Studies of a novel endoplasmic reticulum anion channel from mammalian brain

Alan George Clark

Doctor of Philosophy

The University of Edinburgh

1997

Contents

Abstract

A novel rat brain endoplasmic reticulum (ER) anion channel was investigated. The channel is co-localised with ryanodine-sensitive Ca^{2+}-release channels, and physiologically may function as a charge compensator in the ER membrane to regulate Ca^{2+}-release. Similar channels were reconstituted from sheep brain microsomes and these were partially-purified and reconstituted for macroscopic flux assays.

Brain microsomes were incorporated into voltage-clamped planar lipid bilayers. This is a very powerful technique to study single channels from intracellular membranes such as the ER. Channel gating was voltage-dependent and channels opened in bursts with more activity at positive intra-ER (luminal) voltages. The channel displayed multiple closed states including long "interburst" periods where the channel appeared to be inactive. The single-channel slope conductance was ~70 pS in symmetrical 250 mM Choline Cl with currents saturating at 170 pS in high concentrations of this salt. Exclusion sizing of ions suggested that the pore had a minimum diameter of approximately 7 Å, and the channel was permeant to both anions and cations with anion selectivities $SCN^- > NO_3^- > Br^- > Cl^- > F^-$. The channel displayed 3 subconductance states with relative amplitudes of 22%, 45% and 70% irrespective of the permeant cation. These results suggest that the channel was functionally behaving as a four-barrelled multimer, and openings to subconductance levels were well-described by the binomial equation. A range of putative Cl^- channel blockers were applied. Indanyloxyacetic acid-94 (IAA-94) was studied in detail and found to block the channel from the cytoplasmic side on an intermediate timescale

with a K_i of 35 μM at -30 mV. Block was voltage-dependent, and relieved by negative luminal voltages. 5-nitro-2-(3-phenylpropylamino)-benzoate (NPPB) gave an intermediate use-dependent block at 20 μM, and 4,4'-diisothiocyanatostilbene-2,2'-disulphonic acid (DIDS) completely blocked the channel from the cytoplasmic side at 15 μM. NPPB and DIDS showed irreversible inhibition. HEPES added to both chambers at 10 mM appeared to block individual protomers on a slow timescale.

Single sheep brain ER anion channels showed very similar gating and pharmacological properties to the rat brain channel. The inter-species similarities facilitated use of sheep material to partially-purify the channel by DE52 anion-exchange, Sephadex G-150 gel-exclusion and Concanavalin A lectin chromatography. Proteoliposomes containing the partially-purified protein were used in a $^{36}Cl^-$ efflux assay to correlate flux and pharmacology at a macroscopic level.

Declaration of Originality

I declare that the material presented within this thesis is my own work unless otherwise stated.

Alan G. Clark

Acknowledgements

I would firstly like to thank my supervisor Dr. Richard H. Ashley for all his help and interesting discussions throughout my project, all of my colleagues in lab. 321 past and present and The University of Edinburgh Faculty of Medicine for providing me with a Scholarship. Thanks also to my brother James for proof reading my thesis and Avril for all her support.

Finally, I would like to express my sincere gratitude to the late Jim Manson for giving me insight and direction and also to my Mum for giving me the motivation to succeed.

Abbreviations

9-AC	Anthracene-9-carboxylic acid
AEBSF	[4-(2-Aminoethyl) benzenesulfonylfluoride, HCl]
CHAPS	(3-[(3-Cholamidopropyl)-dimethylammonio]-1-propane-sulfonate)
DIDS	4,4'-diisothiocyanatostilbene-2,2' -disulphonic -acid
DPC	Diphenylamine-2-carboxylic acid
DMSO	Dimethyl sulfoxide
EA	Ethacrynic acid
ER	Endoplasmic reticulum
GABA	γ-aminobutyric acid
HEPES	(N-[2-Hydroxyethyl]piperazine-N'-[2-ethanesulfonic acid])
$InsP_3$	Inositol 1,4,5 trisphosphate
IAA-94	Indanyloxyacetic acid-94
KEGTA	Ethylene glycol-*bis*(β-aminoethylether) N,N,N',N'-tetraacetic acid, K salt
NPPB	5-nitro-2-(3-phenylpropylamino)-benzoate
PC	Phosphatidylcholine
PE	Phosphatidylethanolamine
POPE	Palmitoyloleoyl-phosphatidylethanolamine
POPS	Palmitoyloleoyl-phosphatidylserine
PS	Phosphatidylserine
SDS	Sodium dodecyl sulphate
SR	Sarcoplasmic reticulum

List of Figures

Chapter 1

Chapter 2

Chapter 3

Chapter 4

List of Tables

Chapter 3

Chapter 4

Chapter 1

Introduction

1.1 Ion channels

Ion channels are found in the membranes all cells studied to date, and they are central to the function of cells in the brain. The brain contains approximately 10^{10} neurons in which electrical signalling involves the co-ordinated activities of combinations of ion channels including Na^+, K^+, Ca^{2+}, and Cl^--selective channels. These channels are responsive to specific regulatory elements which control their opening and closing or "gating". Channels are also present in intracellular membranes, including the endoplasmic reticulum (ER) (Figure 1.1) although it is not yet known whether ER membranes are electrically excitable.

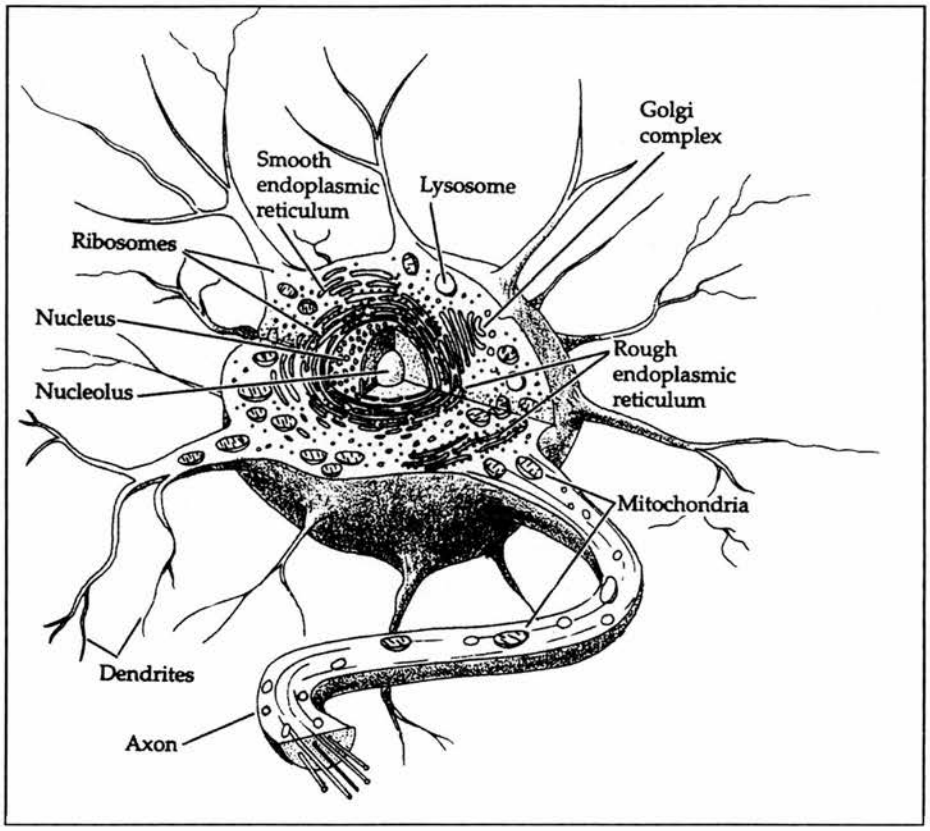

Figure 1.1 Subcellular organelles in the cell body of a neuron.

Adapted from Hall (1992).

1.2 Chloride channels

Chloride (Cl^-) channels are ubiquitous, with diverse biophysical properties and cellular functions. In the plasma membrane these functions include transepithelial ion transport, cell-volume regulation and stabilisation of the resting membrane potential (Strange *et al.*, 1996). Recently, interest in Cl^- channels has increased dramatically following the discovery that the cystic fibrosis transmembrane regulator (CFTR) is a Cl^- channel. To date more than 75 different Cl^- channels have been discovered (Frizzell & Halm, 1990). They have been found in the plasma membranes of many cell types, and also within intracellular membranes including the outer nuclear membrane, mitochondrial membranes and membranes of the endoplasmic and sarcoplasmic reticulum Although CFTR, the voltage-dependent anion channel of the mitochondrial outer membrane (VDAC), ClC voltage-gated channels, γ-aminobutyric acid receptor (GABAR) and Glycine receptor (GlyR) channels can be classified into structural families, many channels can at present be classified according to their functional properties. These functional properties include their conductance, ionic selectivity, voltage and agonist dependence, and sensitivity to blockers.

1.3 Conductance characterisation

Cl^- channels can be characterised according to their single channel conductances:-

(i) Cl^- channels of low-conductance (up to 30 pS).

(ii) Cl^- channels of intermediate-conductance (30-150 pS).

(iii) Large-conductance Cl^- channels (>150 pS).

1.3.1 Low-conductance Cl^- channels

Low-conductance non-ligand gated surface membrane Cl^- channels are active at biologically relevant membrane potentials in the absence of activating ligands such as GABA or ions such as Ca^{2+}. They are found, for example, in *Torpedo* electroplax (Miller & White, 1980, Bauer *et al.,* 1991), in the plasma membranes of epithelial cells (Landry *et al.,*1990), in skeletal muscle sarcolemma (Blatz & Magleby, 1985), and in neuronal cell membranes (Blatz, 1991). In all these locations, they appear to function mainly to regulate membrane excitability, or to control water and electrolyte movements and cell volume (Pusch & Jentsch, 1994).

1.3.2 Intermediate-conductance Cl^- channels

Intermediate-conductance Cl^- channels have a conductance of between 30 and 150 pS and in the main have the same functions as low-conductance Cl^- channels (section 1.3.1). They have been found in various locations such as epithelia (Hanrahan & Tabcharani, 1990), the sarcoplasmic reticulum (Rousseau *et al.*, 1988, Kourie *et al.*, 1996a), endosomes (Reeves & Gurich, 1994), the apical membrane of rectal gland (Greger *et al.*, 1987) and rat brain growth cones (DeBin *et al.*, 1994). These may be termed "background" Cl^- channels.

1.3.3 Large-conductance Cl^- channels

Large-conductance Cl^- channels were the very first to be described at the single-channel level although to date they have been found in relatively few locations and are yet to be fully characterised. The channels are found in very low density and

are only activated after large voltage steps (Blatz and Magleby, 1983). They have been so-named due to their very high conductance (>200 pS in 150 mM Cl) and have been found in the basolateral membranes of urinary bladder, the apical membranes of epithelia (Duszyk *et al.*, 1995) and some epithelial cell lines (Nelson *et al.*, 1984). They have also been found in the plasma membranes of epithelia, amphibian skeletal muscle, macrophages and β-lymphocytes and also in the plasma membranes of cultured cells. Their pore size has been estimated using permeant anions with different cross-sectional areas, and calculated to be between 6-7 Å (Gray *et al.*, 1984).

The selectivity of the channels is similar to that of intermediate-conductance Cl^- channels, with an anion permeability sequence typical for a selectivity filter of "low field" strength (Wright & Diamond, 1977). The field-strength represents selectivities which arise when site-interaction energy and hydration energy depend differently on the ionic radius. The channels are voltage-dependent and are active at potentials around 0 mV but inactivate beyond +/- 20 mV. An exception to this is the channel from amphibian skeletal muscle (Woll *et al.*, 1987) which is active at depolarising potentials up to +60 mV.

The physiological role of large-conductance Cl^- channels is unknown, although it has been suggested it may be part of a gap junction complex (Blatz and Magleby, 1983) or involved in cell volume regulation (Grinstein *et al.*, 1982). A pressure-sensitive channel may act as an osmotic sensor (Martinac *et al.*, 1987).

1.4 Structural characterisation

Only a few Cl^- channels have been cloned and reconstituted to give information on their structure-function relationships. The cloned channels include CFTR , the ClC family and VDAC.

1.4.1 CFTR

Cystic fibrosis (CF) is a lethal genetic disease caused by mutations in CFTR. It belongs to the superfamily of ATP-binding cassette ATPases, and functions as a cAMP-regulated Cl^- channel (Welsh, 1992). Several hundred disease-causing mutations have been identified since the discovery of the gene. One of the most common, ΔF508, results from the deletion of a phenylalanine residue at position 508 and disrupts its biosynthesis and delivery to the apical membrane in epithelia. This leads to defective Cl^- absorption and secretion in airway epithelia.

CFTR is composed of two sections each containing six transmembrane domains and a nucleotide-binding domain (NBD) (Figure 1.1, panel A). A regulatory domain is present between these two sections, and this needs to be phosphorylated for channel opening to occur. To provide insights into the structure and function of CFTR, mutants were made by introducing specific amino-acid changes which alter the properties of the channel. The first site-directed mutagenesis experiments substituted positively-charged amino acids in the transmembrane domains with negatively-charged residues (Anderson *et al.*, 1991). This changed the selectivity of the channel, making I^- more permeant than Cl^-. These charged residues were therefore assumed to be part of the transmembrane pore, and to contribute to the ionic selectivity of the

channel. The R domain of CFTR is responsive to cAMP-activated protein kinases and experiments which deleted the R domain left the channel permanently in the open state. CFTR can still be activated by protein kinase A (PKA) when all consensus phosphorylation sites in the R domain have been eliminated and this activation may be due to cryptic PKA sites. Negatively charged residues at these positions led to channels no longer requiring cAMP for activation. The ATP- binding domains were shown to have a regulatory role as they are suppressed by deletion of the R domain which was speculated to move in and out of the channel in an ATP-dependent manner.

1.4.2 ClC voltage-gated Cl^- channels

The ClC voltage-gated Cl^- channels have now been characterised in many cell types (Pusch & Jentsch, 1994) and comprise a large channel family (Table 1.1). The channels are structurally very similar (Figure 1.1, panel B) although they exhibit functional diversity, and have important physiological functions due to their voltage dependence and tissue distribution including ion secretion, ion balance, cell volume regulation, and stabilisation of membrane potential.

1.4.2.1 CLC-0

Expression-cloning of the voltage-dependent Cl^- channel from *Torpedo* electric organ (ClC-0) (Jentsch *et al.*, 1990) allowed the identification of other members of the family with similar structure. Expression-cloning is the process where clones in a DNA library known to contain the gene of interest are expressed in a

suitable expression system. Screening for functional expression of the gene e.g. Cl^- currents is then carried out to identify DNA fragments from the library that contains the gene.

Expression of the cDNA in *Xenopus* oocytes gave rise to Cl^- currents and the biophysical characteristics of the ClC-0 channel have been extensively studied. The channel has a low conductance of 10 pS and a selectivity sequence of $Cl^- > Br^- > I^-$. The gating involves two different processes namely a slow gate which opens the channel at hyperpolarised potentials with open time constant of several seconds with channel closures even more slowly at depolarised potentials. The second faster gate opens the channel at depolarising potentials with time constants of tens of milliseconds. Channel activity occurred in bursts with two subconductance states suggesting two identical but independent Cl^- conducting protomers in a double-barrelled structure. Channel gating could be described by the binomial equation (Miller & Richard, 1990) and DIDS blocked individual protomers, reinforcing the binomial gating.

The channel consisted of 805 amino acids and a hydropathy plot showed that there were 12 or 13 transmembrane domains (D1 to D13). There was a consensus site for N-linked glycosylation between domains D8 and D9 and this site turned out to be conserved among all members of the ClC family. Removal of the consensus site between D8 and D9 showed that the loop was extracellular. The subunit composition of ClC-0 was investigated using hybrid channels from functionally tagged subunits (Middleton *et al.*, 1996) and this conclusively proved that ClC-0 was a homodimer

containing two independent pores. Similar results were found in an independent study (Ludewig *et al.*, 1996).

1.4.2.2 ClC-1

ClC-1 mRNA is expressed predominantly in skeletal muscle with low levels of expression in heart and kidney (Steinmeyer *et al.*, 1991). Expression in *Xenopus* oocytes gave rise to Cl^- currents with a nearly linear conductance range between -80 to -20 mV but showing inward rectification at positive holding potentials and deactivation at negative holding potentials below -100 mV. ClC-1 contains 965 amino acid residues and has a putative topology like ClC-0 and a similar voltage dependence. This channel is important for skeletal muscle function as defects in the gene lead to the disease myotonia where skeletal muscle becomes hyperexcitable because membrane Cl^- conductance is reduced. This can be manifested as myotonia congenita (Thomsen's disease)(Steinmeyer *et al.*, 1994) as well as generalised myotonia (Becker's myotonia). The single-channel conductance of ClC-1 is very low at 1 pS and was determined by nonstationary noise analysis (Pusch *et al.*, 1994). This probably accounts for the lack of single-channel data from intact skeletal muscle despite its high macroscopic Cl^- conductance (Chua *et al.*, 1991). This makes it difficult to test the hypothesis that the channel functions as a double-barrel like ClC-0.

1.4.2.3 ClC-2

ClC-2 was cloned using ClC-1 cDNA as a probe (Thiemenn *et al.*, 1992). The channel protein contained 907 amino acids and was expressed in many tissues

including rat skeletal muscle, brain, heart, kidney, lung, liver, pancreas, stomach and intestine and also in numerous cell lines. Comparing its characteristics to the currently-known members of the ClC family, ClC-2 was shown to be 55% identical at the amino acid level to ClC-0 and 49% identical to ClC-1. The sequences are most conserved in the hydrophobic domains, and differ greatest at the NH_2 and COOH terminals, and also between domains 12 and 13. Cl^- currents were found when ClC-2 was expressed in *Xenopus* oocytes with slow activation of the channel at high negative potentials and activation by extracellular hypotonicity suggesting a role in volume regulation. The currents were inwardly rectifying, like ClC-1, although ClC-2 lacks the fast activation gate of ClC-0 and ClC-1. The single-channel conductance of the ClC-2 Cl^- channel was 3-5 pS and the conductivity sequence was $Cl^- > Br^- > I^-$. A structure-function study of ClC-2 has been carried out using site-directed mutagenesis with expression in oocytes. Deletion of part of the NH_2 terminal lead to complete abolition of volume and voltage dependence. Other deletions and point mutations showed "modulatory" and "essential" regions within the NH_2-terminal sequence (Gründer *et al.*, 1992).

1.4.2.4 ClC-K

Degenerate PCR primers based on conserved regions of ClC-0, ClC-1 and ClC-2 and the reverse transcriptase-polymerase chain reaction (RT-PCR) techniques were used to clone a new channel (ClC-K1) from whole rat kidney mRNA. (Uchida *et al.*, 1993). Two other ClC members have been described from rat kidney including rClC-K1 and rClC-K2 and in humans two channels have been isolated which show

90% identity to each other on the amino-acid level and 80% to the rat ClC-K channels. These have been termed hClC-Ka and hClC-Kb. ClC-K1 has been functionally expressed in *Xenopus* oocytes although neither rClC-K and hClC-K could be expressed in any expression system. The reason for this is unclear. ClC-K1 expression showed slightly outwardly rectifying Cl^- currents which were time- and voltage-independent. The selectivity sequence differed from other ClC channels, with Br^- being more permeant than Cl^-.

1.4.2.5 ClC-3

ClC-3 cDNA was isolated and expressed from a rat kidney cDNA library (Kawasaki *et al.,* 1994). Although isolated from rat kidney was also abundant in rat brain in the hippocampus, olfactory bulb and the Purkinje cells of the cerebellum. The encoded protein comprosed 760 amino acids in size and the sequence is only 20-24% identical to the other cloned ClC-channels. When ClC-3 cRNA was injected and expressed in *Xenopus* oocytes Cl^- currents were found which were completely blocked with phorbol ester treatment such as 12-o-tetradecanoyl-phorbol 13-acetate. Phorbol esters are activators of PKC, which suggests that PKC directly phosphorylates the protein to render it inactive. It is however possible that PKC directly phosphorylates an associated membrane protein which regulates ClC-3 activity (see 1.5.3.4). The anion permeability sequence is $I^->Br^->Cl^->F^-$ and the channel is Ca^{2+}-dependent and shows outward rectification. When exposed to nominally-free Ca^{2+} conditions the ClC-3 channel shows a middle conductance state of 100 pS (S2) and a high conductance state of 140 pS (S3). It is therefore possible to

hypothesise that the subconductance states could be explained by a triple-barrelled multimer. At 100 nM Ca^{2+}, the 100 pS S2 level is observed together with a smaller 40 pS S3 level. At 200 nM Ca^{2+} only the S3 level was observed which disappeared at 1000 nM. The function of ClC-3 is not defined although it has localised to the parts of the brain involved in short term memory and could be involved in long term potentiation (LTP). PKC may play an important part in the induction and maintenance of LTP (Malenka *et al.*, 1986).

1.4.2.6 ClCN4

The next member to be identified was ClCN4 which was isolated from human using a positional cloning strategy (van Slegtenhorst *et al.*, 1994). This technique involves localising the gene of interest to a specific chromosome region using marker sequences and then narrowing down the region of interest using P1 vectors or libraries to form overlapping clones which can then be narrowed down further. ClCN4 was also independently cloned using an RT-PCR approach (Jentsch *et al.*, 1995). When aligned, ClCN4 shows 78% identity to ClC-3 at the amino acid level. Whereas ClC-3 was ubiquitously expressed, ClCN4 in humans was confined to muscle and brain, where it was the predominant isoform. Rat ClCN4 was found in liver and brain although is was also expressed in heart, muscle, kidney and spleen.

1.4.2.7 ClCN5

Positional cloning was used to identify the 3' region of hClC-K2, and subsequently the isolation and characterisation of the genes complete open reading

Channel	Distribution	Properties	Functional Expression	Reference
ClC-0	*Torpedo* electric organ, skeletal muscle, mammalian brain.	10 pS $Cl^- > Br^- > I^-$ Double-barrel	Yes	Jentsch *et al.*, 1990
ClC-1	Mammals, skeletal muscle.	1 pS $Cl^- > Br^- > I^-$	Yes	Steinmeyer *et al.*, 1991
ClC-2	Mammalian. Many tissues.	3-5 pS $Cl^- > Br^- > I^-$	Yes	Thiemann *et al.*, 1992
ClC-K	Mammalian kidney	? pS $Br^- > Cl^- > I^-$	Yes	Uchida *et al.*, 1993
ClC-3	Mammalian, Many tissues.	140 pS $I^- > Br^- > Cl^- > F^-$	Yes	Kawasaki *et al.*, 1994
ClC-4	Mammalian Many tissues.	nd	nd	Jentsch *et al.*, 1995
ClC-5	nd	nd	nd	Fisher *et al.*, 1995
ClC-6	nd	? pS $NO_3^- > I^- > Br^- > Cl^-$	Yes	Buyse *et al.*, 1997
ClC-7	nd	nd	nd	Brandt & Jentsch, 1995

Table 1.1 The ClC voltage-gated Cl^- channel family
nd = not determined.

frame (ORF) has been described (Fisher *et al.,* 1995). The channel was renamed ClC-5 on the advice of the Genome Database Nomenclature committee. The ORF encoded a protein of 746 amino acids and showed homology to all known members of the ClC-family. Hydropathy analysis of the amino acid sequence showed 12 transmembrane domains which were very similar to the other ClC proteins. Aligning the amino acid sequences showed ClC-5 was most closely related to ClC-3 and ClC-4 but yet only showed 28 % homology to ClC-K. This novel kidney specific gene has been implicated in Dent disease which is a renal tubular disorder characterised by kidney stones (Lloyd *et al.*, 1996).

1.4.2.8 ClC-6 and ClC-7

The most recent members of the ClC family are ClC-6 and ClC-7 (Brandt & Jentsch, 1995). These novel members were cloned from rat and human cDNA libraries using an established sequence tag (EST) and PCR. The ClC-6 protein is 97 kDa and ClC-7 is 87 kDa. ClC-7 is 45% identical at the amino acid level to ClC-6. Both are expressed ubiquitously in many tissues although their function is yet to be elucidated. Initially ClC-4, ClC-5, ClC-6 and ClC-7 did not yield Cl^- currents in *Xenopus* oocytes although recently injection of ClC-6 RNA into *Xenopus* oocytes with a temperature elevation resulted in Cl^- currents identical to the I_{Cln} current (Buyse *et al.*, 1997). Co-injection with other ClC channels failed to yield functional Cl^- channels. This may be explained either by a missing subunit, complex channel regulation, or channels which are resident in intracellular organelles. The function of

ClC-0, ClC-1 and ClC-2 are well characterised, although the physiological significance of the other channels is unknown.

1.4.3 VDAC/mitochondrial porin

The voltage-dependent anion-selective channel of mitochondria (VDAC) sometimes referred to as mitochondrial porin, was first characterised in *Paramecium* by Schein *et al.,* (1976). It was localised to the outer mitochondrial membrane by Colombini *et al.*, (1979). VDAC has a molecular weight of between 30,000 and 35,000 and has been detected in all eukaryotic cells studied to date, including mitochondria from mammals, fish, insects, plants, yeast, fungi and protozoa (Sorgato & Moran, 1993). Although VDAC was originally thought to be exclusively located in mitochondria, it has since been shown to be present in other cell compartments and also in skeletal muscle (Lewis *et al.*, 1994).

1.4.3.1 Biophysical properties

VDAC forms a high-conductance, voltage-gated channel when incorporated into voltage-clamped planar lipid bilayers. The channel has a large single-channel conductance of 650 pS in 150 mM KCl, and its open pore is approximately 3 nm in diameter. The protein adopts multiple conformational states with differing conductances. One open state is slightly anion-selective (P_{anion}/P_{cation} = 2:1) and a large number of anions and cations including $HEPES^-$ and $Tris^+$ are permeant (Roos *et al.,* 1982). The voltage-dependence of VDAC is shown at holding potentials greater than 15-20 mV. The channel switches to a partially-closed subconductance state of 300 pS,

with complete closures at higher potentials. This is consistently seen in all mitochondrial porins except rat brain porin (Mr 35,000), which shows less voltage-dependence. In this case, a transmembrane potential of more than 100 mV was needed to reduce the conductance to 60% (Ludwig *et al.,* 1986). The partially closed substates have a reduced permeability to ions, and are cation-selective.

1.4.3.2 Structure

Mitochondrial porins have been isolated and purified from a number of cells and tissues including rat brain, yeast (*Saccharomyces cerevisiae*), fungi (*Neurospora crassa)*, *Paramecium tetraurelia*, & slime mould (*Dictyostelium discoideum*). A VDAC-like polypeptide with a molecular weight of 36,000 has also been isolated and purified from rat brain (Bureau *et al.*, 1992). The proteins are present in significant amounts in the outer mitochondrial membrane, and have been crystallised to give two dimensional crystals which provide significant structural information (Mannella, 1990). The amino acid sequences of mitochondrial porins from slime mould (Troll *et al.,* 1992), fungi (Kleene *et al.,*1987), & yeast (Mihara *et al.,*1985) have been deduced from their cDNA sequences and the sequence of the mitochondrial porin-like anion channel from rat brain (Bureau *et al.*, 1992) has also been determined. When all the sequences are aligned, only 13 out of approximately 280 residues are conserved (Benz, 1994). This suggests that the β-barrel structure predicted using secondary structure (Kleene *et al.,*1987) and supported by CD-spectra allow extensive amino acid variation without altering the secondary structure and function. The mitochondrial proteins are predominantly hydrophobic, with ~50 % polar residues,

and this distinguishes them from ion channels found in neurons & muscle whose transmembrane domains appear to favour an α-helical structure. The secondary structures of VDAC in yeast, slime mould, & fungi have been analysed in detail (Vogel & Jähnig, 1986), and it has been proposed that the β-sheet crosses the membrane twice with 16 membrane spanning domains. Polar and non-polar residues are present on either side of the β-sheet and folding of this β-sheet into a β-barrel would give a structure of a hydrophilic interior and a hydrophobic exterior ideal for forming an aqueous pore. A VDAC model has been presented as a β barrel formed by between 12 -19 strands, with a short α-helical stretch at the N-terminus.

1.4.3.3 Site-directed mutagenesis

The structure-function relationships of VDAC were investigated by using oligonucleotide-directed site-specific mutagenesis to change 29 amino acids of the cloned yeast VDAC gene. These mutants were expressed in yeast, and the effects of point and multiple mutations were assessed using planar lipid bilayers for reconstitution (Blachly-Dyson *et al.*, 1990). Previous work had shown that lysine was important for channel selectivity (Doring & Colombini, 1985) and therefore selectivity of VDAC was investigated by changing positive lysines to negative residues. The selectivity was measured using reversal potentials with 1 M KCl separated from 0.1 M KCl, and was quite marked in some mutants such as VDAC-E22OK which differed from wild-type VDAC by around 11 mV. Other mutants decreased anion selectivity such as K19E which had a reversal potential of around -2 mV when compared with wild-type. Point or multiple mutations did not have a marked effect on the single-

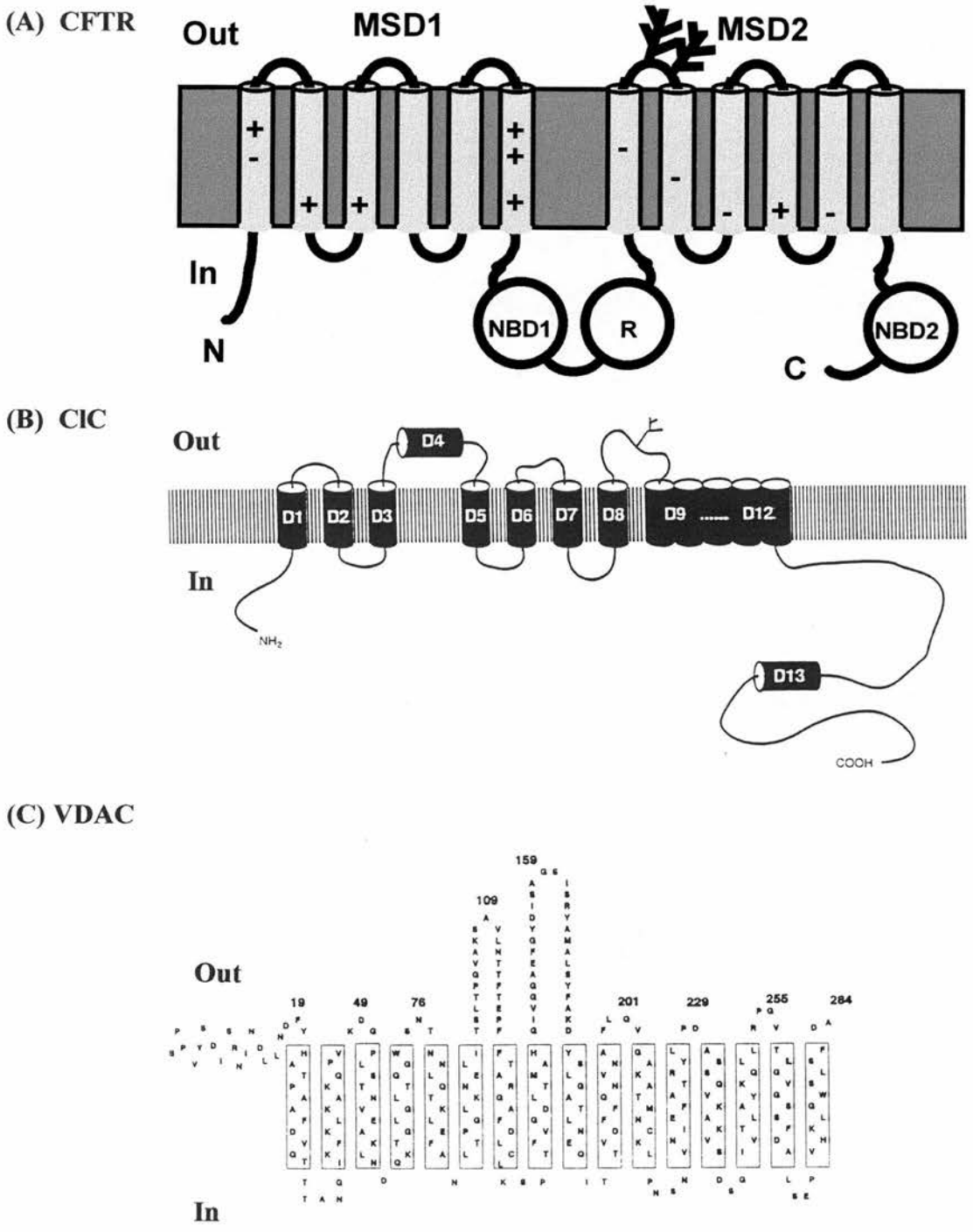

Figure 1.1 Putative membrane topology of known Cl⁻ channel structures. Panel A shows the membrane topology of CFTR (from D. Sheppard) where MSD is the membrane spanning domain, NBD is the nucleotide binding domain and R is the regulatory domain. Panel B shows ClC with D1-D13 representing the domains (adapted from Jentsch *et al.,* 1995). Panel C shows yeast VDAC (adapted from Benz, 1994).

channel conductance, suggesting the pore conformation was not significantly affected by the mutations although multiple mutations did alter channel selectivity from normally anion-selective to cation-selective. The magnitude of the change of charge was highly correlated with the selectivity change, and these were found at 14 sites through the VDAC molecule and are probably found in the pore-lining wall. These results have been used to model the open pathway of the channel with each polypeptide formed by 12 transmembrane β-strands and one transmembrane α-helix.

1.4.4 p64

A putative intracellular chloride channel protein, called p64, has been cloned from a kidney cDNA library (Landry *et al.*, 1993). Modelling based on its predicted amino acid sequence suggested there may be two and possibly four transmembrane domains with potential protein kinase A, protein kinase C and casein kinase II phosphorylation sites. There was no significant homology to any known proteins in the database and the protein was expressed in all cell lines tested. When the cRNA was expressed in *Xenopus laevis* oocytes a protein of a molecular mass of 64 kDa was inserted into intracellular membrane vesicles and not the plasma membrane. It was therefore hypothesised that p64 may be present in intracellular membranes.

1.4.4.1 Purification and cDNA cloning of p64

To purify p64 a high affinity inhibitory ligand Indanyloxyacetic acid-23 (IAA-23) was bound in an affinity column and bovine kidney cortex membranes passed through. The purified material contained four major protein bands following SDS-

PAGE and Ag^+-staining, and these were reconstituted into liposomes to measure $^{36}Cl^-$ uptake, and also into planar lipid bilayers which resulted in Cl^- channel activity (Landry *et al.*, 1989). One of the proteins, a 64 kDa protein was used to prepare an antiserum which immunodepleted all Cl^- channel activity. Thus p64 was speculated to be a Cl^- channel protein.

1.4.4.2 p64 Homologues

Proteins of similar mass (64 kDa) have been located in membranes obtained from T84 human colonic cells, Chinese hamster ovary cells, human fibroblasts and an insect cell line Sf9. Recently a p64 homologue has been identified and characterised in rat tissues including brain, kidney, liver, and lung (Howell *et al.*, 1996). The homologue shows 74% identity to p64. From the predicted amino acid sequence there is one membrane spanning domain with the same membrane topology as the putative chloride channel activator phospholemman and IsK protein (minK). This suggests that it may be a channel regulator or part of a channel complex.

1.5 Channel regulation and activation

1.5.1 Channel regulator proteins

It is not known whether several putative Cl^- channels such as pI_{Cln}, phospholemman and P-glycoprotein are indeed Cl^- channels or possibly regulators activating endogenous channels in the systems used for expression.

1.5.1.1 IsK

IsK protein (minK) was originally shown to be a dual activator of endogenous K^+ and Cl^- channels (Attali *et al.*, 1993). These channels were only observed when large amounts of cRNA (1 μg/μl) was injected in oocytes. The protein had a single membrane-spanning domain and mutations in minK led to a loss of induction of K^+ and Cl^- channels. The model suggested that minK acted as an activator of silent endogenous K^+ or Cl^- channels. Recently, however, it has been shown that co-expression of minK with K_vLQT1, from a novel putative K^+ channel gene *KVLQTI* (Barhanin *et al.,* 1996 and Sanguinetti *et al.*, 1996) forms a functional channel with K^+ currents almost identical to the I_{Ks} cardiac current. Thus IsK induces K^+ currents in *Xenopus* oocytes by interacting with endogenous K_vLQT1 channels.

1.5.1.2 Phospholemman

Phospholemman from cardiac plasma membrane was first considered to be a Cl^- channel (Moorman, 1992) although recent work suggests it may function as a Cl^- channel regulator (Kowdley, 1994). Phospholemman is a small plasma membrane protein of 72 amino acids with a single transmembrane domain. It is a major target for phosphorylation by protein kinase A and protein kinase C (Walaas, 1991). On expression in *Xenopus* oocytes, phospholemman induced Cl^- currents which activated slowly at voltages more negative than -80 mV. This is similar to ClC-2, although the halide selectivity is different ($I^- > Cl^-$) and phospholemman activates faster. The currents can be blocked by extracellular Ba^{2+} and intracellular 9-AC, and are independent of intracellular Ca^{2+}.

1.5.1.3 pI_{Cln}

Injection of cRNA encoding Madin-Darby canine kidney (MDCK) pI_{Cln} into *Xenopus* oocytes gave rise to outwardly-rectifying voltage-dependent Cl^- currents with a permeability sequence of $SCN^- > I^- > Br^- > Cl^-$ (Paulmichl *et al.,* 1992). The currents were inhibited by external ATP and other nucleotides and they were similar to swelling-induced Cl^- currents previously found in other cells including epithelial cells (Kubo & Okada, 1992, Kunzelmann *et al.,* 1989). Injection of RNA into *Xenopus* oocytes with a temperature elevation gave rise to currents identical to those obtained after injection with ClC-6 RNA (section 1.4.2.8). The encoded protein had 235 amino acids and the rat homologue was expressed ubiquitously. Further work has shown that pI_{Cln} is an abundant soluble cytosolic protein ~40 kDa found in mammalian brain, *Xenopus* oocytes, and epithelial and cardiac cells (Krapivinsky *et al.*, 1994). pI_{Cln} associates with other cytosolic proteins such as actin and forms multiple oligomeric complexes. The protein structure predicted from the cDNA shows that there are no transmembrane helices, and it was suggested that pI_{Cln} may make a channel by dimerizing to form a β-barrel pore. Weighing up the evidence suggests that pI_{Cln} may be functioning as a ubiquitous cytoskeleton-associated protein involved in the transduction of cell swelling to channel opening rather than being an ion channel itself. Alternatively, it may insert into the membrane by a porin-like mechanism since they are both acidic proteins and have similar structural characteristics.

1.5.1.4 P-glycoprotein

P-glycoprotein is a member of the ATP-binding cassette (ABC) family of transporters. Even although P-glycoprotein is structurally related to CFTR in membrane topology and nucleotide binding domains, a comparison suggests that it is not a Cl^- channel. Charges in the transmembrane domains of CFTR contribute to its ion-selective pore (Sheppard *et al.,* 1993) but these residues are not conserved in P-glycoprotein. It has been shown to confer drug resistance by actively pumping hydrophobic molecules including substrates and chemotherapeutic drugs from the cytosol out of cells (Diaz *et al.*, 1992). The protein product of the multidrug resistance gene (*mdr1*) is 170 kDa. in size and has been suggested to function both as an ATP-dependent pump and a Cl^- channel (Valverde *et al.*, 1992). When *mdr1* was transfected into fibroblasts which contain no endogenously expressed *mdr1* channels, drug transport activity and also a swelling-activated Cl^- conductance were observed. Only macroscopic whole cell currents were examined, and there were outwardly-rectifying with a conductance of 40 pS. The transport of drugs was also reduced by cell swelling (Sardini *et al.*, 1995) and it has subsequently been shown that P-glycoprotein-mediated drug efflux and swelling-activated Cl^- currents in intact cell lines are separable functions (Ehring *et al.*, 1994). It is possible that P-glycoprotein may function as a swelling-activated Cl^- channel or a Cl^- channel regulator as drugs known to stimulate P-glycoprotein ATPase activity also modify Cl^- channel kinetics.

1.5.2 Cell volume regulation

The cell membranes of most mammmalian cells are highly permeable to water and cells therefore tend to swell. Water-entry may occur by simple diffusion throught the lipid bilayer, bulk transport through ion channels and pumps or even by water transport coupled with solute uptake (Loo *et al.*, 1996). This transport will be regulated by impermeant intracellular charged macromolecules and the osmolarity of the extracellular fluid. The cell volume increase will be counteracted by volume-sensitive ion transport pathways which allow net loss of solutes to shrink the enlarged cells.

Volume-sensitive channels have been found in many cell types. Swelling - activated Cl^- channels have been described in T-lymphocytes, epithelial cells, Ehrlich ascites tumour cells, CFTR, human dermal fibroblasts, and intestinal cells. Hypotonicity also activated an endogenous chloride current, $I_{Cl.swell}$, in *Xenopus* oocytes (Ackerman *et al.,* 1994). The currents were calcium-independent with an anion conductivity sequence of $SCN^- > I^- > NO_3^- > Br^- > Cl^-$, and NPPB and DIDS almost completely blocked the currents at 100 μM. Regulation of cell volume can be achieved indirectly, by activation of separate K^+ and Cl^- channels where swelling-activated Cl^- channels play an important role in triggering and maintaining ionic flux for volume regulation (Cahalan & Lewis, 1994). For example, in hypotonic conditions cells may swell as water enters, triggering a volume sensitive Cl^- channel (Grinstein, 1983). By opening the Cl^- channel the cell is depolarised and this activates voltage-gated K^+ channels (Cahalan & Lewis, 1988). This leads to a subsequent loss of KCl and bulk water contributing to a regulatory volume decrease (RVD). The relevant Cl^-

currents have been shown to be large, outwardly rectifying and were inactive at positive voltages above +80 mV, and also distinct from the cAMP regulated channels. P-glycoprotein has been implicated in cell volume regulation, but it has been shown that volume-sensitive Cl^- channel activity does not depend on endogenous P-glycoprotein (Tominaga *et al.*, 1995). Volume-sensitive Cl^- channels may also have an important role in organelle volume regulation including the endoplasmic reticulum (section 1.8.2). For the present, the molecular identity of Cl^- channels regulating cell volume is not known.

1.5.3 Cell signalling

Regulation of Cl^- channels can occur through interaction with second messengers, receptors, G-proteins and protein kinases. The mechanisms by which they interact may be relatively simple, or involve highly complex signalling cascades.

1.5.3.1 Ca^{2+}

Ionised calcium (Ca^{2+}) is an important messenger in cells of the nervous system and other cells of the body. The cytosolic concentration of free Ca^{2+} is maintained at 50-100 nM and extracellular [Ca^{2+}] at ~1 mM. Rapid increases in the cytosolic concentration acts as a regulatory signal in neuronal function. In the surface membrane, a Na^+/Ca^{2+} exchange protein and a plasma membrane calcium pump maintain the steep gradient, and in the ER an ATP-dependent calcium dependent pump concentrates Ca^{2+} in one or more intracellular storage pools. Ca^{2+} is responsible for regulating some Cl^- channels either by increasing their probability of being open or

by causing Ca^{2+}-induced inhibition. Ca^{2+}-dependent Cl^- channels have been found in many locations including receptor cells (Bader *et al.*, 1982), oocytes (Matsuoka *et al.*, 1996), *Ascaris* parasite (Valkanov *et al.*, 1994), rat lacrimal cells (Evans & Marty, 1986), endocrine cells (Taleb *et al.*, 1988), skeletal muscle (Kourie *et al.*, 1996b), endosomes (Reeves & Gurich, 1994), neuronal cells (Owen *et al.*, 1986) and the plasmalemma of cardiac myocytes (Zygmunt *et al.*, 1991). A Ca^{2+}-activated outwardly-rectifying Cl^- channel was found in the apical membrane of distal nephron epithelium, where insulin increased the single-channel conductance by dephosphorylating the tyrosine of the channel through activation of protein tyrosine phosphatase (Shintani & Marunaka, 1996). Their physiological roles of Ca^{2+}-dependent Cl^- channels include electrolyte secretion in exocrine cells, volume regulation in animal cells and control of turgor in plant cells.

1.5.3.2 cAMP-dependent protein kinase

Cyclic AMP-dependent protein kinase (PKA) can regulate channels by phosphorylating them. It is a tetramer of two heterodimers each comprising a catalytic and a regulatory subunit. The regulatory subunits bind to catalytic subunits to inhibit activity. PKA is activated by cAMP which binds to the regulatory subunits releasing the active catalytic subunits. This results in phosphorylation of serine and threonine residues on proteins, using the γ phosphate from ATP. These serine and threonine residues are found in consensus sequence sites are found in many different proteins.

PKA-regulated channels are found in many locations including basolateral membranes of the mouse thick ascending limb (Guinamard *et al.*, 1995), gastric

parietal cells (Malinowska *et al.*, 1995), chick heart cells (Hall *et al.*, 1995), pancreatic duct cells (Gray *et al.*, 1993), endothelial cells (Vaca *et al.*, 1993), proximal tubules (Bae & Verkman, 1990) and sarcoplasmic reticulum (Kawano *et al.*, 1992). The physiological role of these channels includes modulation of voltage gating and regulation of pH. CFTR is also regulated by PKA and this was first shown when cAMP increased the Cl^- permeability of normal but not CF epithelia. Abnormal regulation of the Cl^- conductance pathway in CFTR reduces ductal fluid secretion and leads to the disease phenotype. Cytochalasin D, an actin filament disrupter, was also shown to activate CFTR in the presence of PKA, but this was cAMP independent (Fischer *et al.*, 1995). It is believed to function by releasing a cellular inhibitor which is held in place by F-actin.

1.5.3.3 cGMP-dependent protein kinase

Cyclic GMP-dependent protein kinase (PKG) contains its regulatory and catalytic domains in a single subunit. Unlike PKA which is expressed in all areas of the brain, PKG is only predominantly found in Purkinje neurons in the cerebellum where it is found with guanylyl cyclase. The heat stable toxin from *E. coli,* STa, stimulates Cl^- secretion with elevated levels of guanosine 3'-5' -cyclic monophosphate (cGMP). It is unknown however, whether the Cl^- secretion is regulated by cGMP directly, or via PKG.

1.5.3.4 Protein kinase C

Protein kinase C (PKC) is a ubiquitous enzyme which requires both 1,2-diacylglycerol (DAG) and Ca^{2+} for activity. Many membrane proteins are phosphorylated by PKC which participates in a variety of functions including long-term potentiation in the hippocampus and gating of ion channels. Activation of PKC can occur with some hydrophobic phorbol esters which mimic DAG.

ClC-3 is a second messenger-gated Cl^- channel. The cDNA is expressed in *Xenopus* oocytes, and phorbol esters completely block the Cl^- current (Kawasaki *et al.*, 1994). It has been hypothesised that PKC directly phosphorylates ClC-3 or a membrane-associated protein which regulates channel activity. Consensus sites for phosphorylation exist in ClC-3 at Ser-51 and Ser-362, and phosphorylation of these residues may lead to inactivation of the channel. The R domain of CFTR has several consensus sequences for PKC phosphorylation, and the addition of phorbol esters is known to increase Cl^- secretion. PKC-activated Cl^- channels were also found in hepatocytes (Koumi *et al.*, 1995) and show similarities to those found in renal and airway epithelia, although are not activated by PKA. Physiological roles for these channels may include cell volume regulation in hepatocytes, and stimulation of Cl^- secretion in airway epithelia.

1.5.3.5 Nucleotides

Nucleotides have been shown to regulate ion transport and intracellular Ca^{2+} in human normal and cystic fibrosis airway epithelium (Mason *et al.*, 1991). ATP enhanced a basal Cl^- conductance in lysosomal membranes (Tilly *et al.*, 1992) while

other nucleotides were ineffective. ATP has also been shown to directly modulate Cl^- conductance in the zymogen granules of rat pancreas (Thévenod *et al.*, 1990), ER-enriched pig pancreatic microsomes (Bégault *et al.*, 1993) and rat brain synaptosomal membranes (Yuto *et al.* 1997). ATP may function by phosphorylation of Cl^- channels or regulator proteins, but currently the mechanisms of its action are unclear.

1.5.3.6 GTP-binding proteins

G-proteins are known to modulate enzymes and ion channels. The process involves hormone receptor activation of the regulatory proteins G_S and G_p which activate adenylate cyclase or phospholipase C to produce the second messengers cAMP and Ca^{2+}. GTP and its non-hydrolysable analogue guanosine -5'-o-(3-thiophosphate) (GTPγS) activated a Cl^- channel in the apical membrane of cultured renal cortical collecting duct (Schwiebert *et al.*, 1990). GTP and GTPγS have also been shown to modulate Cl^- channels in apical membranes from human colonocytes (Tilly *et al.*, 1991).

1.6 Ligand-gated Cl^- channels

Ligand-activated Cl^- channels are regulated by neurotransmitters which open and close the ion pore by binding to a site on the channel protein. They can be classified into gene families which include the acetylcholine receptor and serotonin receptor permeable to cations and the GABA receptor (GABAR), glycine receptor (GlyR), which conduct anions. The amino acids GABA and glycine are the two major inhibitory neurotransmitters in the mammalian central nervous system, and increases

in Cl^- conductance have an inhibitory effect on postsynaptic neurons by producing hyperpolarisation and preventing neuronal firing.

1.6.1 GABA

GABA is the most widely distributed inhibitory neurotransmitter in the vertebrate central nervous system and was originally shown to activate bicuculline-sensitive Cl^- channels. Later it was shown to activate cation channels which led to the formation of two new classes namely $GABA_A$ and $GABA_B$ (Hill & Bowery, 1981).

1.6.1.1 Receptor types of GABAR

$GABA_A$ receptors were sensitive to bicuculline but insensitive to baclofen whereas $GABA_B$ were stimulated by baclofen but insensitive to bicuculline. The $GABA_A$ receptor also has modulatory binding sites for barbiturates, benzodiazepines, neurosteroids and ethanol (MacDonald *et al.,* 1994) which open Cl^- channels directly via allosteric interactions. $GABA_B$ receptors open Ca^{2+} and K^+ channels via a GTP-binding protein mediated system and second messengers. There now appears to be a third class of GABA receptors which are insensitive to both bicuculline and baclofen (Johnston, 1994). These have been designated $GABA_C$ and are found in retinal neurons (Feigenspan *et al.,* 1993). The receptor appears to be far simpler than $GABA_A$ and is activated at lower concentrations of GABA. The single-channel conductance of the $GABA_AR$ is ~30 pS and is higher than $GABA_C$ (~8 pS). The most potent $GABA_C$ receptor agonists are muscimol and *trans*-4-aminocrotonic acid (TACA), and it is antagonised by picrotoxonin.

1.6.1.2 Subunit structures of GABA receptors

The $GABA_A$ receptor was initially thought to have two polypeptide chains: α (Mr = 48,000-53,000) which binds benzodiazepines, and β (Mr = 55,000-57,000) which binds GABA (Sigel *et al.,* 1983). The subunit composition was thought to be $\alpha_3\beta_2$. Additional subunit families (γ, δ, ρ) were subsequently identified (Shivers *et al.,* 1989) with each of the subunits forming multiple subtypes except δ (α1-6, β1-4, γ1-3, ρ1,2). Expression of the subunits in *Xenopus* oocytes showed that each can form part of a functional hetero-oligomeric channel and therefore must have a binding site for GABA. The γ subunit itself does not bind GABA or benzodiazepines but confers high-affinity binding of benzodiazepine when paired with α and β subunits in the oocyte expression system. The stoichiometry of ligand binding is still poorly understood, with potential binding sites on α, β, γ and δ subunits. $GABA_C$ has been shown to be composed of ρ subunits and when expressed in *Xenopus* oocytes, a homo-oligomeric Cl^- channel is formed which is insensitive to bicuculline but sensitive to picrotoxonin (Cutting *et al.,* 1991).

1.6.2 Glycine

Glycine receptors (GlyRs) are ligand-gated Cl^- selective ion channels. The resting potential for Cl^- is near the resting potential of the cell, so that activation of GlyRs results in an inhibitory effect on action potentials like GABARs. GlyRs differ from GABARs in their pharmacology, and whereas GABA predominantly functions in the brain, Glycine is found in the spinal cord where it serves as the major inhibitory neurotransmitter (Aprison, 1978).

1.6.2.1 Subunit structures of GlyRs

The proposed quaternary structure of the GlyR is believed to be a pentameric arrangement with two types of subunits, namely a ligand-binding α subunit of 48,000 and a structural β subunit of 58,000 (Betz, 1992) forming the anion channel. The α-subunits exist in developmentally-regulated isoforms identified generated by alternative mRNA splicing (α_1 to α_4) (Grenningloh *et al.*, 1990a), but the β subunit exists on its own (Grenningloh *et al.*, 1990b). After affinity-purification a polypeptide of 93 kDa was also observed which was cytoplasmically located and was believed to have an anchoring function at the postsynaptic membrane.

1.6.2.2 GlyR subtypes

GlyRs have been shown to be developmentally-regulated. This was demonstrated during rodent spinal cord development which shows neonatal GlyRs ($GlyR_N$) at birth and then the adult receptor ($GlyR_A$). $GlyR_N$ have reduced affinities for strychnine and other agonists including β-alanine and taurine (Schmieden *et al.*, 1992). The adult α-subunit replaces the neonatal subunit 2-3 weeks after birth.

1.6.2.3 Agonist sensitivity of GlyRs

GlyRs in spinal cord neurons were activated by α- and β-amino acids with the order of potency being glycine > β-alanine > taurine > L-alanine > proline (Werman *et al.*, 1968). Ligand binding has been investigated using site-directed mutagenesis and it has shown to have three main binding domains in the extracellular amino-terminal region. Domain I is responsible for taurine activation (Schmieden *et*

al., 1992), domain II determines the order of activity and potency of the amino acids (Kuhse *et al.*, 1990) and domain III has been shown to confer agonist-antagonist discrimination (Vandenberg *et al.*, 1992).

1.6.2.4 Specificity of antagonists of GlyRs

The plant alkaloid strychnine can block glycine-induced currents in *Xenopus* oocytes and neurons with high affinity at 20 to 50 nM (Young & Snyder, 1973). Derivatives of strychnine (RU 5135 and 1,5-diphenyl-3,7-diazaadamantan-9-ol) can also block the receptor with RU5135 having the highest affinity of all glycinergic ligands (3 nM).

1.7 Pharmacology of Cl^- channels

Compared with cation channel blockers such as tetrodotoxin (TTX), tetraethylammonium ion (TEA^+), and nifedipine, compounds known to block Cl^- channels have been very poorly-characterised. Most is known about the GABA Cl^- channels, and studies from amphibian and mammalian skeletal muscle. Pharmacological experiments on ionic channels are very important to probe their functional architecture and also for their purification and isolation where high-affinity ligands must ideally bind with K_Ds in the sub-micromolar range. It is helpful to determine the inhibitory potency of blockers of Cl^- channels by assessing their half-maximal concentration for inhibition (IC_{50}).

1.7.1 Putative Cl^- channel blockers

Cl^- channel blockers can be placed into three main categories including inorganic anions, cations and aromatic acids. The interacting anions include SO_4^{2-}, Br^-, NO_3^-, ClO_4^- and cation blockers include H^+, Cu^{2+}, Cd^{2+} and Zn^{2+} (Franciolini & Nonner, 1987). The aromatic acid Cl^- channel blockers include polycyclics such as (9-AC), benzoates such diphenylamine-2-carboxylic acid (DPC), 5-nitro-2-(3-phenylpropylamino)-benzoate (NPPB), frusemide and niflumic acid. Phenoxyacetates such as ethacrynic acid and indanyloxyacetic acid-94 (IAA-94) and sulphonic acids such as (N-[2-hydroxyethyl]piperazine-N'-[2-ethanesulfonic acid]) (HEPES) and 4,4'-diisothiocyanatostilbene-2,2'-disulphonic acid (DIDS) (Figure 1.3) also block Cl^- channels. It is unknown whether these blockers act on a specific receptor site or whether their action is non-specific.

1.7.2 Structure-activity relationships

Studies have been carried out on Cl^- channels in apical vesicles from bovine tracheal mucosa (Landry *et al.*, 1987) and nephron basolateral membrane (Wangemann *et al.*, 1986) to assess and optimise the inhibitory potency of the blockers tested. In epithelia, potent blockers were identified from the indanyloxyacetic acid and anthranilic acid series to Cl^- channels in the apical membranes from bovine tracheal mucosa. These included IAA-94 with an IC_{50} of ~ 1-2 μM and an anthranilic acid derivative AA-130B with an IC_{50} of 0.1 μM. In the nephron basolateral membrane a study was carried out with diphenylamine-2-carboxylate. The drug was modified to create 219 new compounds which were individually assessed for

A) Polycyclic aromatic: anthracene-9-carboxylic acid (9-AC)

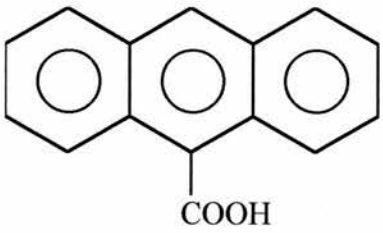

B) Benzoate: 5-nitro-2-(3-phenylpropylamino)-benzoate (NPPB)

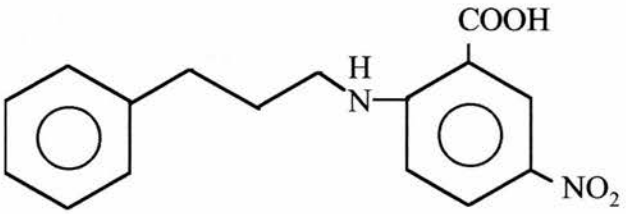

C) Phenoxyacetate: indanyloxyacetic acid-94 (IAA-94)

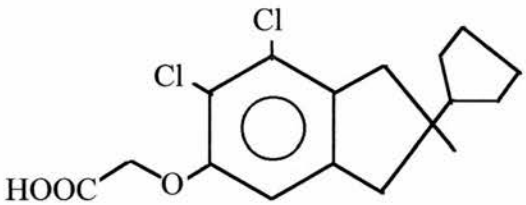

D) Sulphonic acid: (N-[Hydroxyethyl]piperazine-N'-2-ethanesulfonic acid]) (HEPES)

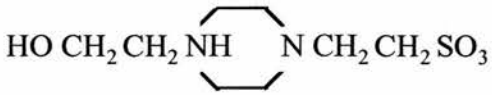

Figure 1.3 Specimen structures of some Cl^- channel blockers.

inhibitory potency. This led to the discovery of very potent blockers such as 5-nitro-2-(3-phenylpropylamino)-benzoate with an IC_{50} of 8×10^{-8} M.

1.8 Intracellular Cl^- channels

It is known that Cl^- channels are found in intracellular membranes including the outer nuclear membrane (Tabares, 1991), mitochondrial membranes (Colombini, 1994) and the sarcoplasmic (Smith *et al.*, 1985a, b, Rousseau *et al.*, 1988, Tanifuji *et al.*, 1987) and endoplasmic reticulum (Ashley, 1989, Schmid *et al.*, 1988). The ER of non-contractile tissues such as the brain is similar to the SR and plays an important role in Ca^{2+}-signalling (Berridge, 1993). Compared with the Cl^- channels found in plasma membranes, intracellular channels have been very poorly characterised. One of the few intracellular Cl^- channels to be characterised is p64, a putative Cl^- channel from bovine kidney cortex although it remains to be seen whether it is indeed functioning as a Cl^- channel or merely as a Cl^- channel regulator. Some of the putative functions for intracellular Cl^- channels include charge compensation, organelle volume regulation and electrical shunting for acidification of cellular compartments.

1.8.1 Co-localisation of Cl^- channels with Ca^{2+}-release channels

The specialised sarcoplasmic reticulum (SR) accumulates, stores and releases Ca^{2+} to initiate muscle contraction. Work has traditionally been focussed on SR although interest is rapidly growing in the ER. It is the major intracellular structure involved in the uptake and release of Ca^{2+} and contains Ca^{2+}-release channels including the ryanodine receptor. It was first shown in SR of skeletal muscle using

planar lipid bilayers that Cl^- channels were co-localised with intracellular ryanodine-sensitive Ca^{2+}-release channels (Smith *et al.*, 1985a). These co-localisation experiments were later repeated in brain by incorporating rat cerebral cortex microsomal membrane vesicles into planar lipid bilayers (Ashley, 1989). This showed that Ca^{2+}-release channels were also co-localised with Cl^- channels in brain ER and a Poisson analysis supported the idea that brain microsomes were effectively channel "packets" containing approximately equal numbers of Ca^{2+} and Cl^- channels. Cl^- channels were also shown to be present in isolated membrane vesicles (Bégault *et al.*, 1993) and in ER-associated membranes from brain (Pozzan *et al.*, 1994). While SR Cl^- channels have been studied in reasonable detail, ER Cl^- channels have been very poorly studied.

1.8.2 Putative roles of intracellular Cl^- channels

In lysosomes, golgi and endosomes the intracellular Cl^- channels regulate the intraorganelle pH (Glickman *et al.,* 1983). This is achieved by shunting the electrogenic membrane potential produced by the H^+-ATPase to allow acidification of intracellular compartments. The role of Cl^- channels in the ER may be to function as charge compensators to modulate Ca^{2+} release *in vivo.* Charge compensation has been hypothesised to maintain electroneutrality after Ca^{2+}-release from intracellular stores (Palade *et al.*, 1989, Kemmer *et al.*,1987, Bayerdörffer *et al.*, 1984). The mechanism implicitly assumes that the ER membrane is polarised. There is some evidence that the ER may develop a transmembrane potential, as some channels found in the SR and ER show voltage-dependent gating (Martin & Ashley, 1993 and Schmid *et al.*, 1990).

This suggests that the ER membrane or subdomains may be "excitable" (subject to repolarisation and depolarisation).

It is important for intracellular organelles like the ER to maintain a consistent volume and Cl^- channels play an important role (Zizi *et al.*, 1991). Cl^- channels depolarise the cell membrane which leads to a regulatory volume decrease. By analogy it is possible that outwardly rectifying chloride currents may also be mediated by Cl^- channels in the ER membrane.

Chapter 2

Materials & Methods

2.1 Materials

Chemicals of the highest purity available were obtained from Sigma-Aldrich Chemical Co. Ltd., Poole, Dorset, U.K. unless otherwise stated.

2.1.1 Brain tissue

Forebrains were obtained from Sprague-Dawley rats supplied by MFAA, Edinburgh, and sheep material was obtained from Edinburgh Meat Markets, Slateford Road abbatoir.

2.1.2 Planar lipid bilayers

POPE and POPS lipids were obtained from Avanti lipids, Alabaster, Alabama, U.S.A and n-decane from Aldrich Chemical Co. Ltd., Dorset, UK. The lipids were shipped as powders on dry ice, and kept in unopened O_2-free vials for up to 3 months before use at -70°C. Primary stock solutions of POPE and POPS were prepared in $CHCl_3$ (50 mg/ml). These were pulsed with a stream of N_2 before storing at -70°C.

2.1.3 Liposome preparations

PE, PC, PS, and cholesterol were obtained from Avanti lipids, Alabaster, Alabama, USA. $^{36}Cl^-$ from ICN Radiochemicals, Thame, Oxfordshire, UK and [^{3}H]-inulin was from Amersham Life Science, Little Chalfont, Buckinghamshire,UK.

2.1.4 Blockers

NPPB was a kind gift from Dr. Rainer Greger, Freiburg, Germany and DPC was a kind gift from Dr. Malcolm Wright, Edinburgh, UK. IAA-94 was obtained from Alexis Corporation (UK) Ltd., Bingham, Nottingham, UK and niflumic acid from ICN Biomedicals, Inc., Aurora, Ohio, USA.

2.1.5 Purification

The DE52 column was obtained from Whatman Chemical Separation Ltd., Wirral, Merseyside, UK and Spectra/por dialysis tubing was from Spectrum Medical Industries, Inc., Los Angeles, California, USA.

2.1.6 Other chemicals

AEBSF was obtained from Calbiochem-Novabiochem (UK) Ltd., Beeston, Nottingham, UK and Ultima Gold MV scintillation liquid was from Packard Instrument B.V.-Chemical Operations, Groningen, The Netherlands. Acrylamide/bis solution (40%) w/v 39:1 was obtained from Bio-Rad, Hercules, California, USA.

2.2 Methods

2.2.1 Isolation of membrane vesicles

Microsomal membrane vesicles were obtained from rat cerebral cortex as previously described (Ashley, 1989). Briefly, cerebral cortices from adult male and female Sprague-Dawley rats were rapidly dissected on ice in a petri dish, chopped into

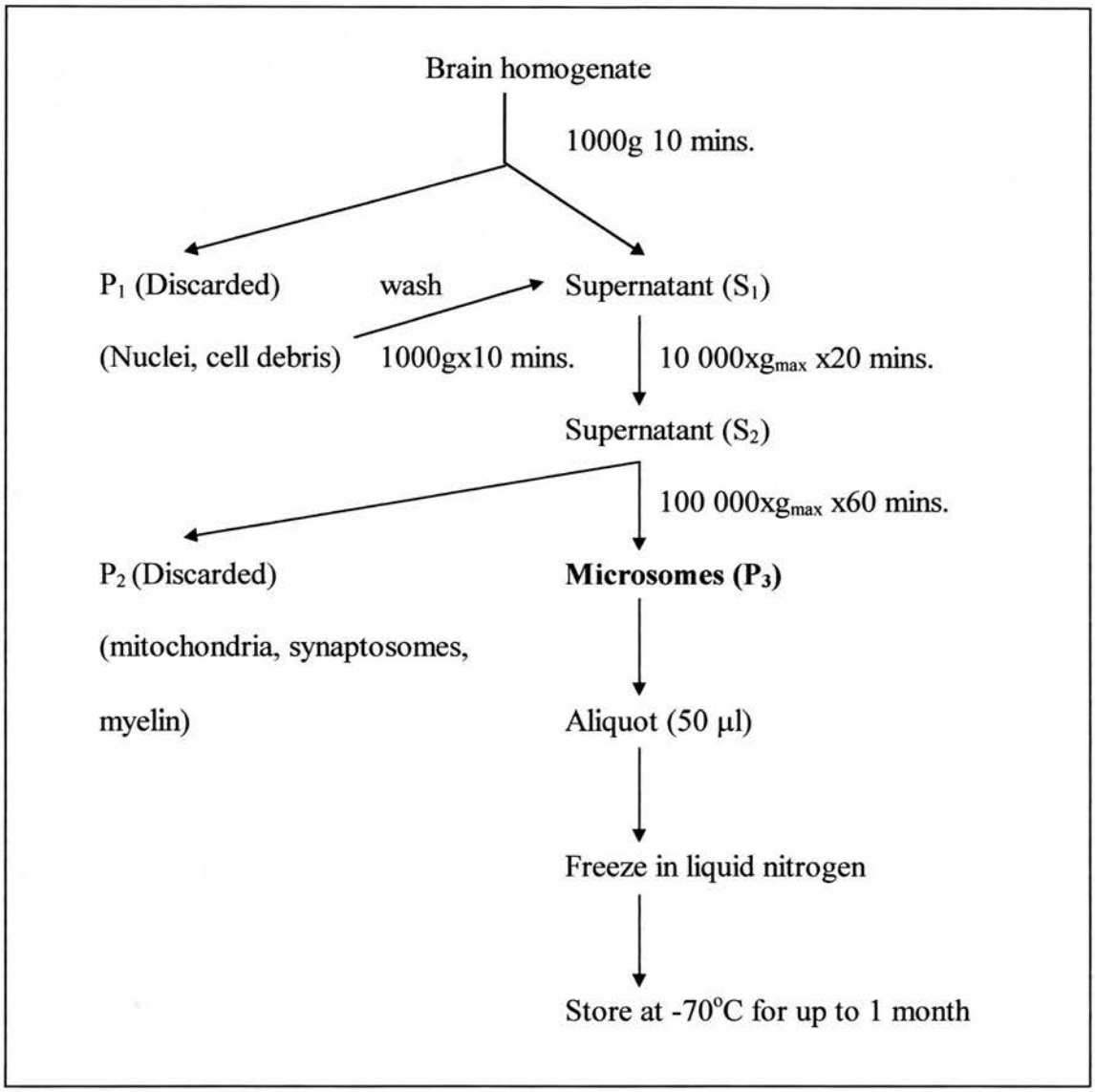

Figure 2.1. Preparation of brain microsomes by differential centrifugation.

1-2 mm cubes, and suspended in ice-cold 0.32 M sucrose, 5 mM Tris-HCl (pH 7.4) containing antiproteases (0.2 mM AEBSF, 10 μg/ml soybean trypsin inhibitor, 150 μg/ml benzamidine, 1 μg/ml leupeptin, 0.5 μg/ml pepstatin A and 0.5 μg/ml aprotinin) without added Ca^{2+}. This prevented the action of Ca^{2+} dependent proteases such as the calpains. HEPES buffer was excluded from all solution preparations as it was known to block other anion channels (Yamamoto & Suzuki, 1987 and Hanrahan & Tabcharani, 1990). Whilst dissecting the forebrains, brain myelin (white matter) was removed as far as possible while leaving the cerebral hemispheres intact. The tissue was rinsed in 9 volumes of 0.32 M sucrose 5 mM Tris-HCl with antiproteases (pH 7.4) before homogenising with 12 up and down strokes in a teflon glass homogeniser at 800 rpm, cooling mid-way on ice. The sheep cerebral cortex was prepared in a similar way and was stripped of meninges before chopping into 5-10 mm cubes and suspending in ice-cold 0.32 M sucrose, 5 mM Tris-HCl with antiproteases (pH 7.4). In this case the tissue was homogenised using an 'Ultra-Turrax TP 18-10' homogeniser avoiding frothing. The rat and sheep brain homogenate then underwent a classical differential centrifugation to yield the final microsomal membrane fraction which was resuspended in 0.32 M sucrose. The brain microsomes were snap frozen immediately in liquid N_2 in 50 μl aliquots containing 10-20 mg protein per ml and stored at -70° C for up to 1 month (Figure 2.1).

2.2.2 Planar lipid bilayers

The lipid for planar bilayers consisted of a 50 % decane suspension of

palmitoyl-oleoyl phosphatidylethanolamine (POPE) and palmitoyl-oleoyl phosphatidylserine (POPS) (each 15 mg/ml). The bilayers were cast at room temperature from lipid suspension prepared fresh daily from -70°C chloroform stock solutions. A plastic stick with a small amount of lipid (~1 μl) was drawn across a 300 μm hole in a polystyrene partition separating two solution-filled chambers (600 μl) which were designated *cis* and *trans*. Bilayers formed spontaneously as observed optically, using a low-power (x 20) microscope, and electronically, by monitoring the increase in membrane capacitance which accompanied thinning. The bilayer capacitance was measured using a triangle waveform pulse of 100 Hz at 100 mV. The current amplitude is proportional to the membrane capacitance which can be measured using an AC voltmeter. Membranes were discarded unless their capacitance reached at least 250-300 pF and they remained electrically stable for 10-15 mins, with a background conductance below 5 pS.

The planar lipid bilayer system was constructed by Mr Richard Montgomery, National Heart and Lung Institute, London, UK. The electronics consisted of a standard resistor-feedback (10 GOhm) high-impedence current amplifier, connected to the *cis* and *trans* chambers with Ag/AgCl electrodes and 2% (w/v) agar bridges containing 3 M KCl. The *cis* chamber was voltage-clamped relative to the *trans* chamber, which was grounded (Figure 2.2). The standard electrophysiological conventions for current and voltage were adopted and membrane potentials were defined as the cytoplasmic minus ER luminal potential, with positive "outward" (cytoplasm to ER lumen) currents shown as "upgoing" traces. This is consistent when

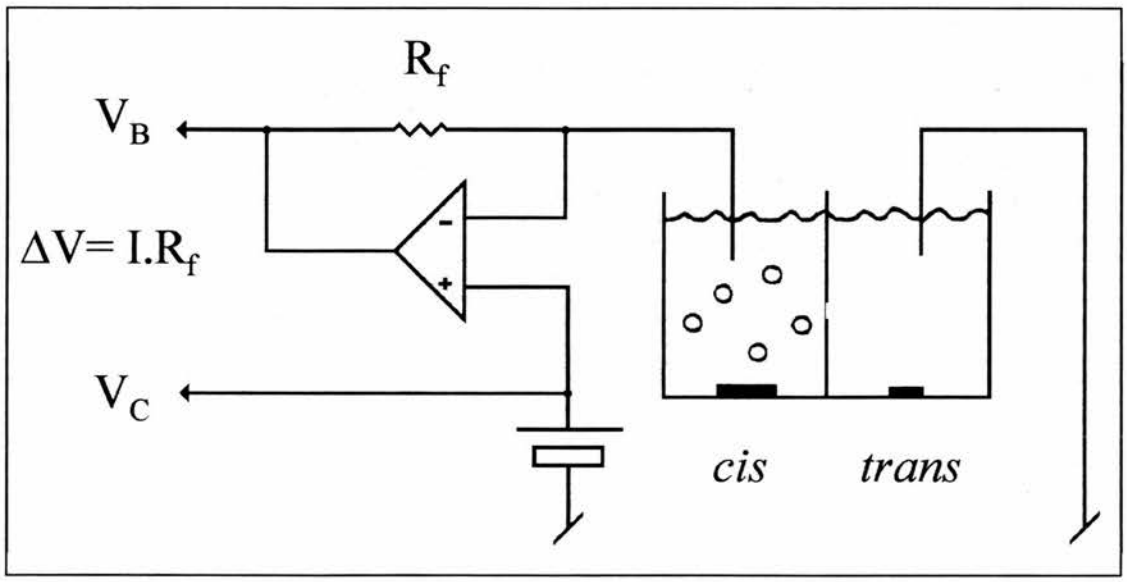

Figure 2.2 The planar lipid bilayer system.
The *cis* chamber is voltage clamped (V_C) relative to the *trans* chamber which is held at actual ground, using an opamp configured as a current to voltage converter. When ion channels are incorporated, the opamp keeps the inverting (-) and non-inverting (+) inputs the same by adjusting the backoff potential (V_B) across the feedback resistor (R_f). The ion channel currents are given $-[V_B - V_C / R_f]$. (Adapted from Ashley, 1995).

right-side out vesicles fuse with the bilayer. The ion channel currents were digitised, low-pass filtered at 10 kHz (-3 dB point, Bessel-type response), and recorded on videotape using a modified audio processor. Similar procedures, and typical apparatus, have been described in detail by Alvarez (1986), Labarca & Lattorre (1992) and Williams (1995).

The bilayers were initially bathed in 50 mM Choline Cl containing 5 mM Tris-HCl (pH 7.4) and 2 mM $CaCl_2$. Microsomal membrane vesicles (final concentration 5-10 μg protein per ml) were added to the *cis* chamber, and a *cis>trans* osmotic gradient was established to encourage fusion of vesicles with the bilayer (Figure 2.2). Fusion normally occurred between 15-30 minutes and often led to the incorporation of multiple channels. The protein concentration was titrated in subsequent additions to obtain single channels. After the fusion of single channels the contents of the *cis* chamber was perfused with 10 volumes of solution to remove unfused vesicles in order to prevent further channel incorporation. Salt concentrations in each chamber were adjusted with the addition of small aliquots (up to 40 μl) of concentrated 3 M stock solutions and drugs and other compounds were added directly to the required chamber from DMSO or ethanol stocks kept at -20° C. The carrier solvents had no effect on bilayers at the concentrations used. Typical experiments normally lasted up to 20 minutes, and were terminated with bilayer breakage or spontaneous channel inactivation.

2.2.3 Partial purification of sheep brain microsomal anion channel

Sheep brain P_3 (Figure 2.2) was added to solubilisation buffer (20 mM Tris-HCl, 1.5% (w/v) CHAPS, 1 mM EDTA, 0.2 mM AEBSF 150 μg/ml benzamidine, 1 μg/ml leupeptin, 0.5 μg/ml pepstatin A and 0.5 μg/ml aprotinin, pH 7.6) to give an optimal protein concentration for solubilisation of 2-2.5 mg/ml. This was incubated at 4 °C with slow stirring for 90 minutes before spinning at 100,000g for 55 minutes. The solubilisate was concentrated to ~10 ml (Amicon Ultrafiltration Cell) and then loaded onto a DE52 anion-exchange column. This was run overnight at a flow-rate of 1 ml/min with a salt gradient of 0 to 600 mM KCl, and fractions were collected with a 'LKB 2211 superrac' fraction collector. The absorbance at 280 nm was plotted against fraction number to show the elution profile and the efflux assay described later (section 2.2.4) was used to identify Cl^- transporting activity. These fractions were pooled and concentrated to ~ 4 ml before loading onto a Sephadex G150 column and running overnight at a flow-rate of 0.5 ml/min. Fractions containing maximal Cl^- transport activity were again identified and pooled. Lectin affinity chromotography has previously been used to purify a SR Cl^- channel (Ide *et al.,* 1991), and it has been shown that p64, a putative intracellular Cl^- channel, possesses two consensus glycosylation sites. Therefore Concanavalin A (ConA), a lectin from *Canavalia ensiformis*, was used in a further stage of purification. A Con A-sepharose B column was pre-equilibrated with washing buffer containing 1 mM each of Mg^{2+} and Ca^{2+} (Cl salts) and incubated for 60 minutes with very gentle mixing. These divalent cations were required for binding of the Con A to sugar residues. Bound protein was eluted

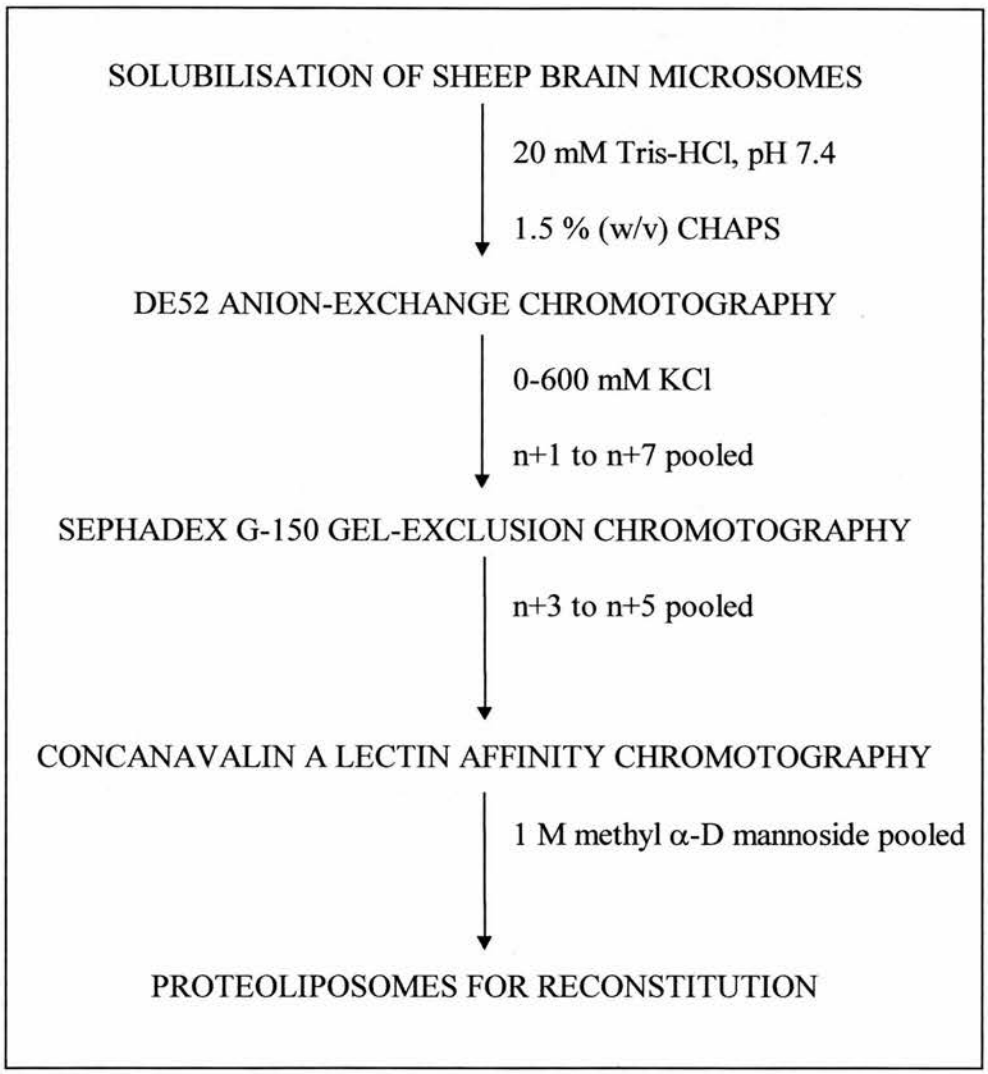

Figure 2.3 Partial purification protocol for sheep brain anion channel.

after treatment with 0.2 M and 1 M methyl α-D mannoside. The 0.2 and 1 M methyl α-D mannoside fractions were dialysed overnight with Spectra/por molecular porous membrane tubing, molecular weight cut-off 12-14 000, to remove the sugar before reconstituting proteoliposomes (Figure 2.3).

2.2.4 Preparation of liposomes and proteoliposomes for efflux assay

Liposomes were formed from a mixture of phosphatidylethanolamine (PE), phosphatidylserine (PS), cholesterol and phosphatidylcholine (PC) in the ratio 5:2:2:1 (each 20 mg/ml). Lipids were dried under a stream of nitrogen from $CHCl_3$ stocks and resuspended in 20 mM Tris-HCl, pH 7.4. After vortexing for 5 minutes the lipid suspension was probe sonicated on ice (Sanyo Soniprep 150) to form liposomes.

Proteoliposomes were formed by mixing an equal volume of liposomes (50 µl) and solubilisate (50 µl) and passing it through 1 ml Sephadex G-50C columns by spinning at 800 rpm. The proteoliposomes formed as the CHAPS was removed. ^{36}Cl (1 µCi) and [^{3}H]-inulin (1 µCi) were added at this stage and the proteoliposomes were snap frozen in liquid nitrogen and stored at -70 °C to preserve the activity of the reconstituted protein for up to 2 weeks.

2.2.5 Efflux Assay

The Cl^- transporting fractions were identified from DE52, Sephadex G-150 & Concanavalin A columns using a $^{36}Cl^-$ efflux assay. The efflux assay is essentially a "trapped volume ratio" assay where the [^{3}H]-inulin trapped volume remains relatively

high but the $^{36}Cl^-$ trapped volume decreases as Cl^- leaks out. The ratio of $^{36}Cl^-/[^3H]$-inulin will correpondingly decrease. The proteoliposomes containing entrapped $^{36}Cl^-$ and $[^3H]$-inulin were thawed and sonicated for 10 seconds using a probe sonicator (Sanyo Soniprep 150) to complete the freeze-thaw-sonication cycle. $^{36}Cl^-$ efflux was initiated by diluting the proteoliposomes 10-fold in 20 mM Tris-HCl, pH 7.4 and then at timed intervals passing 100 µl through 1 ml Sephadex G-50C columns at 800 rpm to remove external $^{36}Cl^-$. The pooled samples, together with relevant controls, were then scintillation counted.

2.2.6 Scintillation counting of ^{36}Cl and $[^3H]$-inulin

"Ultima Gold MV" scintillation fluid (2 ml) was added to 100 µl samples obtained from the efflux assay. This included duplicate samples for direct counting of $^{36}Cl^-$ and $[^3H]$-inulin and duplicate samples for the column fractions. These were then counted using a Packard 1900CA liquid scintillation analyser. The $[^3H]$-inulin counts were adjusted for a 5-7 % $^{36}Cl^-$ crossover.

2.2.7 SDS-polyacrylamide gel electrophoresis

Glass plates were cleaned with detergent, distilled water and methanol and then assembled in a Hoefer "SE 250 Mighty Small II" gel apparatus using 1 % (w/v) agarose as a sealing gel. A 10% separating gel (10 ml) was prepared with distilled water (3.43 ml), 40 % (w/v) acrylamide/bis solution 29:1 (2.5 ml), 10% (w/v) SDS (0.1 ml), 1 M Tris-HCl, pH 8.8 (3.76 ml), 25 mg/ml ammonium persulphate (0.2 ml)

and TEMED (10 µl). This was poured between the plates filling up to 1 cm below the comb. A small amount of butanol was added to give a level gel edge. The exclusion of oxygen aided polymerisation by preventing the generation of free radicals by ammonium persulphate and encouraging cross-linking. The excess butanol was poured off when the gel had set and a 3.5 % stacking gel (5 ml) was prepared with distilled water (3.163 ml), 40% (w/v) acrylamide/bis solution 29:1 (0.438 ml), 0.5M Tris-HCl, pH 8.8 (1.25 ml), 10% (w/v) SDS (50 µl), 10% ammonium persulphate (0.1 ml) and TEMED (5 µl). While the stacking gel was polymerising samples were denatured by heating to 100 °C for ~5 minutes in gel loading buffer consisting of 50 mM Tris-HCl (pH 6.8), 100 mM dithiothreitol, 2% (w/v) SDS, 0.1% (w/v) bromophenol blue, 10% (v/v) glycerol. Once the stacking gel had set, the comb was removed and the gel and reservoirs were filled with running buffer which consisted of 25 mM Tris-HCl/ 250 mM glycine (pH 8.3) and 0.1% (w/v) SDS. The samples (up to 50 µl) were loaded into the wells and a current of 60 mA was applied until the dye front had migrated through the stacking gel. Once in the separating gel the current was increased to 90 mA for ~2 hours.

2.2.8 Coomassie staining

The mini-gel apparatus was disassembled and the the gel was placed in a glass tray with 0.25 % (w/v) coomassie stain (~20 ml) which contained coomassie blue R-250 (0.625 g), 40% (v/v) methanol (100 ml), acetic acid (17.5 ml), in distilled (250 ml). Gels were stained for 1 hour and then destained overnight. The destain (~20 ml)

consisted of 40% (v/v) methanol (70 ml), acetic acid (50 ml), and distilled water to 1000 ml.

2.2.9 Analyses of single channel records

Cl^- channel currents were identified as "single-channel" when there was a single main open-state or "unit" current usually at negative holding potentials, where Po was high (~0.7). The channel recordings were displayed using Axotape 2 and analysed using the pClamp 6 suite of programs (Axon Instruments). In-house programs were used for other analyses including the binomial analysis of substate behaviour. The overall resolution of the current recordings was set by the background noise of the bilayer membrane, rather than by noise from the electronics as expected. The rise-time of the current amplifier was <200 μs, and the electrical noise was typically up to 1.5 pA peak-to-peak at 0.25 kHz (low-pass -3 dB Bessel), rising to ~8 pA at 1 kHz. Single-channel currents were post-filtered at 0.05-0.25 kHz (-3 dB, 8 pole Bessel or digital Gaussian filter). The exact filter values depended on the analysis being carried out, and the precise conditions are given for each experiment. For channel lifetime analysis, a semi-empirical iterative approach to determine the minimum cut-off frequency, as the extent of low-pass filtering is crucial. This low-pass filtering effectively eliminated high frequency bilayer noise and the bilayers also had good baseline current stability compared to many patch-clamp experiments. The -3 dB point for each bilayer recording was set as high as possible, using control recordings to ensure that "false-openings" to the lowest amplitude level of the channel

would not be detected. This lowest channel amplitude was observed in a Cl^- channel containing bilayer. The shortest event durations that could be accurately measured have a rise-time of $0.33/f_c$, where f_c is the -3 dB point in kHz (Colquhoun & Sigworth, 1983). For example, a cut-off frequency of 0.15 kHz would allow event durations of no less than 2.2 ms to be measured. Switches in voltage-clamp potential also gave rise to bilayer capacitative transients (lasting up to 5 s), but since the recordings were essentially at equilibrium no effort was made to cancel these out.

The Goldman-Hodgkin-Katz (GHK) voltage equation was used to measure relative ionic permeabilities and in biionic conditions the monovalent anion permeabilities were measured using the relationship:-

$$P_X/P_Y = [X]/[Y].\exp(-zFE_r/RT)$$

where P_X/P_Y, the relative permeabilities of anions X and Y in the *cis* and *trans* chambers, were related to the reversal potential, E_r. R is the gas constant, T is the absolute temperature and F is Faraday's constant and z is the valency. In a single salt, relative anion-cation permeabilities, P_{anion}/P_{cation}, were calculated from:-

$$P_{anion}/P_{cation} = [n-\exp(E_r/k)]/[n.\exp(E_r/k)]$$

Where n represents the *cis:trans* salt concentration ratio and k = RT/F (26 mV at room temperature). It is stated whether concentrations have been corrected to ionic

activities.

The probability for channel "protomers" (total number = N) being open, $Po_{(Protomer)}$ or p was calculated when carrying out the binomial analysis. Channel data were fitted to a binomial model where the proportion of time (Pi) spent in each state or conductance level, i = 0, 1,....N, was given by:-

$$Pi = \{N!/[i!(N-i)!]\}.\ p^{i}(1-p)^{N-i} \qquad I = 0,1,....N$$

Binomial statistics should apply whenever there are mutually exclusive, independent outcomes and the probability of the outcomes are equal e.g. independent and mutually exclusive gating of individual protomers. Data were fitted by maximising the likelihood of E(Fi)ln(Pi), where Fi was the relative proportion of time in level i (Hayman & Ashley, 1993). For channels in which protomer openings correspond to a binomial distribution, $Po_{(Protomer)}$ is given analytically by:-

$$Po_{(Protomer)} = 1/N.EPi(n)$$

In this case Pi(n) is the proportion of events at level n or higher, and n is at least the first substate (protomer) level. A similar algorithm is used within pClamp6.

Chapter 3

Reconstitution and single channel properties of a rat brain ER anion channel

3. Reconstitution and single channel properties of a rat brain ER anion channel

In non-contractile cells the ER has been shown to be the main calcium storage organelle involved in calcium regulation (Meldolesi *et al.*, 1990). The SR of muscle cells contains at least three types of ion channels including Ca^{2+}-release channels, K^+ channels and Cl^- channels. Brain microsomes were fused with planar lipid bilayers to investigate whether the ER contains similar channels compared to the more specialised SR from muscle. Single channels were reconstituted from brain ER, and these included ryanodine-sensitive Ca^{2+}-release channels, calcium-activated K^+ channels and Cl^- channels. Attention was focussed on the Cl^- channel, as intracellular anion channels have been very poorly characterised. It has been shown in SR that Cl^- channels are co-localised with Ca^{2+}-release channels (Smith *et al.*, 1985) and the same occurs in ER (Ashley, 1989). Physiologically, these channels may have an important function as "charge compensators" during Ca^{2+} uptake and release in the ER system.

3.1 Characterisation of the microsomal membrane fraction

Ion channels present in rat brain microsomes were identified by fusing membrane vesicles with voltage-clamped planar lipid bilayers (Figure 2.2). The fusion process was promoted by the addition of 2 mM Ca^{2+} to the *cis* chamber (side of vesicle addition), stirring, and the presence of negatively-charged lipids in the bilayer. Fusion normally took place between 15-30 mins after the addition of vesicles and was never observed in the absence of gradient or Ca^{2+}. The microsomal protein concentration was important and if it was too high it resulted in multiple channels

whereas if it was too low then no fusions took place. Therefore addition of vesicles were titrated to give rise to single anion channels. Although the process of fusion is poorly understood, it is believed that a pre-fusion bridge occurs between Ca^{2+} and POPS to bring the channel-containing vesicles into close proximity with the bilayer. An osmotic gradient established on the side of vesicle addition drives the swelling of the pre-attached vesicles to reconstitute the channels. The brain ER microsomal vesicles may be "inside-out" or "outside out". It has been previously shown during co-localisation experiments with the ryanodine-sensitive Ca^{2+}-release channel that in almost all cases the vesicles which fuse with the bilayer are in the "outside out" configuration (Ashley, 1989). That is, the adenine nucleotide sensitivity of the incorporated ryanodine-sensitive Ca^{2+}-release channel faces the *cis* chamber.

Calcium-activated K^+ channels could be readily incorporated in the presence of KCl . These channels were silent in Choline Cl as it is a quaternary ammonium compound which blocks K^+ channels. The presence of these channels suggests either contamination by plasma membranes or that the ER contains maxi-K^+ channels. Fusion of the microsomes also led to the incorporation of ryanodine-sensitive Ca^{2+}-release channels, and to the incorporation of Cl^- channels displaying subconductance states.

Typical traces at a range of holding potentials are shown for a calcium-activated K^+ channel in 250/50 KCl *cis/trans* before and after the addition of 2 mM K_2EGTA(Figure 3.1.1) which did not affect the pH. The free [Ca^{2+}] was calculated after the addition of EGTA using an apparent K_D of 0.15 μM and was found to be 300 nM. A ryanodine-sensitive Ca^{2+}-release channel was shown in symmetric 50/50

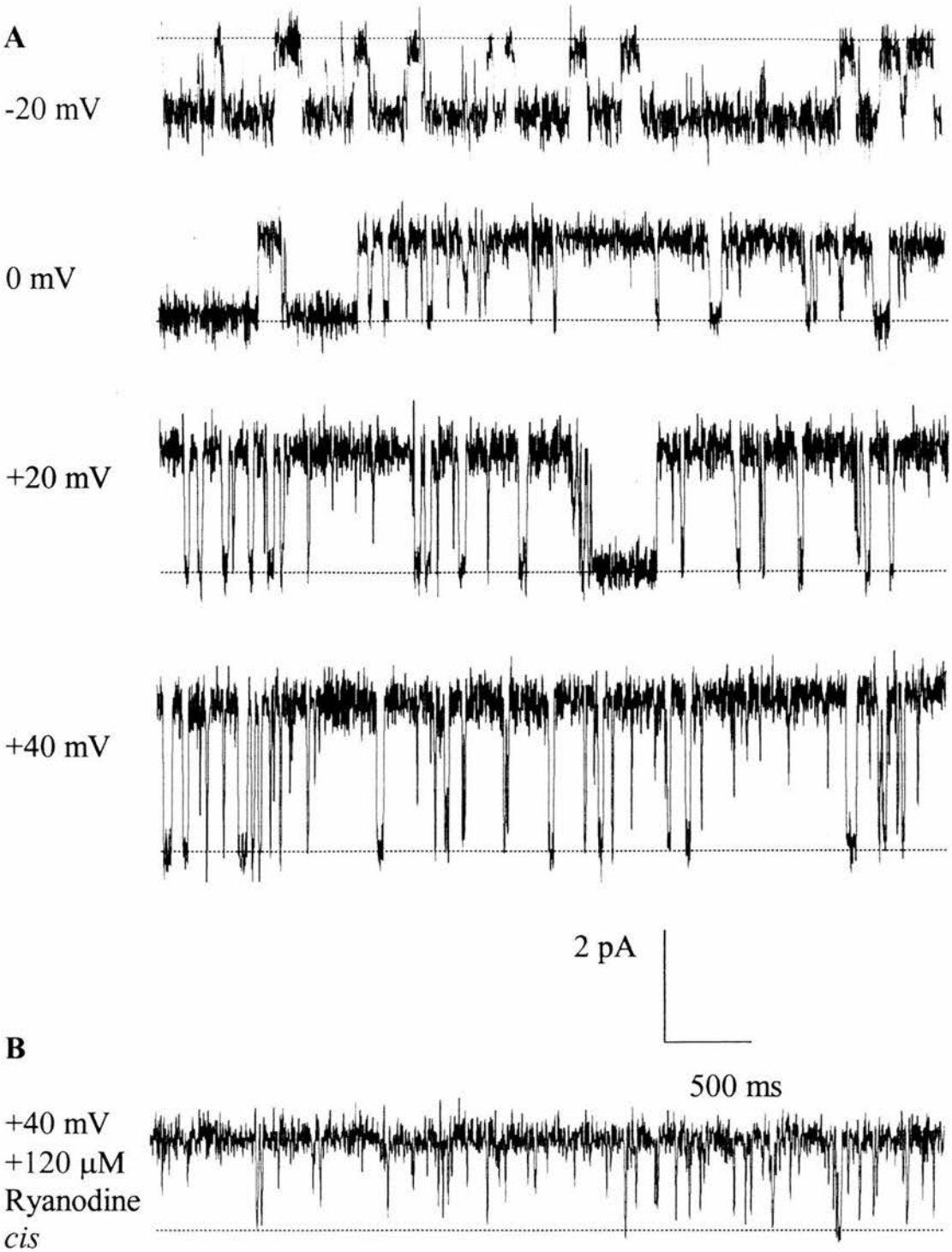

Figure 3.1.1 Ryanodine-sensitive Ca^{2+}-release channel reconstituted from rat brain microsomes. Single channel currents shown in symmetric 50 mM Choline Cl, 5 mM Tris-HCl, pH 7.4 with 100 mM KCl *cis*: 0 mM KCl *trans*. Potentials are *cis-trans* (cytoplasm-ER lumen) and positive currents are shown going upwards. Panel A shows the channel at a range of holding potentials after the addition of 1 mM MgATP and Panel B at -40 mV after the addition of 120 μM Ryanodine. The closed, non-conducting levels are indicated (...). Low-pass filtered at 0.15 kHz.

ChCl with 100/0 KCl (Figure 3.1.2) and was shown to be blocked to a 40 % substate (Ashley, 1989) on addition of 120 μM ryanodine. The conductance of the channel was 35 pS which is less than normally expected but is probably due to $Choline^{+}$ block. The intermediate-conductance rat brain Cl^{-} channel co-localised with the ER Ca^{2+} release channel (Ashley, 1989) was investigated and forms the subject of this thesis.

3.2 Conductance and gating behaviour of the rat brain ER anion channel

Ion conduction was mostly examined in symmetric Choline Cl (Figure 3.2.1) but also shown in symmetric KCl (Figure 3.2.2) and symmetric Tris-HCl (Figure 3.2.3). The current /voltage (I/V) relationship for the different salts are shown in Figure 3.2.4. The single-channel conductances in Choline Cl, KCl and Tris-HCl were 82 pS, 85 pS, and 73 pS, respectively, and the main open state and substate slope conductances were linear and showed no rectification over the voltage range examined (Figure 3.2.5). Channel gating was voltage-dependent, with openings in bursts, with greater activity at negative (cytoplasm-lumen) than positive holding potentials. At negative potentials the channel resided in higher-conductance substate levels, and the main open state. At positive potentials the channel had long interburst levels, with the channel residing in lower substates and very rarely in the main open state.

The conductance-concentration relationship for the main open state was examined as a function of the concentration of Choline Cl (Figure 3.2.5). The data are fitted by non-linear least squares analysis to a Michaelis-Menten model, $g = [S]/(Km + [S])$. g_{max}, where g is the single-channel conductance (and g_{max} is the maximal

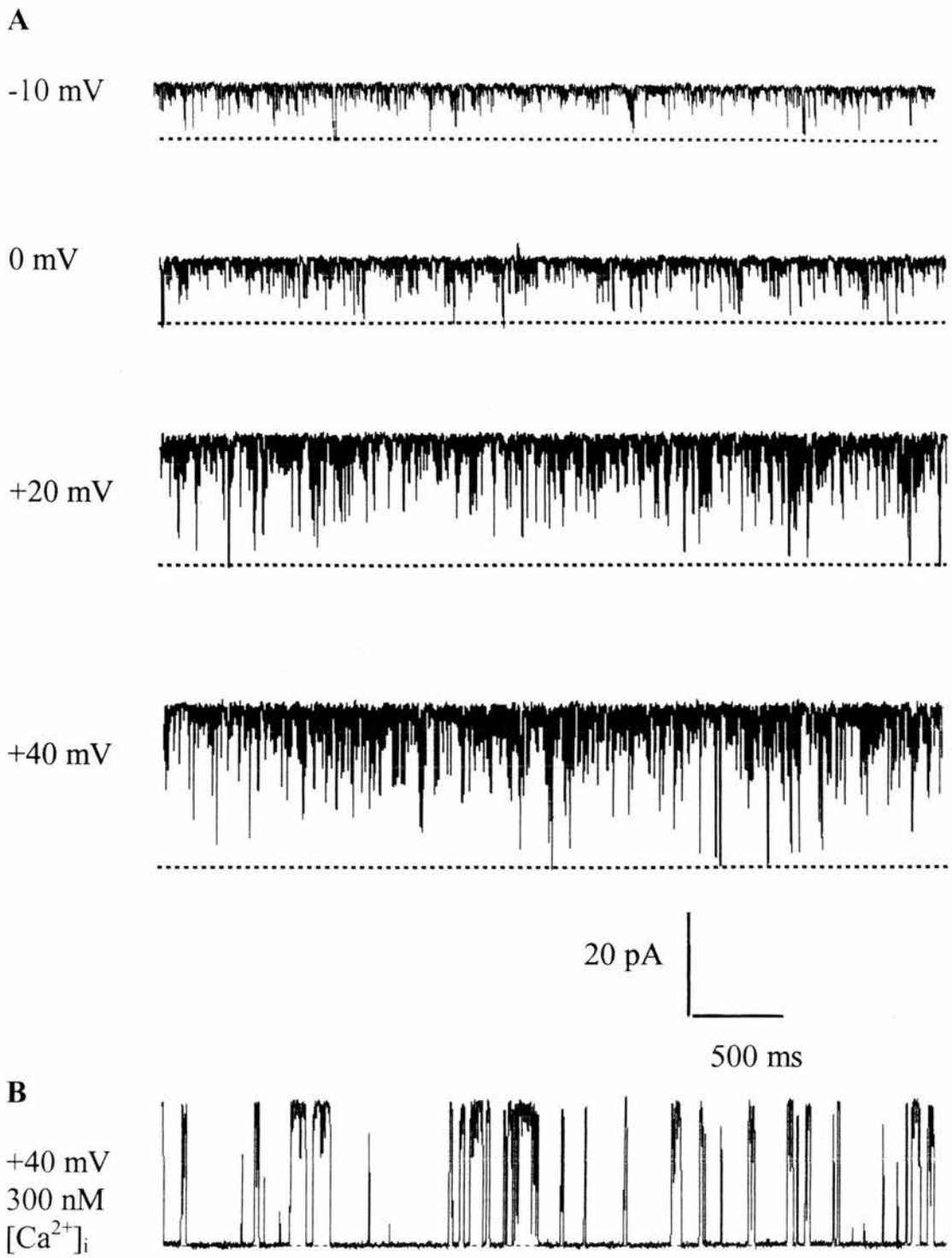

Figure 3.1.2 Calcium-activated K^+ channel reconstituted from rat brain microsomes. Panel A shows a single channel at a range of holding potentials in asymmetric 250 mM:50 mM *cis/trans* KCl, 5 mM Tris-HCl, pH 7.4, $[Ca^{2+}]$ = 2 mM. Panel B shows the channel at +40 mV after the addition of 2 mM KEGTA, $[Ca^{2+}]_i$ = 300 nM . The closed levels are indicated (...). Low-pass filtered at 0.15 kHz.

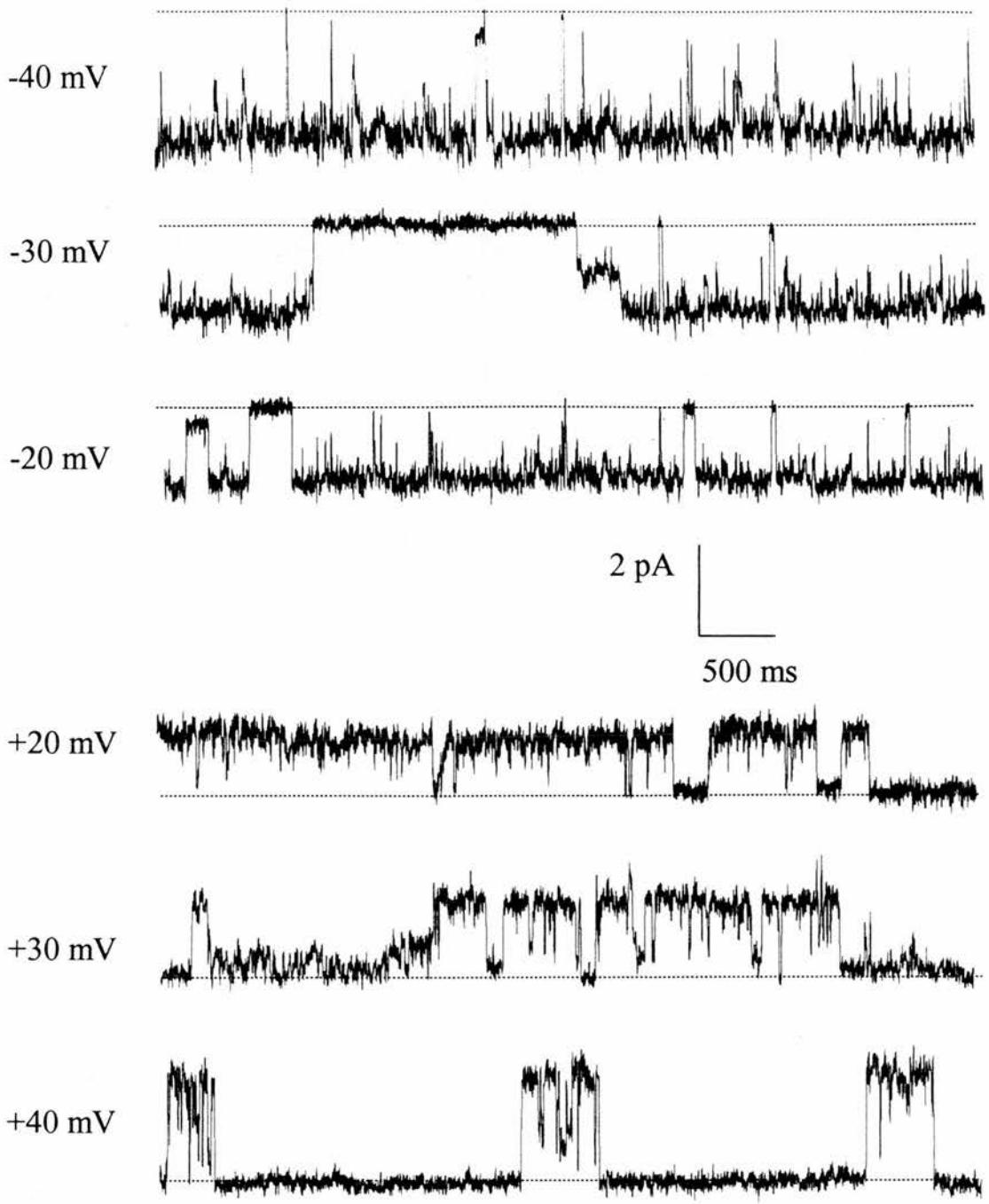

Figure 3.2.1 Single-channel recording of the rat brain ER anion channel in symmetric 250 mM ChCl. The conductance behaviour of a single anion channel is shown at a range of holding potentials in symmetric 250 mM Choline Cl, 5 mM Tris-HCl, pH 7.4. The closed levels are indicated (...). Low-pass filtered at 0.15 kHz.

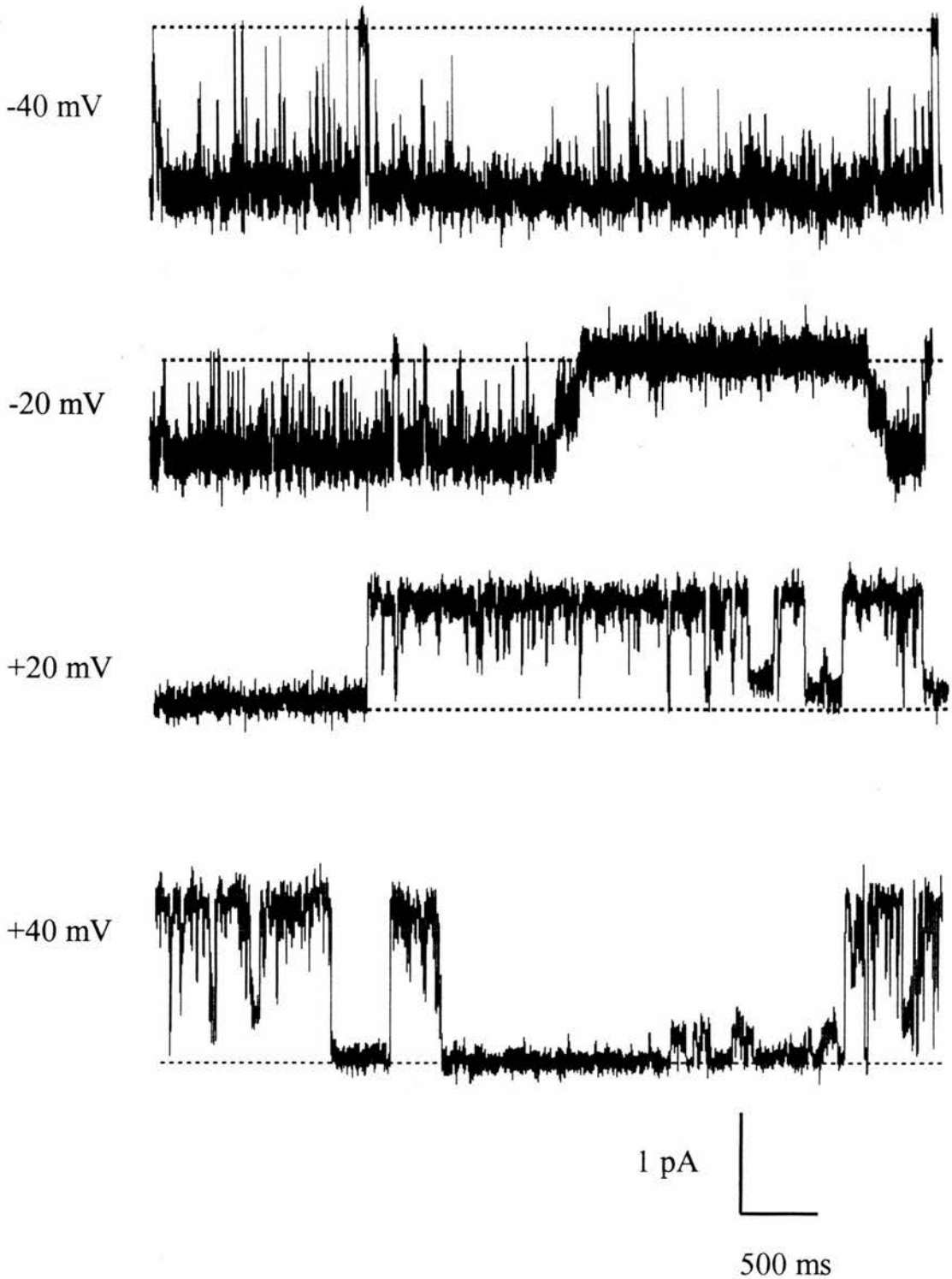

Figure 3.2.2 Single-channel recording of the rat brain ER anion channel in symmetric 250 mM KCl. The conductance behaviour of a single anion channel is shown at a range of holding potentials in symmetric 250 mM KCl, 5 mM Tris-HCl, pH 7.4. The closed levels are indicated (...). Low-pass filtered at 0.15 kHz.

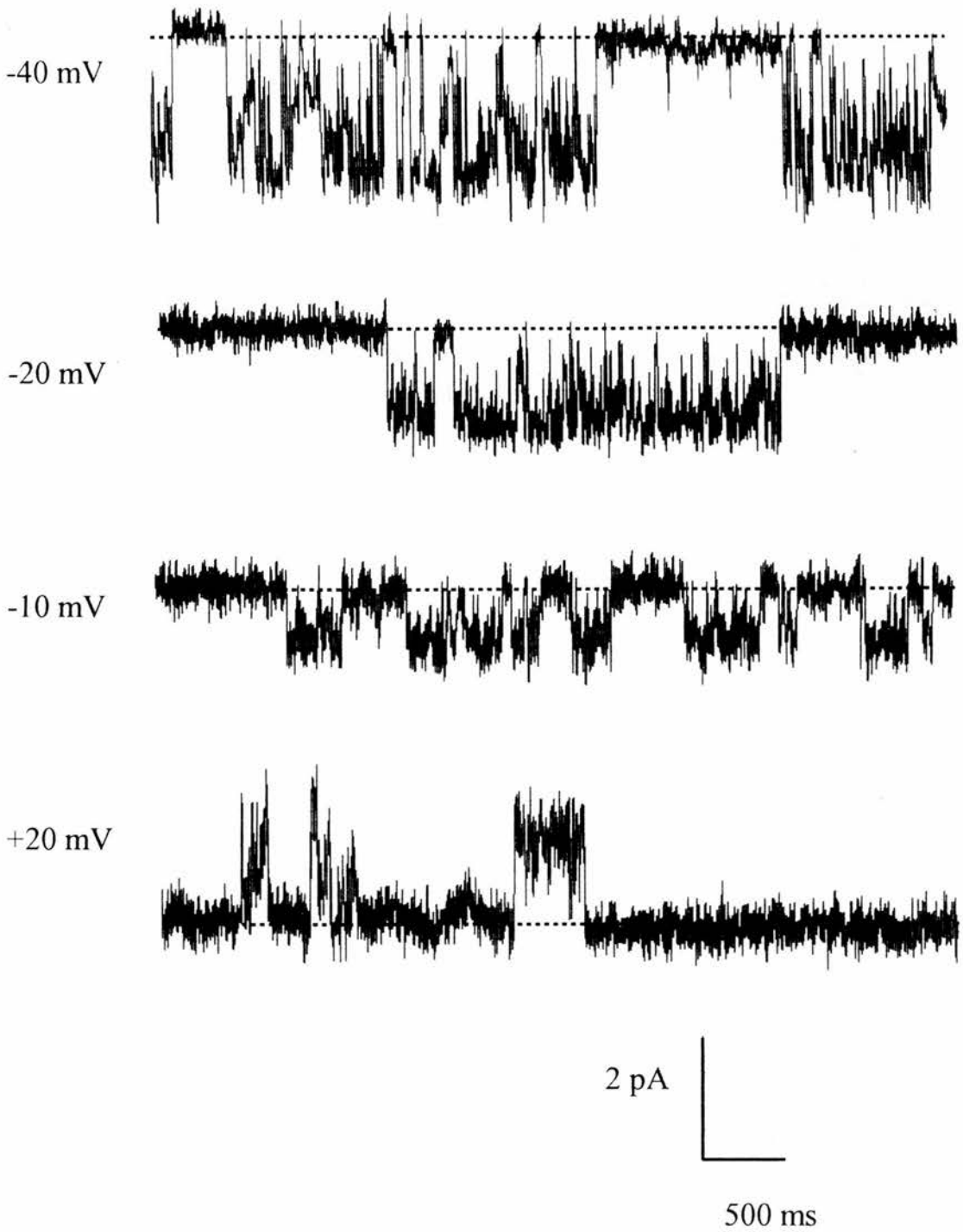

Figure 3.2.3 Single-channel recording of the rat brain ER anion channel in symmetric Tris-HCl. The conductance behaviour of a single anion channel is shown at a range of holding potentials in symmetric 250 mM Tris-HCl, pH 7.4. The closed levels are indicated (...). Low-pass filtered at 0.15 kHz.

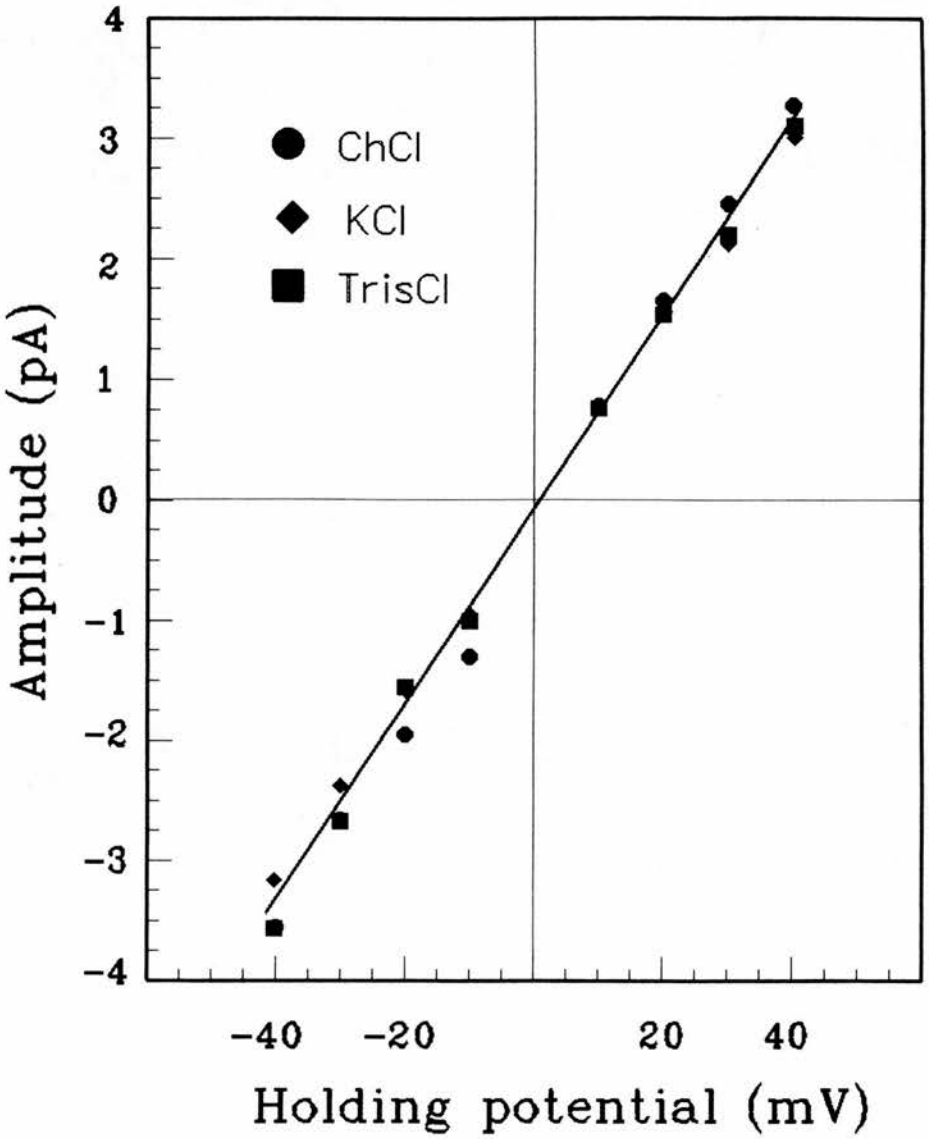

Figure 3.2.4 I/V relationships in different symmetric salts
The corresponding current/voltage relationships in symmetric ChCl, KCl, and Tris-HCl solutions are shown.

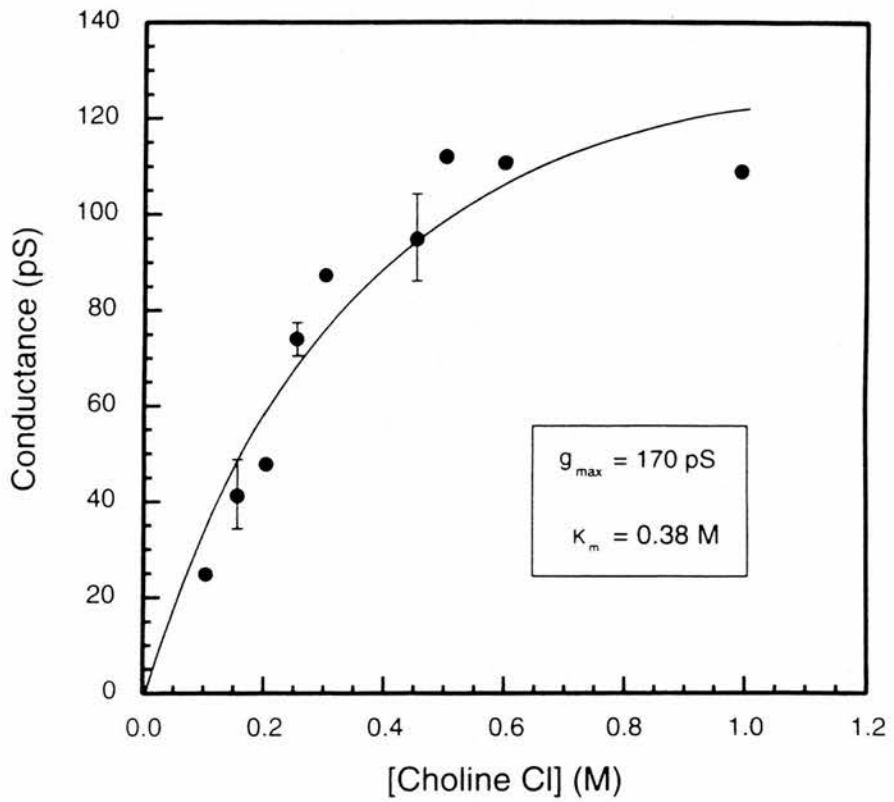

Figure 3.2.5 Single-channel conductance-concentration relationship in symmetric Choline Cl. All points are averages of at least 2 determinations, or +/- SEM (n = 4 to 12) where indicated.

conductance, [S] is the concentration of Choline Cl and Km is the Michaelis constant. The maximal conductance is 170 pS and the channel has an apparent Km for Choline Cl of 380 mM.

3.3 Substate behaviour of the rat brain ER anion channel

One of the most striking and interesting characteristics of the brain ER anion channel was its substate behaviour. The channel displayed three subconductance levels together with the low current level representing the closed state and the highest current level as the main open state. The channel often showed one or more substates in sections of the recording, but only rarely were all observed at any one time (Figure 3.3.1). The channel never displayed more than three substates at intervals of 22% $\pm$ 2.1% (n=16), 45% $\pm$ 4.4% (n=22), and 70% $\pm$ 3.9% (n= 22) of the main open state irrespective of the permeant cation (Figure 3.3.2), shown $\pm$ standard deviation (SD) for n experiments (some data from D. Murray). Similar substate amplitudes were shown in 20 experiments in Choline Cl, 7 in KCl, and 6 in Tris-HCl, +/- SD (KCl & Tris-HCl data from D. Murray, unpublished observations). To illustrate the substate behaviour all-points histograms were created from short recordings at different holding potentials. All of the substates are shown at a holding potential of +60 mV (Figure 3.3.3, Panel A), the 70% substate and main open state are prevalent at +40 mV (Figure 3.3.3, Panel B), and the ~22% and 45% substate are prevalent from a recording at +20 mV (Figure 3.3.3, Panel C). Current-voltage relationships for the main open state and the three substates are shown (Figure 3.3.4). The slope conductances were linear and the main open state slope conductance was 72 pS with

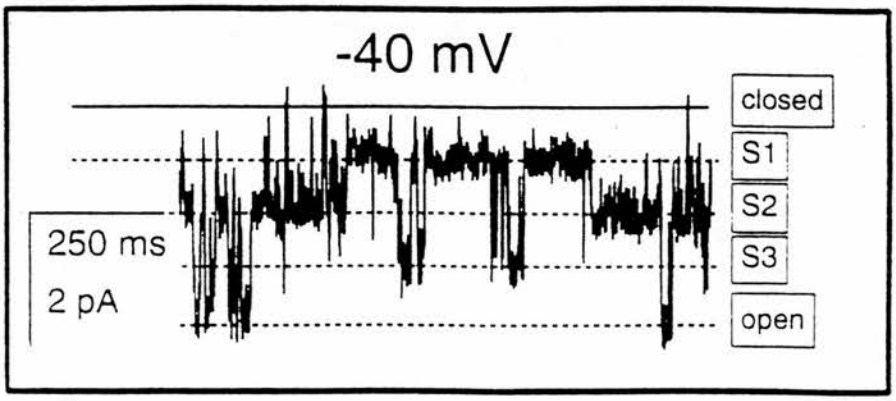

Figure 3.3.1 Substate levels of the rat brain ER anion channel.
A single channel is shown at a holding potential of -40 mV in 250 mM symmetric Choline Cl, 5 mM Tris-HCl, pH 7.4. A continuous line shows the closed state, with dotted lines representing the substates and main open state. Low-pass filtered at 0.15 kHz.

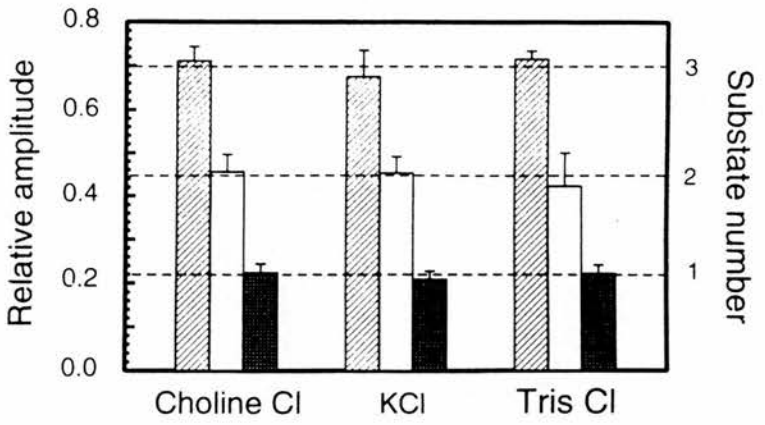

Figure 3.3.2 Relative substate amplitudes in different solutions.
Relative substate amplitudes are shown +/- SD in Choline Cl, KCl and Tris-HCl. The closed and main open state amplitudes are set to 0 and 1.0 respectively.

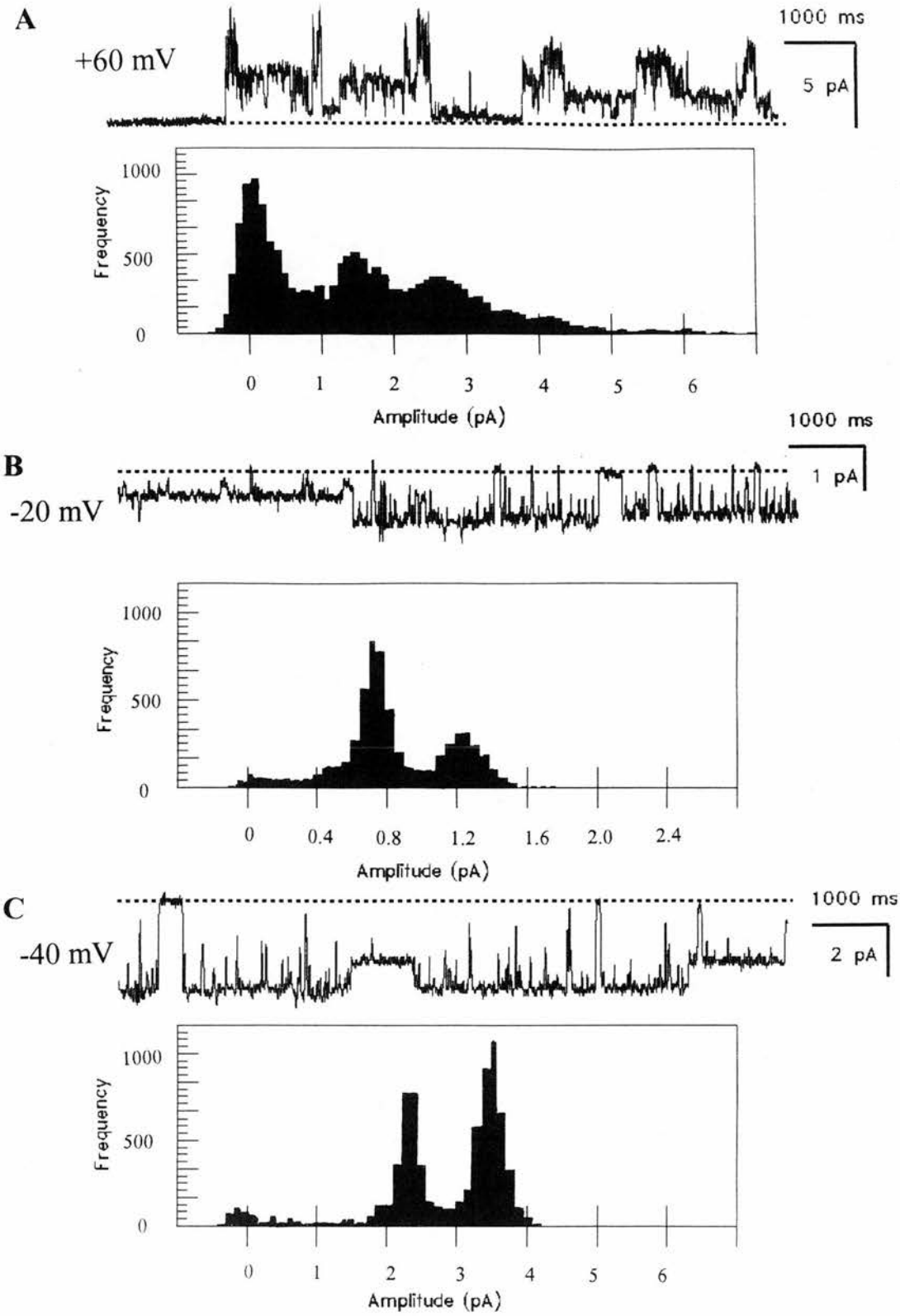

Figure 3.3.3 Examples of recordings with corresponding all-points amplitude histograms. Panels A, B, and C show all-points amplitude histograms from three independent channels at different holding potentials in 250 mM Choline Cl, 5 mM Tris-HCl, pH 7.4. The closed levels are indicated (...). Low-pass filtered at 0.15 kHz.

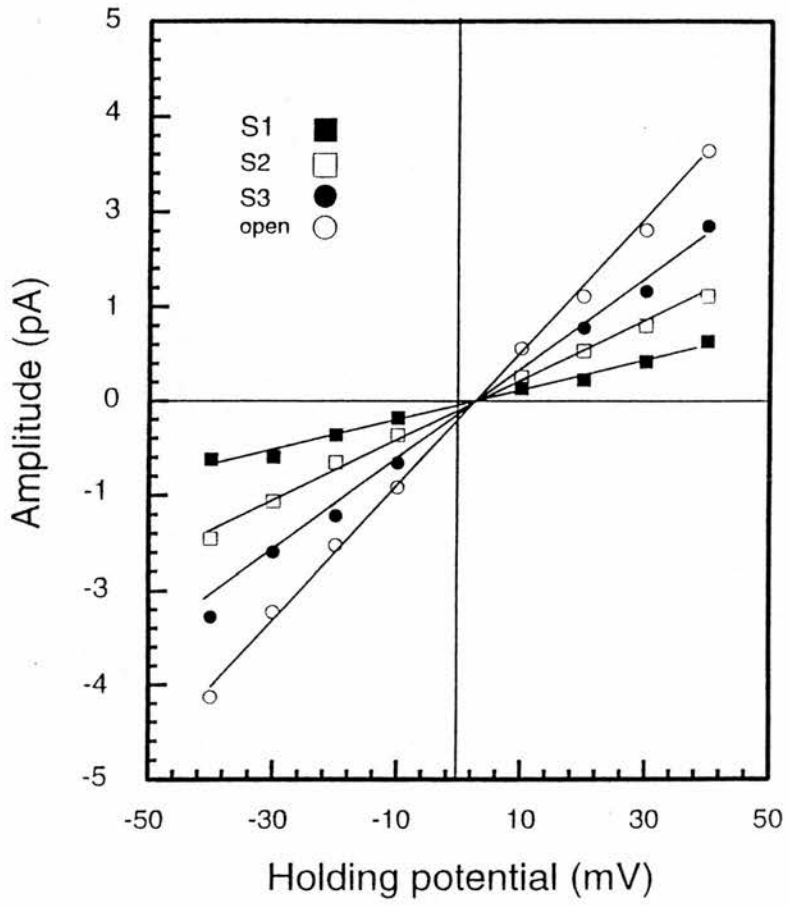

Figure 3.3.4 I/V relationship for the main open state & three substates. The current-voltage relationship for the main open state and the three substates are shown.

a junction potential of +4 mV. A binomial analysis of substate behaviour will be described later (section 3.7).

3.4 Equilibrium anion and cation selectivities

The relative permeabilities of a range of anions were obtained by perfusing the *cis* and *trans* chambers with different K salts. Using activities calculated from activity tables (Robinson & Stokes, 1955) the anion permeabilities versus Cl^- were P_{SCN} (2.2 +/- 0.8) > P_{NO3} (1.4 +/-0.2) > P_{Br} (1.3 +/-0.3) > P_{Cl} (=1.0) > P_F (0.6). This shows +/- SD for 3 or 4 experiments or an average of 2 experiments. The results show that the channel is poorly-selective between anions although there is a statistical preference ($P>0.05$) for SCN^- over Br^- and Cl^-. The number of experiments performed was relatively low due to the appearance of co-incorporated K_{Ca} and Ryanodine-sensitive Ca^{2+}-release channels on perfusion with K salts.

The GHK equation (section 2.2.7) was used to measure the selectivity for anions over cations. P_{anion}/P_{cation} for Cl^- versus K^+ was 1.6 +/-0.3 (mean +/- SD, n=5) (data from D. Murray), Cl^- vs. $Choline^+$ was 2.2 +/-0.2 (n=5), and Cl^- vs. $Tris^+$ was 6.1 +/-0.2 (n=6) (data for $Tris^+$ from D. Murray and R.H. Ashley, unpublished observations). The single channel conductances for K^+, $Choline^+$ and $Tris^+$ were 74 +/- 9 pS, 71 +/- 3 pS and 71 +/- 13 pS respectively.

Choline Cl was the choice of solution for most of the experiments and the concentration dependence of $P_{Cl}/P_{Choline}$ was calculated. The reversal potential in 250/50 (*cis/trans*) Choline Cl was +18.8 +/- 6 mV (mean +/- SD, n=8) and the permeability ratio of $P_{Cl}/P_{Choline}$ was 3.2 +/- 1.2. This was statistically different from

data obtained in 450/150 Choline Cl ($P<0.05$). P_{Cl}/P_{Cs} was also concentration-dependent and comparing 250/50 and 150/50 solutions gave of P_{Cl}/P_{Cs} of 4.3 +/- 0.43 (mean +/- SD, n=3) and 2.4 +/- 0.2 (mean +/- SD, n=3) respectively. These were corrected for activities (D. Murray, unpublished observations). These findings suggest that the relative permeabilities are concentration-dependent suggesting the channel has a multi-ion pore.

3.5 Molecular modelling of permeant ions

Space-filling models of permeant ions were constructed and energy minimised using Alchemy III, Tripos Associates with help from Dr. Richard J. Martin, Preclinical Veterinary Sciences, Edinburgh, UK. The models show the end-elevation of the ions $Choline^+$, $Tris^+$ and K^+ which were all permeant through the channel (Figure 3.5.1).

3.6 Binomial analysis of substate behaviour

A binomial analysis was performed to investigate the probability of the individual channel "protomers" being open and following a binomial distribution. The channel appeared to have periods of relative inactivity referred to as interburst intervals and a closed lifetime analysis was performed on single channels selected for binomial analysis to identify the long interburst durations. This was necessary to exclude the interburst closures and separate them from intraburst closures. In Figure 3.6.1, lifetime analysis was performed on a 108 s recording in symmetric Choline Cl. Event durations of less than 5 ms excluded from the main histogram. The intraburst closures were fitted by maximum-likelihood analysis to a double exponential

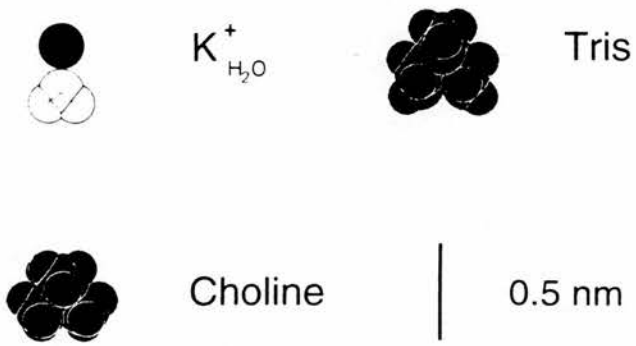

Figure 3.5.1 Space-filling models of permeant cations.
Panels A,B and C show minimal cross-sectional profiles for the permeant cations Choline$^+$, Tris$^+$ and K$^+$ (with single water of hydration). Scale bar is shown.

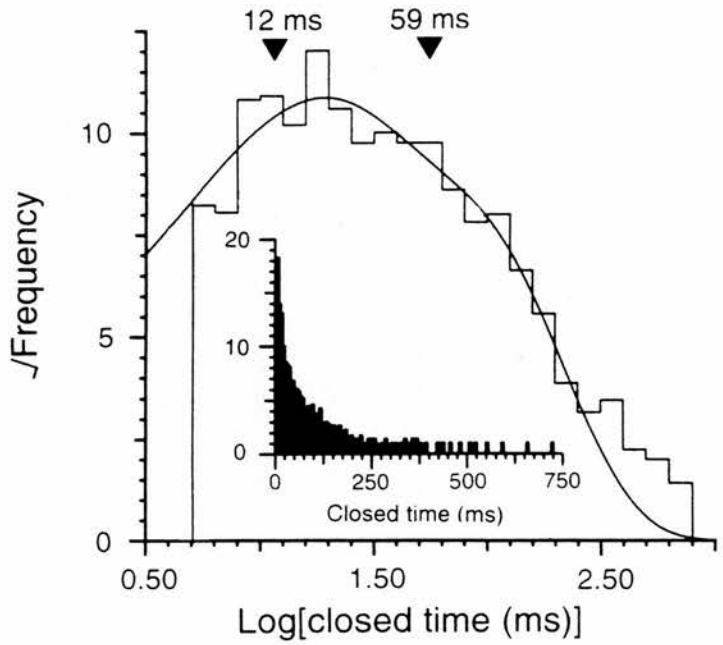

Figure 3.6.1 Closed lifetime analysis.
The closed lifetime distribution is shown on a logarithmic scale and inset on a linear time scale for a single channel at -40 mV in symmetric Choline Cl. The two closed time constants are indicated.

distribution for closed durations between 5 ms and 250 ms. This gave mean lifetimes of 12 ms and 59 ms. Data collected from 6 single channels in symmetric Choline Cl (30-120 s recordings at -40 mV) gave mean closed times of 5.9 +/- 1.6 ms and 47+/- 11 ms (means +/- SD, n=6). Similar results were obtained at +40 mV with mean closed lifetimes of 7.7 +/- 2.9 ms and 48 +/- 12 ms (+/- SD, n=5). Although the frequency of the long interburst closures were low they occupied much of the recording time and could bias the binomial analysis of closed states. Thus before proceeding with the binomial analysis closures three times greater than the ~50 ms intraburst closed time constant were excluded as on the basis of an exponential distribution 3 SDs remove 95 % or so of "false" events. The data have been fitted by least-squares to multi-component Gaussian distributions to derive Pi for each amplitude level. From the Pi measurements, the best-fit $Po_{(protomer)}$ values for -40 mV was 0.69 and at +40 mV it was 0.19. These values were used to construct the theoretical distributions inset with the peak variances matched with the original data (Figure 3.6.2). The channel displayed certain substates in the recordings but rarely many substates at any one time (Figure 3.2.1). If the residence in a certain substate comprised >10 % of the events they were excluded from maximum likelihood fitting. Measured and predicted residence times at each amplitude level for 6 channels were compared under similar ionic conditions at a holding potential of -40 mV (average values +/- SEM, n = 6) (Figure 3.6.3). The inset shows a highly-significant correlation ($P<0.001$ by t-testing) between the measured and predicted Pi values (slope is 0.97) thus reinforcing the binomial analysis. $Po_{(protomer)}$ values were calculated at a range of positive and negative potentials. These data were fitted to the Boltzmann equation:-

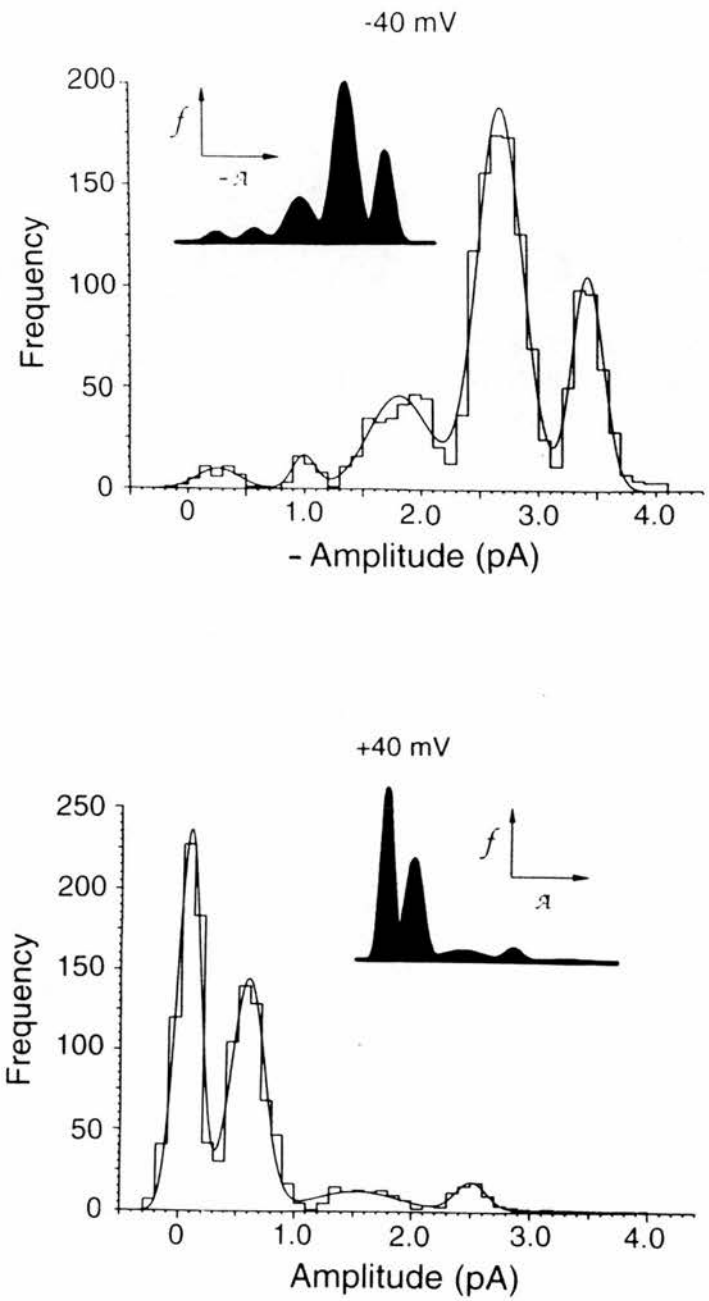

Figure 3.6.2 Amplitude histograms in symmetric Choline Cl.
Panels A and B show all-level amplitude histograms from 30 s recordings of a single channel in symmetric Choline Cl, at holding potentials of -40 mV and +40 mV respectively. The insets show theoretical binomial distributions calculated from best-fit $Po_{(protomer)}$ values.

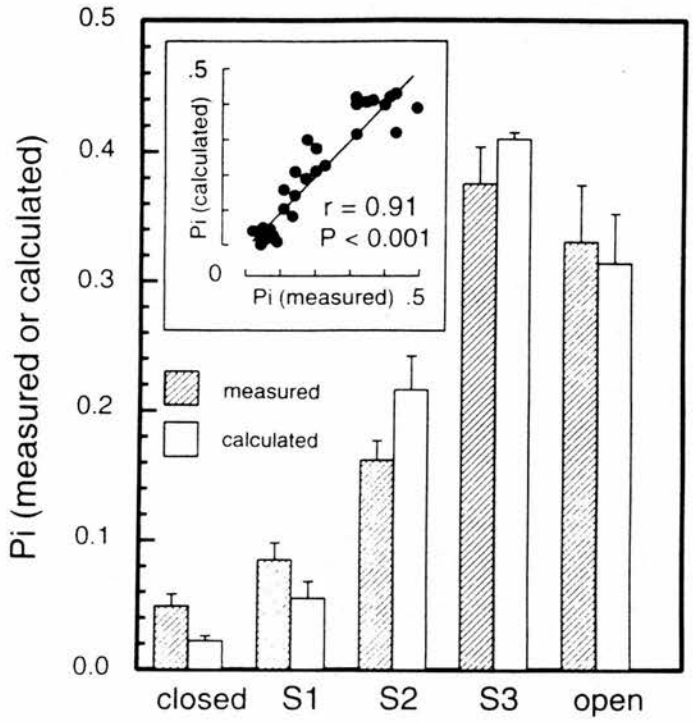

Figure 3.6.3 Measured vs. predicted residence time at different amplitude levels. The measured vs. predicted residence time at each ampitude level is shown for recordings in symmetric 250 mM Choline Cl, 5 mM Tris-HCl, pH 7.4 at -40 mV.

$Po_{(protomer)} / 1\text{-}Po_{(protomer)} = \exp [-zF/ RT (V\text{-}Vo)]$

Where V is the membrane potential, Vo is the potential where $Po_{(protomer)} = 0.5$ (this was -3.5 mV) and gating charge z is 0.84. Extrapolated $Po_{(protomer)}$ values approach a maximum of 1 at -100 mV and a zero value at approximately +100 mV (Figure 3.6.4).

3.7 Channel block

A library of putative Cl^- channel blockers belonging to different structural groups were accumulated in order to assess their potency on the brain ER anion channel (Table 3.7.1). These putative inhibitors were used at concentrations which had been shown to block other anion channels, and they were stirred into either the *cis* or *trans* chambers, or both. The mode of blocking was either described as "slow" if the individual blocking events could be easily resolved on the time-scale of the recordings, and "intermediate" if there was prominent flickering. The dissociation rate of "fast" blockers meant that the residence time of the blocker in the channel cannot be distinctly resolved on the time-scale of the recordings, resulting in an apparent reduction in single-channel conductance.

The stilbene derivative 4,4'-diisothiocyanatostilbene-2,2' -disulphonic-acid (DIDS) induced a complete block when added to the *cis* chamber at 100 μM (Figure 3.7.1, Panel A). The effect was irreversible despite thorough perfusion. DIDS has been shown to eliminate Cl^- currents irreversibly in other intracellular membranes including the SR (Kasai & Kometani, 1979 and Suarez-Isla *et al.,* 1986). The divalent cation Zn^{2+}, when added to the *cis* chamber, induced a "fast" block at 0.5 mM and a

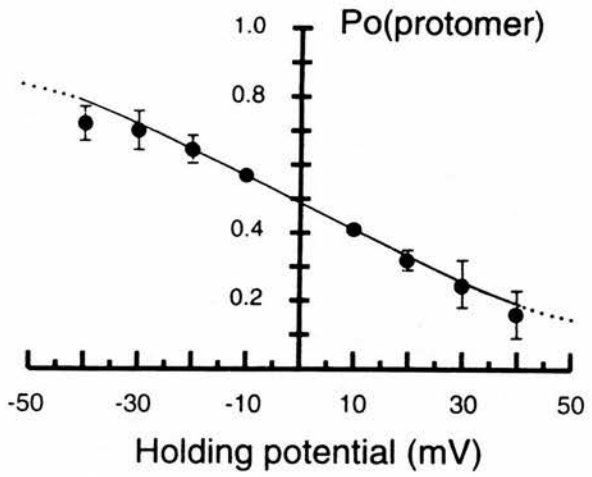

Figure 3.6.4 Voltage-dependence of open probability.
The voltage-dependence of $Po_{(protomer)}$ between -40 mV and +40 mV is shown. Values are averages of at least two determinations, +/- SEM (n = 4 -7 channels).

complete block at 1 mM. This was reversible on perfusion (Figure 3.7.1, Panel B). When added to the *trans* chamber at 0.5 mM, a complete reversible block was observed (data not shown). Zn^{2+} has been shown to block Cl^- channels in other membranes including rat brain hippocampal neurons (Franciolini & Nonner, 1987).

The effect of the proton buffer HEPES on the Cl^- channel was studied. The buffer was added to both chambers at 10 mM and appeared to block individual protomers giving rise to "slow" blocking events lasting hundreds of milliseconds (Figure 3.7.2, Panel A). This further suggested that the channel may function as four protochannels which can be blocked independently. Frusemide also induced a slow block when added to both chambers at 100 μM (data not shown).

Ethacrynic acid (EA) when added to both chambers induced an "intermediate" block at 200 μM (Figure 3.7.2, Panel B). 5-nitro-2-(3-phenylpropylamino)-benzoate (NPPB) was added to both chambers at 100 μM and induced a time-dependent flickery or "intermediate" block which was irreversible after washout of *cis* and *trans* chambers (Figure 3.7.3). The flickery block was also observed with a concentration as low as 10 μM (data not shown). 9-AC was added to the *cis* chamber at 100 μM and also induced a flickery or "intermediate" block which was time-dependent but was reversible on perfusion (Figure 3.7.4). A detailed analysis was carried out on the block induced by IAA-94. As the concentration of IAA-94 was increased the single channels became less active although the time resolution was still satisfactory to observe the fully open state (Figure 3.7.5). The flicker therefore did not represent a "fast" block. $Po_{(Protomer)}$ was measured as a function of [IAA-94] and voltage to give a K_D of 35 μM at -30 mV (Figure 3.7.6). Block was voltage-dependent and was more

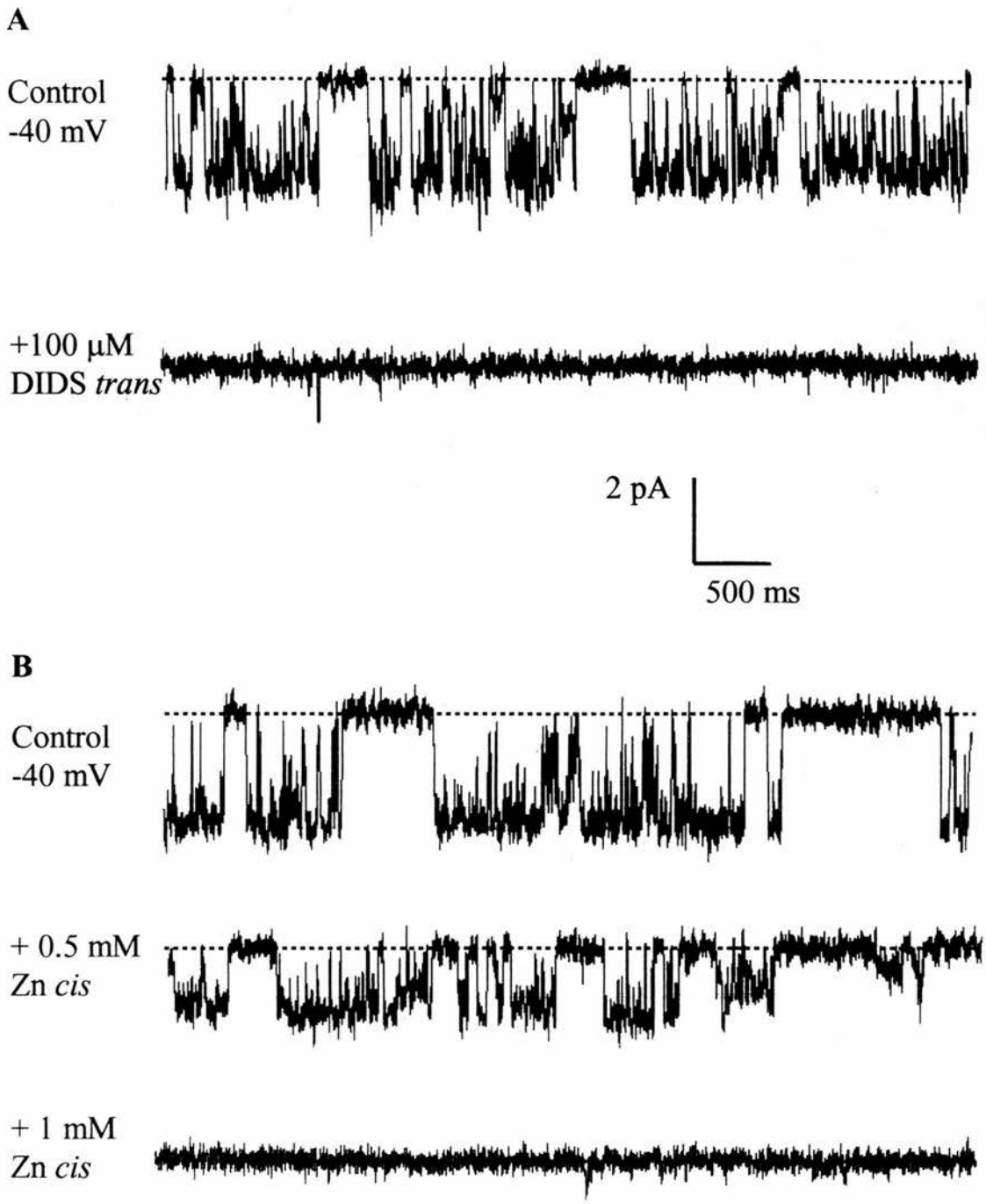

Figure 3.7.1 Channel block by DIDS and Zn^{2+}.
Panels A and B show the effect of adding 100 μM DIDS to the *trans* chamber and 1 mM Zn^{2+} to the *cis* chamber. The data are from two independent experiments in 250 mM ChCl at -40 mV. The closed levels are indicated (...). Low-pass filtered at 0.15 kHz.

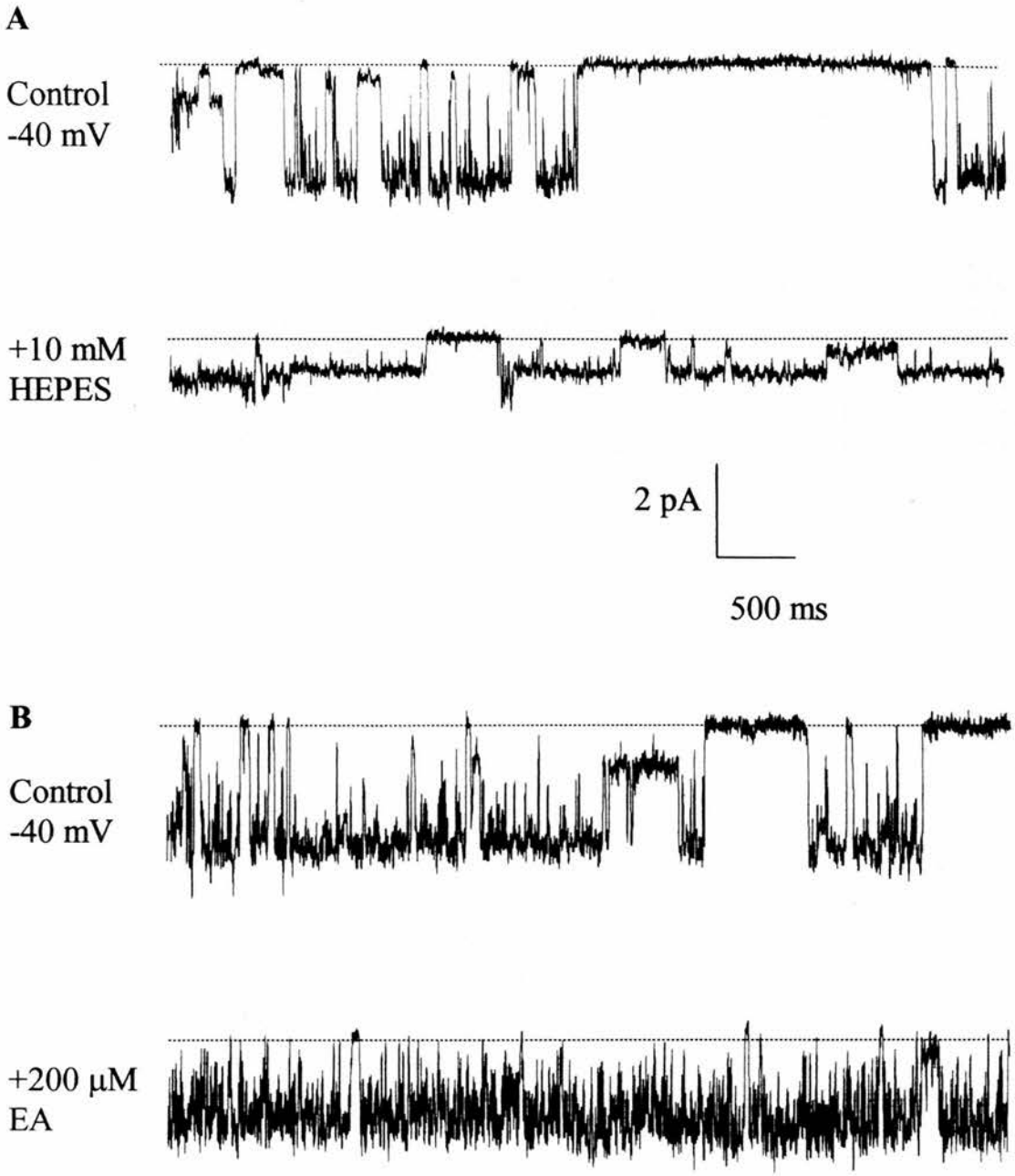

Figure 3.7.2 Channel block by HEPES and EA.
Panels A and B show the effect of adding 10 mM HEPES, and 200 μM EA to both chambers. The data are from two independent experiments in 250 mM ChCl at -40 mV. The closed levels are indicated (...). Low-pass filtered at 0.15 kHz.

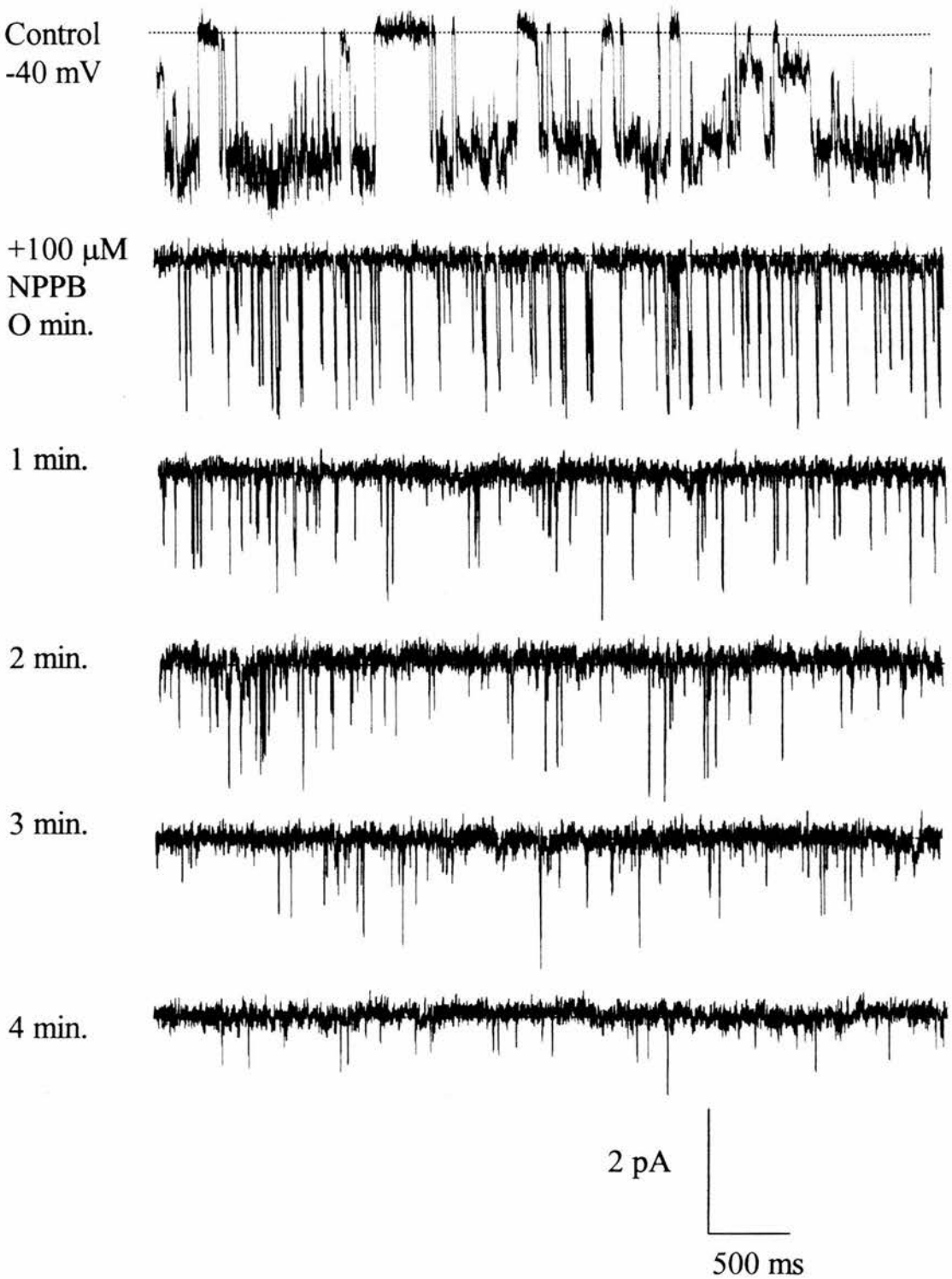

Figure 3.7.3 Time-dependence of NPPB block.
A single channel was recorded in symmetric 250 mM ChCl at -40 mV. 100 μM NPPB was added to both chambers and the time-dependent decrease in channel activity is shown. The closed levels are indicated (...). Low-pass filtered at 0.15 kHz.

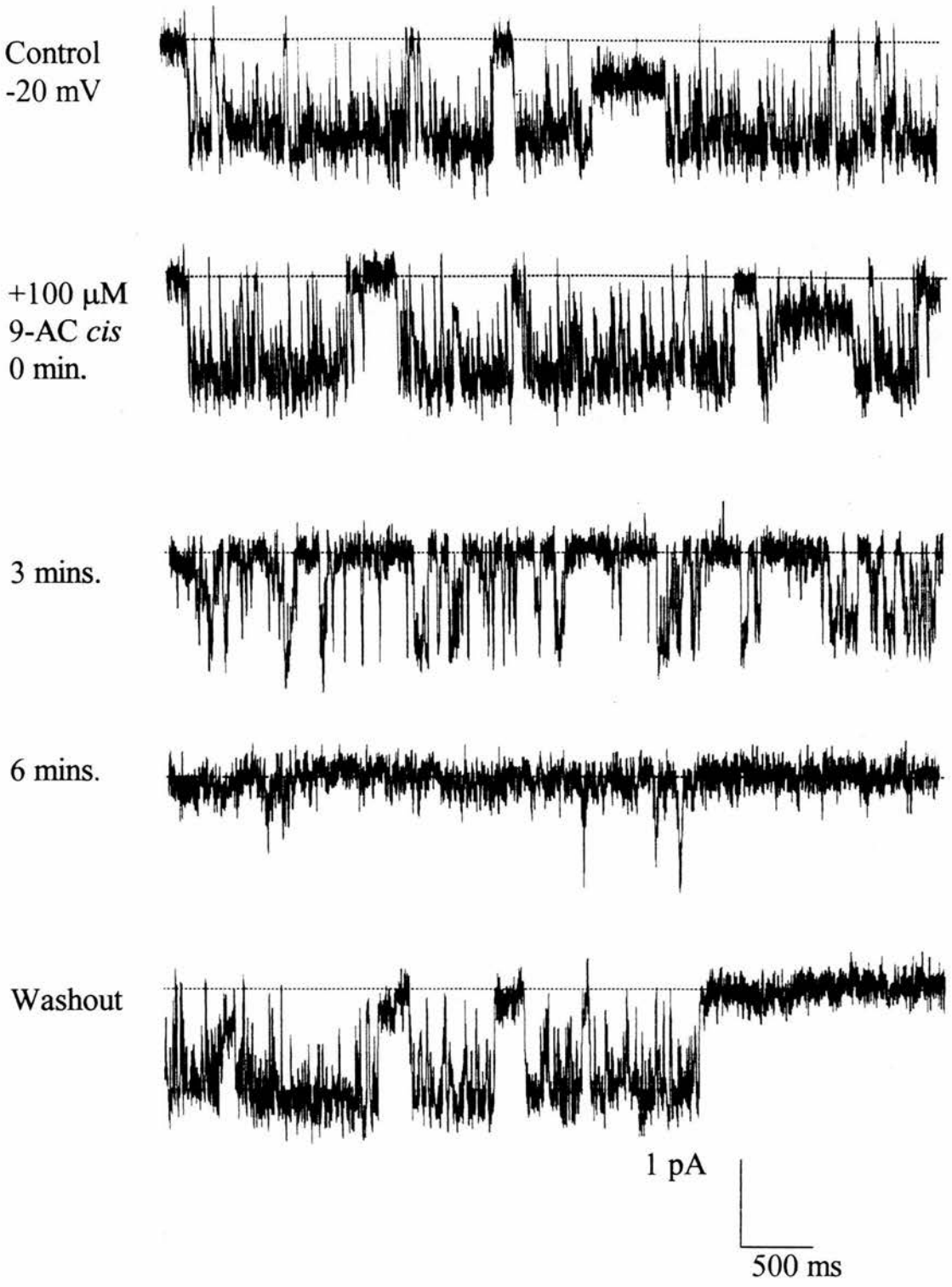

Figure 3.7.4 9-AC block.
A single channel is shown in 250 mM symmetric ChCl at -20 mV. 100 μM 9-AC was added to both chambers and the time-dependence decrease in channel currents is shown. Currents returned to normal after washout. Closed levels are shown (..). Low-pass filtered at 0.15 kHz.

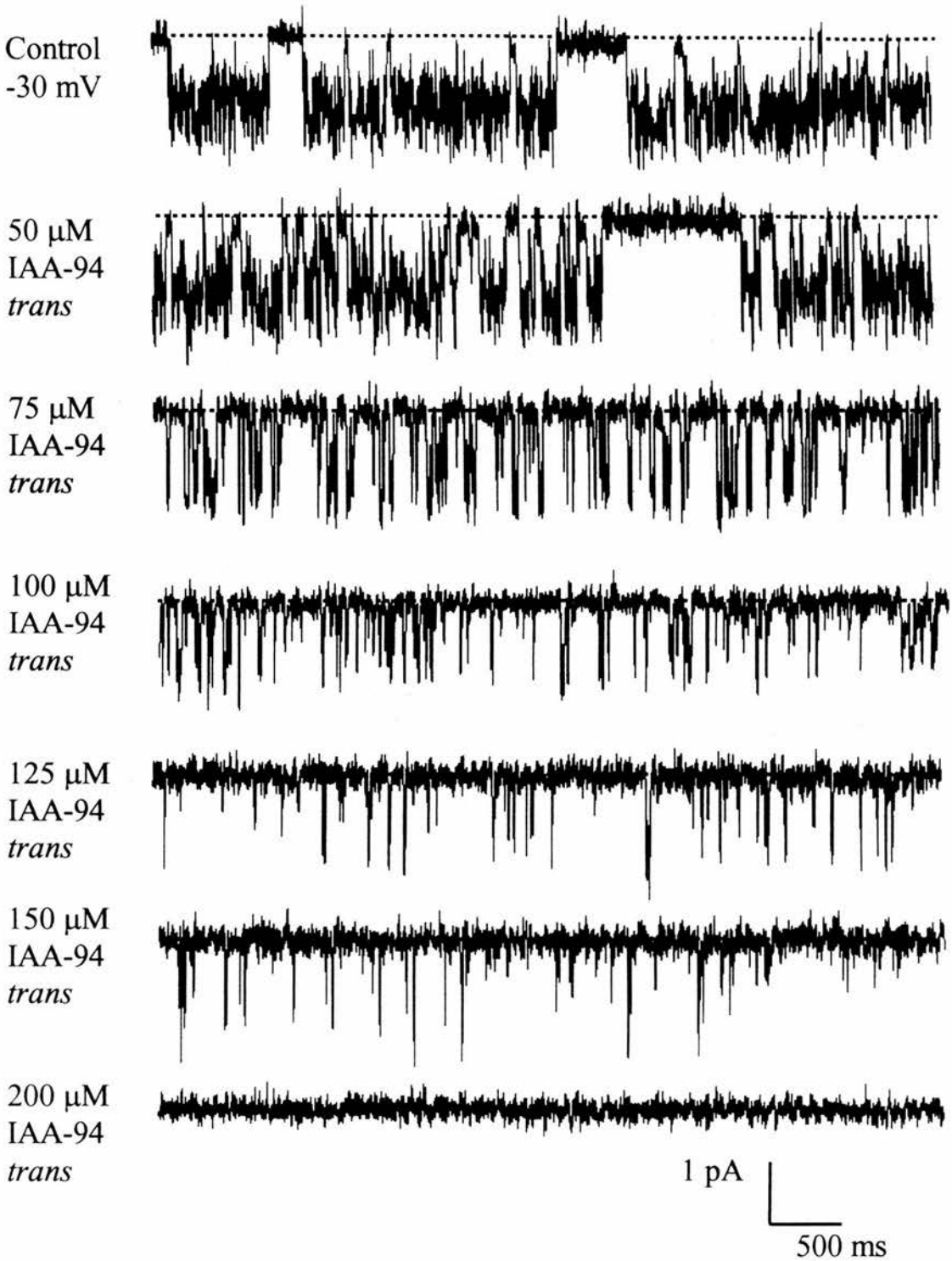

Figure 3.7.5 IAA-94 block.
A single channel is shown in 250 mM symmetric ChCl at -30 mV before and after sequential additions of IAA-94 to the *trans* chamber to give the indicated concentrations. Closed levels are shown (...). Low-pass filtered at 0.15 kHz.

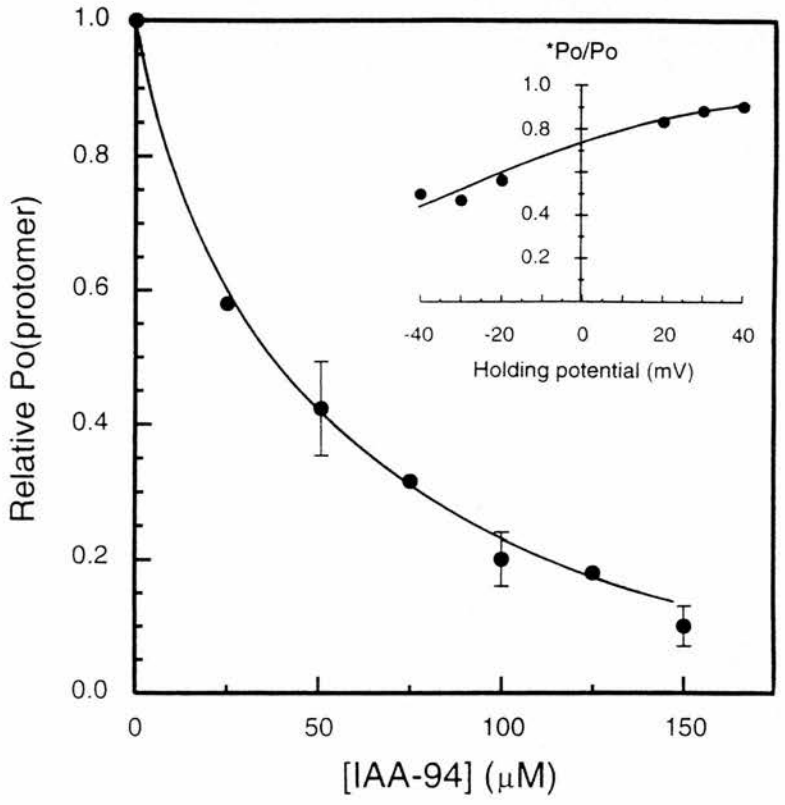

Figure 3.7.6 Dose response curve and voltage dependence of IAA-94 block. Po $_{(protomer)}$ was measured over a range of IAA-94 concentrations, and the data were fitted by non-linear least-squares analysis to a single-site inhibition curve. Each point is an average from at least two independent channels, +/- SEM for n = 3 measurements. The inset shows the voltage-dependence of the block induced by 50 μM IAA-94 added to the *cis* chamber. *Po and Po represent with and without drug respectively.

Table 3.7.1 Effect of anion channel blockers on the rat brain ER anion channel.

Inhibitor	Conc.	Block	Reversible	Sidedness	*n*
9-AC	100 μM	Flickery	+/-	*cis*	3
DIDS	15-100 μM	Complete	-	*cis*	7
DPC	100 μM	No effect	/	Both	3
EA	200 μM	Intermediate	nd	Both	4
Frusemide	100 μM	Slow	nd	nd	2
HEPES	10 mM	Slow	nd	Both	3
IAA-94	25-200 μM	Flickery	+	*cis*	14
Niflumic acid	100 μM	No effect	/	/	2
NPPB	10-100 μM	Flickery	-	*cis* or *trans*	10
Puromycin	100 μM	No effect	/	Both	2
TBA	10-50 mM	No effect	/	Both	3
Zn^{2+}	0.5-2 mM	Fast/complete	+	*cis*	10
	0.5-2 mM	Complete	+	*trans*	9

+ = reversible, +/- = partially reversible, - = irreversible.
nd = not determined, / = not applicable.

marked at negative holding potentials. This voltage-dependence suggests that the binding site(s) were located within the electric field.

Using the Woodhull equation,

$$*Po_{(Protomer)}/ Po_{(Protomer)} = *Po/Po = \{1+[B]/ K_D(0).\exp(-z\delta FV/RT)^{-1}$$

where *Po and Po are $Po_{(Protomer)}$ with (*) and without blocker, and zδ, the "effective valence" of the blocking reaction, is the compound of valency and the electrical distance of the blocker binding site (Woodhull, 1973). Assuming a valency of -1, δ was 0.78 of the distance across the membrane electric field when block was induced by 50 μM IAA-94 added to the *cis* chamber, and K_D (0 mV) for IAA-94 was 135 μM (Figure 3.7.6).

The addition of 2 mM MgATP to bilayers containing the brain ER anion channel led to destabilisation and ultimately breakage of the membrane seconds after addition (data not shown). Mg^{2+} added as a control had no adverse effect on bilayer stability. Many ion channel proteins have consensus phosphorylation sites although the ATP-destabilising effect prevented any attempt to uncover functional evidence for protein-kinase A-mediated phosphorylation (Vaca & Kunze, 1993), for example. Finally neither DPC (100 μM), niflumic acid (100 μM), TBA (50 mM) or puromycin (100 μM) had any effect on Cl^- chanel activity (data not shown).

3.8 Discussion

Rat brain microsomal membrane vesicles were fused with planar lipid bilayers leading to the incorporation of anion channels. There is a theoretical possibility that these anion channels may have originated from a contaminating membrane fraction such as the plasma membrane. This does not appear to be the case because they were shown to be co-localised with brain ER ryanodine-sensitive Ca^{2+}-release channels, based on a Poisson analysis in addition to coincident incorporation (Ashley, 1989). These results are consistent with the presence of intracellular Cl^- channels in muscle SR (Smith *et al.*, 1985,1986, Tanifuji *et al.*, 1987, Rousseau *et al.*, 1988).

These brain ER channels do not represent protein-translocating pores (Simon & Blobel, 1991) occupied by nascent polypeptide chains which restrict permeation of ions. Upon addition of puromycin to protein-conducting channels, peptidyl puromycin is removed, revealing single channel conductances of 220 pS. This is significantly higher than the conductance of the brain ER anion channel, and puromycin had no effect after brain ER vesicles were fused with the bilayer. Protein-conducting channels also close when the salt concentration is raised to 150-400 mM due to ribosomes detaching from the membrane. The brain ER anion was open well beyond this threshold when investigating the conductance-concentration relationship.

The channel discriminated poorly between different anions and was poorly selective between anions and cations (e.g. $P_{Cl}/P_K = 1.6$). The ER Cl^- channel was more poorly selective than ClC channels and SR Cl^- channels ($P_{Cl}/P_K = 0.012$) (Townsend & Rosenberg, 1995). Testing different permeation models for the brain ER anion channel to explain the mixed anion and cation permeation (Franciolini & Nonner,

1994) was made difficult by the co-incorporation of cation channels in the present study although evidence for multi-ion pores includes the concentration-dependence of relative anion vs cation permeabilities. The channel may therefore have an interesting permeation mechanism. By exclusion sizing of ions, the pore has a diameter of approximately 7 Å which corresponds to the combined size of $Tris^+$ and Cl^- which are permeant in the channel. The saturating single-channel conductance is lower than would be expected when physical laws are applied to a hypothetical cylindrical pore of approximately 7 Å (Hille, 1984). If the channel is comprised of four protochannels then a conductance of over 1 nS would be expected. However, conductance-concentration data from a similar intermediate-conductance Cl^- channel from SR displayed a maximal conductance of 154 pS (Rousseau *et al.*, 1988). This channel also displayed a prevalence of substates which makes it possible that intracellular channels may have unusual gating mechanisms to explain the data.

The multiple subconductance states observed do not represent multiple channels as only four levels were ever seen when the channel was held at maximally active negative holding potentials. The subconductance states may be explained either by the gating of "multimeric" channel complexes or by changes that occur within a single pore. The "multimeric" channel model displays subconductance states when only some of the protochannels are open at any one time, and conductance levels occur at regular fractions of the fully-open state. In this model the protomers may open and close independently. Subconductance states may also arise from changes in a single pore including long-lived conformational states, alterations in rapid fluctuations between conformational states, or because of alterations in the

electrostatic properties in the channel vestibules (Dani & Fox, 1991). The analysis of the gating behaviour of the brain ER anion channel shows that functionally it behaves as a "multimeric" channel complex, although this is not definitive in the absence of detailed molecular studies. The strongest support for the "multimer" hypothesis comes from the the fact that HEPES interacts with individual protochannels and also that the protomers open and close independently of each other which is very unlikely in a "single-pore" channel. The gating of the channel also displayed openings from closed levels to the fully open state. This is probably due to the poor time resolution of the recordings so that the openings of 3 or 4 protochannels may appear to be superimposed, especially at high negative potentials when the $Po_{(Protomer)}$ is quite high (~0.7).

The kinetics of the channel can be represented by the following gating scheme with the four levels corresponding to the independent gating of the four protomers:-

$$Cl \rightleftarrows \begin{bmatrix} C2 \rightleftarrows C3 \rightleftarrows (C4) \rightleftarrows O1 \\ C2 \rightleftarrows C3 \rightleftarrows (C4) \rightleftarrows O1 \\ C2 \rightleftarrows C3 \rightleftarrows (C4) \rightleftarrows O1 \\ C2 \rightleftarrows C3 \rightleftarrows (C4) \rightleftarrows O1 \end{bmatrix}$$

C1 corresponds to the long interburst closures when the channel was in a long-lived closed or "inactive state", and was excluded from the binomial analysis of channel gating. This state was favoured at positive (cytoplasm-lumen) potentials, and its presence suggests that there is a gate which can close all four protomers simultaneously. O1 corresponds to the open state(s) of the channel, although this state

has not been analysed. Intraburst behaviour of each of the four protomers corresponds to:-

$$[C2 \rightleftarrows C3 \rightleftarrows (C4) \rightleftarrows O1]$$

There were more closed states in the gating scheme than could be adequately resolved such as C4. The complicated intraburst behaviour is represented by C2 and C3 and O1 represents the open state(s). Only closed states could be analysed as it was not possible to tell which protomer was open at any one time. The problem is analagous to the difficulty encountered when analysing open lifetimes in multichannel records.

A number of blockers were found to have an effect on the brain ER anion channel. One of the best known Cl^- channel blockers is the stilbene derivative DIDS. The effect of DIDS has been extensively studied in anion channels (Marten *et al.*, 1993) and also to compare various anion transporters (Cabantchik & Greger, 1992) including a study carried on Band 3, an anion antiporter in mammalian erythrocytes. DIDS interacted with at least two amines on lysine residues via its two isothiocyanate (SCN^-) side groups resulting in an intramolecular cross-link and block of the

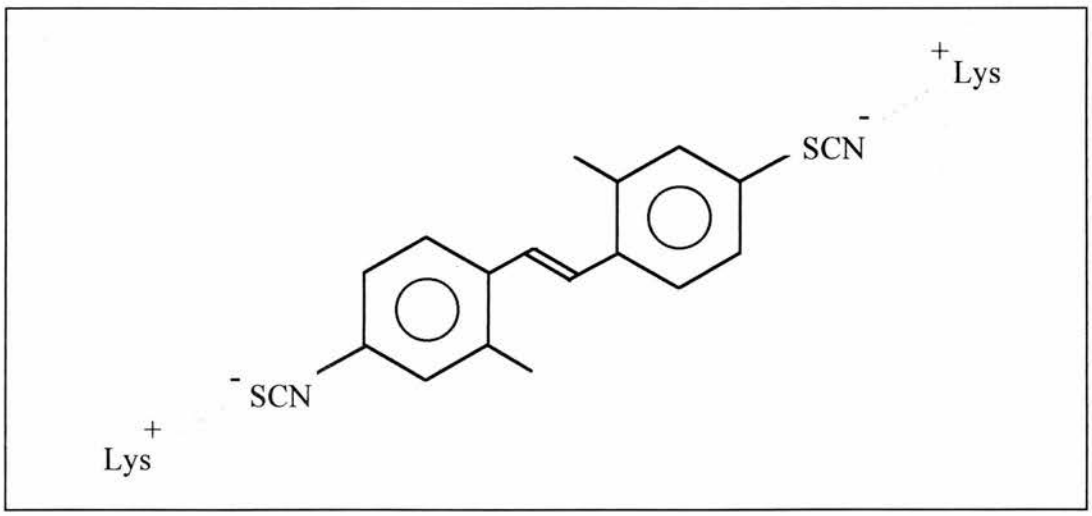

Figure 3.8.1 Hypothetical binding of DIDS to lysine residues in the channel.

transporter. It is therefore possible that there may be a Lys-stilbene-Lys interaction in the brain ER channel giving rise to the complete irreversible block (Figure 3.8.1). Zn^{2+} blocked the channel and gave a "fast" block at 0.5 mM *cis* and a complete block at 1 mM *cis* and also at 0.5 mM *trans*. It has been shown to block plasma membrane anion channels from a range of cells including human T lymphocytes (Pahapill & Schlichter, 1992), hippocampal neurons (Franciolini & Nonner, 1987), and foetal rat brain growth cones (DeBin *et al.*, 1994). It has been suggested that Zn^{2+} may interact with histidine or cysteine residues within the pore and it is possible that the Zn^{2+} binding site in the channel pore may be analagous to Zn^{2+} finger proteins where a Zn^{2+} ion can be coordinated to a pair of cysteines and a pair of histidines in up to nine repeating domains. Zn^{2+} has been used to probe the major skeletal muscle Cl^- channel, hClC-1 (Kürz *et al.*, 1997).

The block by NPPB increased with time (Figures 3.7.2). This time-dependence may be explained by the drug partitioning into the membrane to gain access to its binding site. This argument is supported by the fact that NPPB is lipophilic in its protonated form and the drug is active from either side of the membrane (Table 3.7.1). 9-AC also blocked the channel in an "intermediate" time-dependent manner although the block was partially reversible (Figure 3.7.4). It has previously been shown in Cl^- channels from skeletal membranes that 9-AC produces its effect by partly or completely partitioning into the membrane (Palade & Barchi, 1977). This would increase membrane fixed negative surface charge density and retard transmembrane anion movement. Alternatively, the amphipathic nature of 9-AC may allow the hydrophobic ring to partition into the lipid phase leaving the charged carboxyl residue

at the membrane-water interface and again retard movement of anions. These suggestions are speculative although they tie in with the time-dependence of block. The 9-AC may only partially partition into the membrane as the block is partially reversible (Hedrich & Kurkdjian, 1988).

HEPES appeared to interact with individual protomers (Figure 3.7.2) similar to the effect observed in neuronal Cl^- channels from *Drosophila* (Yamamoto & Suzuki, 1987). The block by IAA-94 supported the idea that the blocker interacted with individual channel protomers on an "intermediate" timescale (Figure 3.7.5) although the affinity of IAA-94 at 35 μM is probably too low to consider affinity purifying the brain ER anion channel using the compound.

Chapter 4

Single channel recordings, partial purification & macroscopic assays of a sheep brain ER anion channel

4. Single channel recordings, partial purification & macroscopic assays of a sheep brain ER anion channel.

The study of the brain ER anion channel was extended to another mammalian system, partly in an attempt to isolate the channel protein and also to investigate any inter-species similarities with the rat brain channel. The use of sheep material increased the microsomal yield due to larger brain size and facilitated the development of a partial purification protocol. Data in this chapter reports an ER anion channel from sheep brain microsomes which displayed similar gating and pharmacological properties to the rat brain channel. After this identification the channel was partially-purified and reconstituted into liposomes for characterisation at a macroscopic level.

4.1 Characterisation of the microsomal membrane fraction and conductance behaviour of sheep brain ER anion channel.

Ion channels present in sheep brain microsomes were identified in the same way as rat brain vesicles by fusion into voltage-clamped planar lipid bilayers (Figure 2.1.2). The fusion process was again promoted by the addition of 2 mM Ca^{2+} to the *cis* chamber (side of vesicle addition) stirring, and the presence of negatively-charged lipids in the bilayer. Fusion normally took place between 15-30 mins after the addition of vesicles in the presence of a *cis/trans* osmotic gradient. The microsomal protein concentration was again important and the addition of vesicles was titrated to give rise to single anion channels.

Calcium-activated K^+ channels such as maxi-K^+ could be readily incorporated in the presence of KCl (data not shown). Fusion of the microsomes also led to the incorporation of a different higher conductance Cl^- channel and also a very similar Cl^- channel to that found in rat brain. In general, it was more difficult to obtain channels from sheep brain microsomes and they had higher background "noise" than those obtained from rat brain microsomes. This may be due to a preponderence of contaminating small leak channels or possibly the lipids in the preparation had been oxidised. There were fewer single-channel fusions with the bilayer and the microsomes were only viable for up to 2 weeks at -70^{O}C.

A sheep brain ER anion channel was identified which seemed to be very similar to the rat brain channel. Typical traces at a range of holding potentials are shown in 450/50 Choline Cl *cis/trans* (Figure 4.1.1) and also an independent experiment recorded in 350/150 KCl (Figure 4.1.2). The single-channel conductance of the channel in 450/50 ChCl was 71 pS. The channel showed typical bursting gating behaviour observed in the rat brain channel but was much less active at positive holding potentials. An example of the higher conductance Cl^- channel was shown in 250/50 Choline Cl (Figure 4.1.3). Here the single-channel conductance was 115 pS. These currents were never seen in the rat brain microsomal fraction. As before, the potentials are quoted *cis* to *trans* (cytoplasm-lumen) and positive currents are shown as upward deflections. Although co-localisation experiments were not carried out on the sheep brain anion channel, similarities with the rat brain ER anion appears to suggest that the channel also originates from the ER.

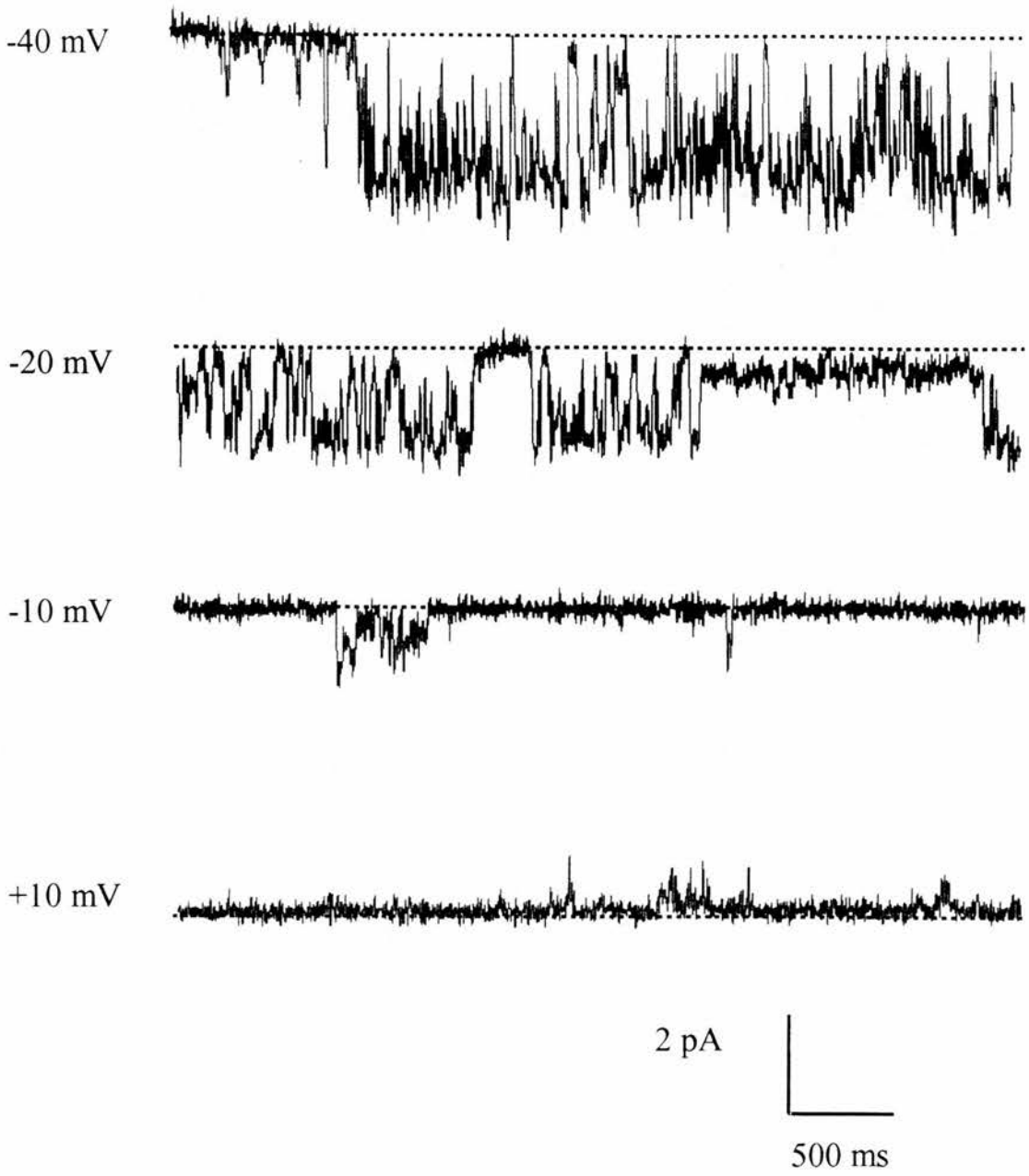

Figure 4.1.1 Single-channel recording of a sheep brain ER anion channel in Choline Cl. The conductance behaviour of a single anion channel is shown at a range of holding potentials in asymmetric 450 mM/50 mM Choline Cl, 5 mM Tris-HCl, pH 7.4. The closed levels are indicated (...). Low-pass filtered at 0.15 kHz.

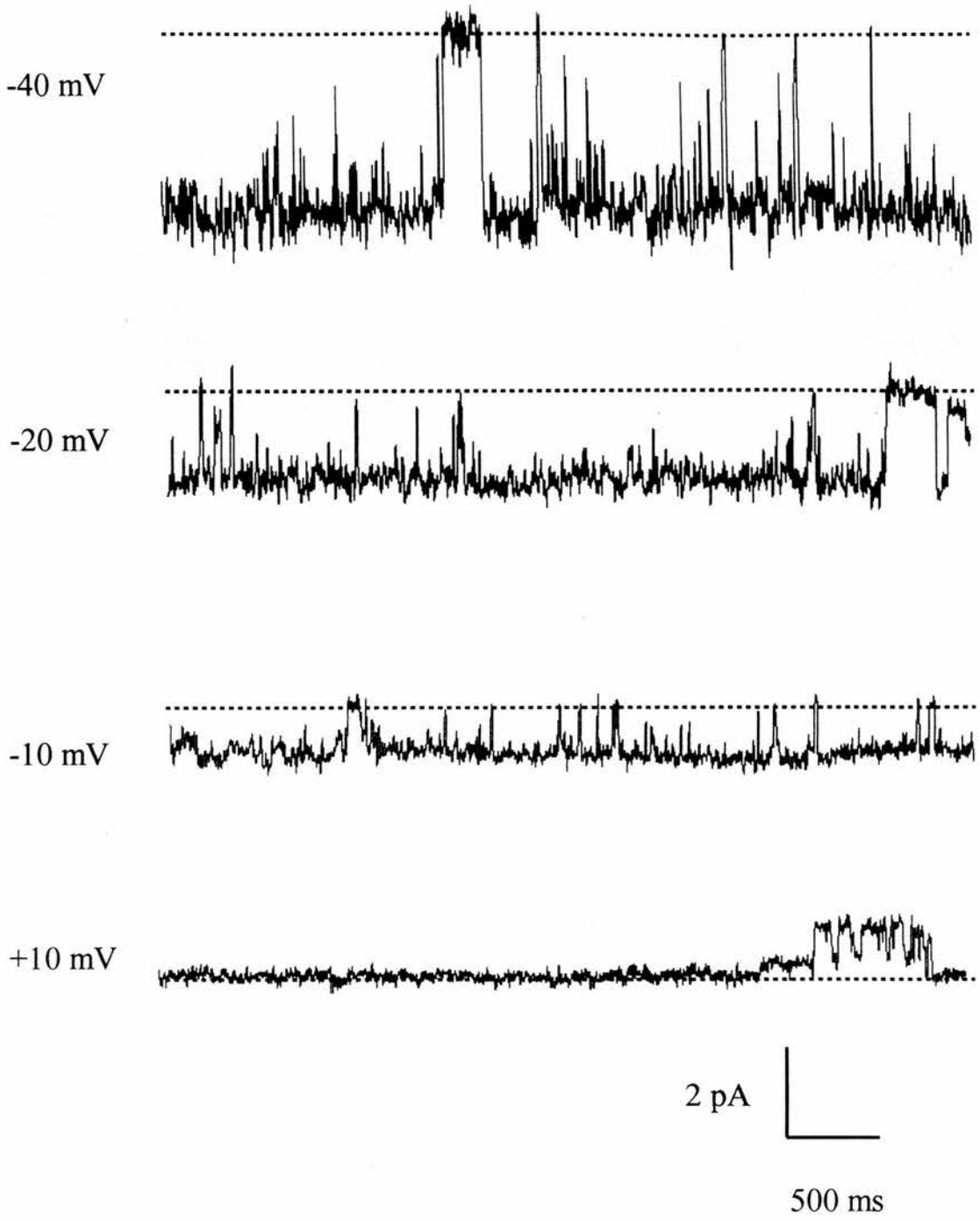

Figure 4.1.2 Single-channel recording of a sheep brain ER anion channel in KCl. The conductance behaviour of a single anion channel is shown at a range of holding potentials in asymmetric 350 mM/150 mM KCl, 5 mM Tris-HCl, pH 7.4. The closed levels are indicated (...). Low-pass filtered at 0.15 kHz.

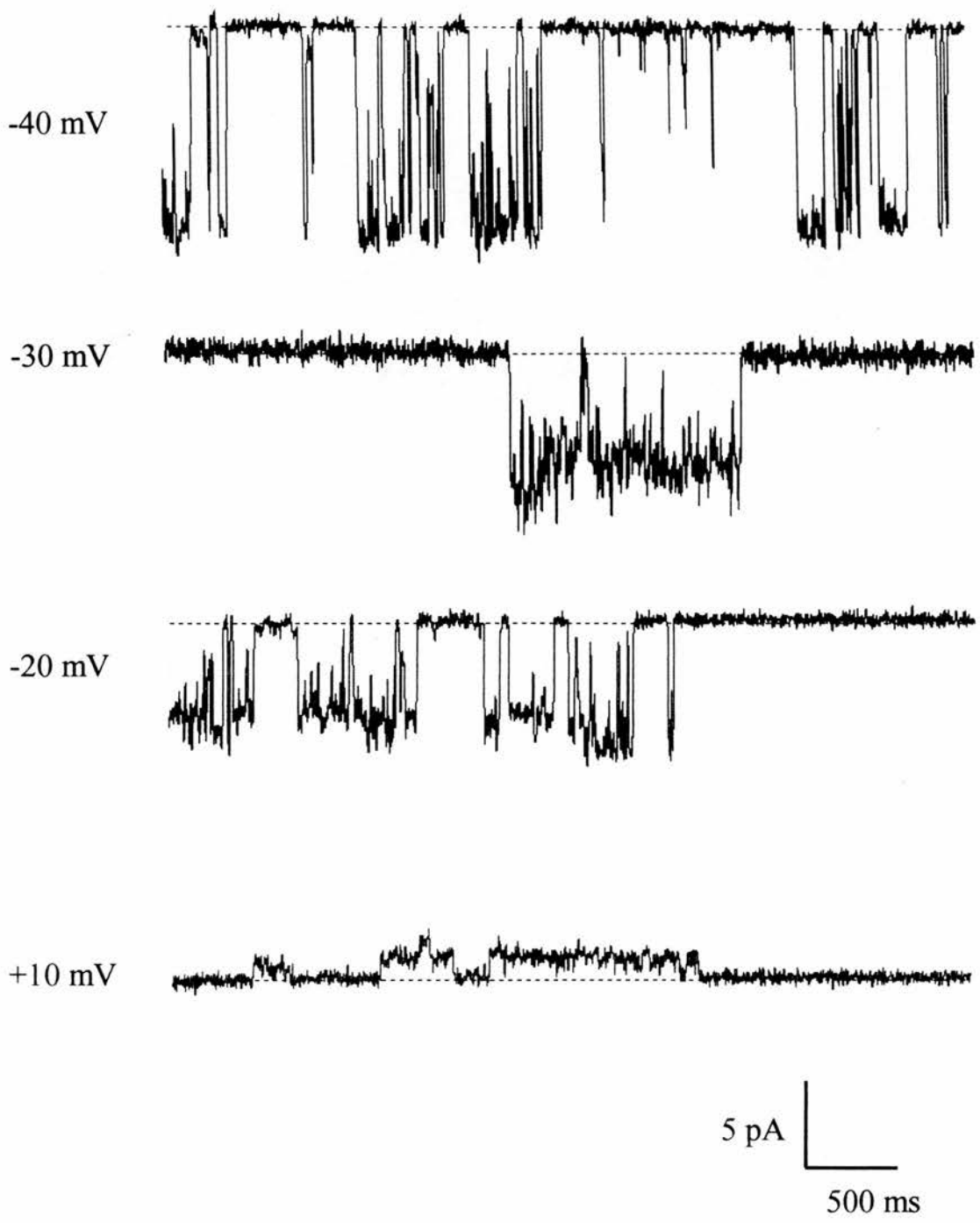

Figure 4.1.3 Single channel recording of a higher-conductance sheep brain anion channel in Choline Cl. The conductance behaviour of a single anion channel is shown at a range of holding potentials in asymmetric 250 mM/50 mM Choline Cl, 5 mM Tris-HCl, pH 7.4. The closed levels are indicated (...). Low-pass filtered at 0.15 kHz.

4.2 Substate behaviour of the sheep brain ER anion channel

One of the most striking similarities between the rat and sheep brain ER anion channels was their substate behaviour. The sheep ER channel also appears to display three subconductance levels at approximately 25%, 50% and 75% of the main open state, which were also difficult to capture in the same short section of recording. The closed, 25 %, 75 % and open states are shown in symmetric 250 mM Choline Cl (Figure 4.2.1, Panel A) and also the prevalence of the 50 % substate in another section of recording in the same conditions (Figure 4.2.1, Panel B).

4.3 Channel block

Cl^- channel blockers were used at concentrations known to have an effect on the rat brain ER anion channel. These blockers were stirred into either the *cis* or *trans* chambers, or both, and the block was characterised (Table 4.2.1). A detailed block analysis could not be carried out on the sheep brain channel due to difficulty in obtaining single channel data due to contaminating channels. A basic pharmacological screen was thus carried out as an inter-species comparison with the rat brain channel.

The most effective blockers of the rat brain channel (IAA-94, NPPB, DIDS and Zn^{2+}) were investigated on the sheep brain channel. DIDS was added to the *cis* chamber at 100 μM and completely blocked the channel (Figure 4.3.1, Panel A). Zn^{2+} also completely blocked the channel when added to the *cis* chamber at 1 mM (Figure 4.3.1, Panel B). Addition of NPPB at 100 μM to both chambers gave a flickery or "intermediate" time-dependent block (Figure 4.3.2) very similar to the block found in the rat brain channel (Figure 3.7.3).

A

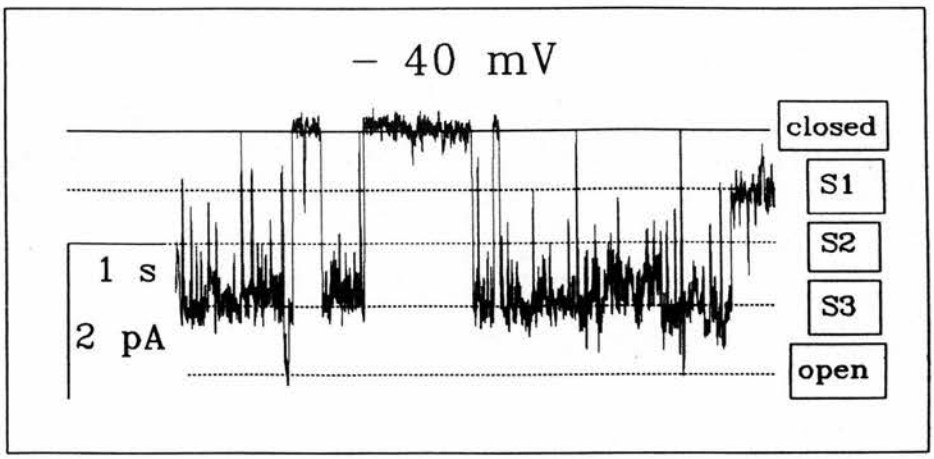

B

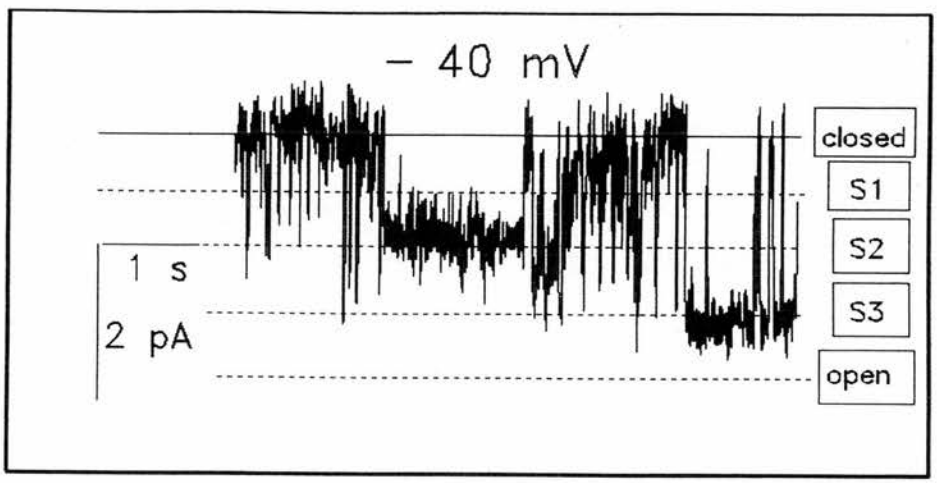

Figure 4.2.1 Substate levels of the sheep brain ER anion channel.
Panels A and B show a single channel at a holding potential of -40 mV in 250 mM symmetric Choline Cl, 5 mM Tris-HCl, pH 7.4. A continuous line is marked to show the closed state with dotted lines representing the substates and main open state. Low-pass filtered at 0.15 kHz.

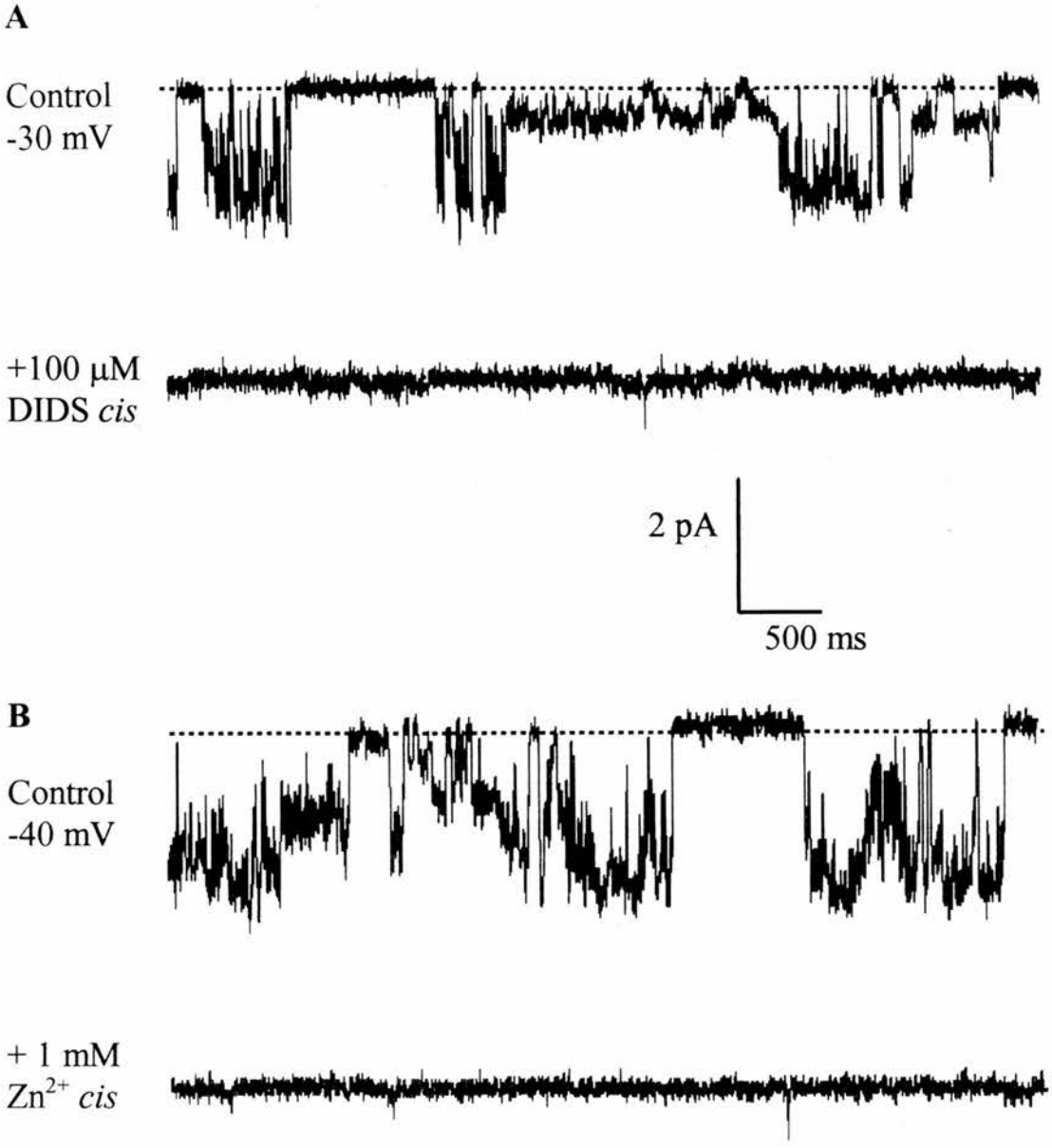

Figure 4.3.1 Channel block by DIDS and Zn^{2+}.
Panel A shows a single channel in symmetric 250 mM ChCl at -30 mV and Panel B shows an independent experiment in the same ionic conditions at -40 mV. The effect of adding 100 μM DIDS *trans* and 1 mM Zn^{2+} *cis* is shown. Closed levels are indicated (...). Low-pass filtered at 0.15 kHz.

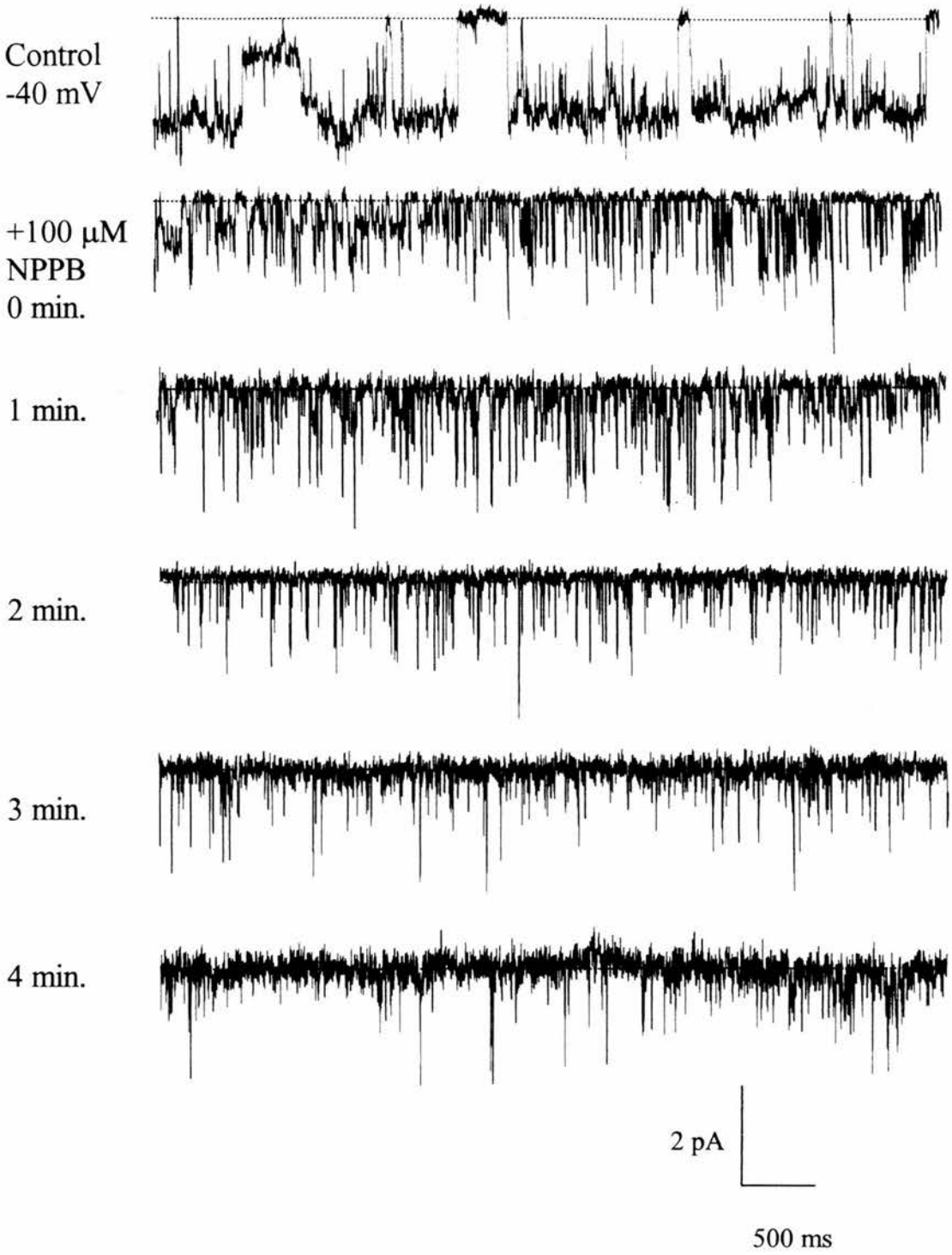

Figure 4.3.2 Time-dependence of NPPB block.
A single channel was recorded in symmetric 250 mM ChCl at -40 mV. 100 μM NPPB was added to both chambers and the time-dependent decrease in channel activity is shown. Closed levels are indicated (...). Low-pass filtered at 0.15 kHz.

IAA-94 was added to both chambers at 100 μM and induced a flickery or "intermediate" block (Figure 4.3.3). Unfortunately due to problems in obtaining single channel data due to noisy data, fewer single-channel fusions the dose-response and voltage dependence of IAA-94 block could not be investigated. The block obtained in the sheep brain ER channel for all the blockers tested was remarkably similar to that observed in the rat brain channel.

4.4 Development of other macroscopic assays

Other potential assay sytems were developed alongside the efflux assay to measure Cl^- transporting activity. Concentrative uptake assays have been described previously in systems with an abundance of Cl^- channels and used by Goldberg & Miller (1991).

4.4.1 Development of the concentrative uptake assay

The steps of the assay were to obtain essentially electrically "tight" liposomes for measurement of the concentrative uptake of $^{36}Cl^-$ through an ionophore or the Cl^- channel itself. Also, a good recovery of liposomes was required together with a high trapped volume. These criterion were monitored using the internal marker [^{3}H] inulin.

4.4.1.1 Formation of liposomes

Various combinations of lipids were tested in an attempt to form "tight" liposomes for the assay. PE (Nutfield lipid products, Surrey, U.K.), PE/PS (Nutfield), PC IVS (Sigma), PC IVS/PS (Sigma/Nutfield) at concentrations of 10 mg/ml were

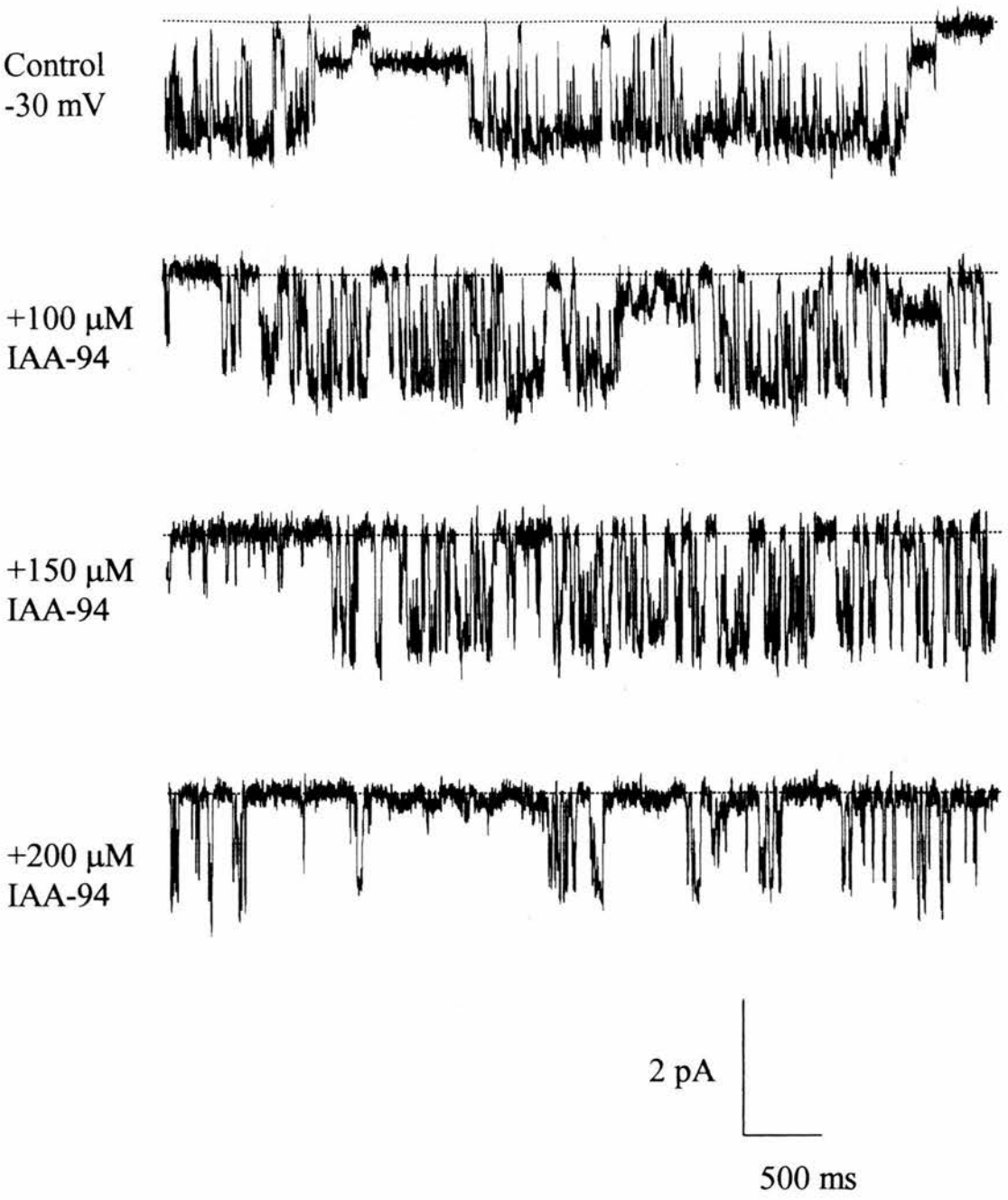

Figure 4.3.3 Channel block by IAA-94.
A single channel is shown in symmetric Choline Cl before and after adding sequential additions of IAA-94 to both chambers at the indicated concentration. Closed levels are shown (...). Low-pass filtered at 0.15 kHz.

Table 4.3.1 Effect of anion channel blockers on the sheep brain ER anion channel.

Inhibitor	Conc.	Block	Reversible	Sidedness	*n*
DIDS	15-100 μM	Complete	nd	*cis*	2
IAA-94	100 μM	Flickery	nd	*cis*	2
NPPB	100 μM	Flickery	nd	*cis* or *trans*	3
Zn^{2+}	0.5-1 mM	Fast/complete	nd	*cis*	6
	nd	nd	nd	*trans*	nd

+ = reversible, - = irreversible.
nd = not determined.
n= number of independent experiments

used, and were resuspended in 50 mM Tris-HCl before probe-sonicating on ice until the lipid suspension became translucent. Freeze-thaw sonication was used to form large unilamellar liposomes.

4.4.1.2 Removal of detergent.

To monitor the integrity of the liposomes and mimic the process of forming proteoliposomes the same lipid combinations were used and resuspended in 150 mM Tris-HCl, pH 7.4 containing 1.5 % (w/v) CHAPS. This was sonicated before passing through Sephadex (G50-F or G25-C columns) to remove CHAPS and form the liposomes. [^{3}H] Inulin was added as an internal marker to monitor the integrity of the liposomes through the steps. Both gels worked well.

4.4.1.3 Concentrative uptake assay

Exchanging the external Tris-HCl with Tris-glutamate was optimised by passing the liposomes through 1 ml of pre-swollen Biogel, Sephadex G50-F, Sephadex G50-C or Sephadex G25-C. The most efficient was found to be Sephadex G50-C. The object of this was to create an inside positive potential, and the liposomes were diluted five-fold in 50 mM Tris-Glutamate to ensure negligible Cl^- remained. 1μCi/ml $^{36}Cl^-$ was then added to the liposomes. Before scintillation-counting of $^{36}Cl^-$ in the liposomes the external Cl^- had to be removed. Removal was assessed with either a filter manifold or Dowex columns. At various time intervals 300 μl of liposomes were added to a double filter on a Millipore manifold and washed through with Tris-glutamate. Alternatively, 100 μl of liposomes were passed through 1 ml

equilibrated Dowex columns and washed with 1 ml Tris-glutamate. The eluate from the Dowex column or the dried filters were mixed with scintillation liquid and counted. A satisfactory concentrative uptake was not observed. In the absence of a purified Cl^- channel protein potential ionophores were used such as Tributyltin. This did not work as the compound was probably working as a Cl^-/OH^- exchanger rather than a problem with the assay itself.

4.5 Partial purification

The sheep brain microsomal membranes were solubilised with 1.5% (w/v) CHAPS and then passed through DE52 anion-exchange chromotography. Maximal Cl^- transporting activity was consistently found in proteoliposomes containing fractions n+1 to n+7 and these were pooled (Figure 4.5.1). Two peaks of activity were found after separation by Sephadex G-150 gel-exclusion chromatography and these were termed fraction I and fraction II (Figure 4.5.2). Proteoliposomes containing fraction II contained more Cl^- transporting activity and therefore fractions n+3,4,5 were pooled. Reconstitution of fraction I into planar lipid bilayers gave K^+ channels (Figure 4.5.3) which were not found in fraction II. Cl^- channels were not found in fraction I or II. An efflux assay on the active fractions after Sephadex G150 in the presence of the inhibitors NPPB, IAA-94 and DIDS showed no inhibition (Table 4.5.1). Other leak pathways may exist that were unaffected by the inhibitors. Molecular weight standards ran through Sephadex G150 indicate that the Cl^- activity exists at ~170 kDa. (Table 4.5.2) (data from S. Howell). A 7.5 % Coomassie-stain SDS-gel is shown (Figure 4.5.4). There is a diversity of proteins after the relatively

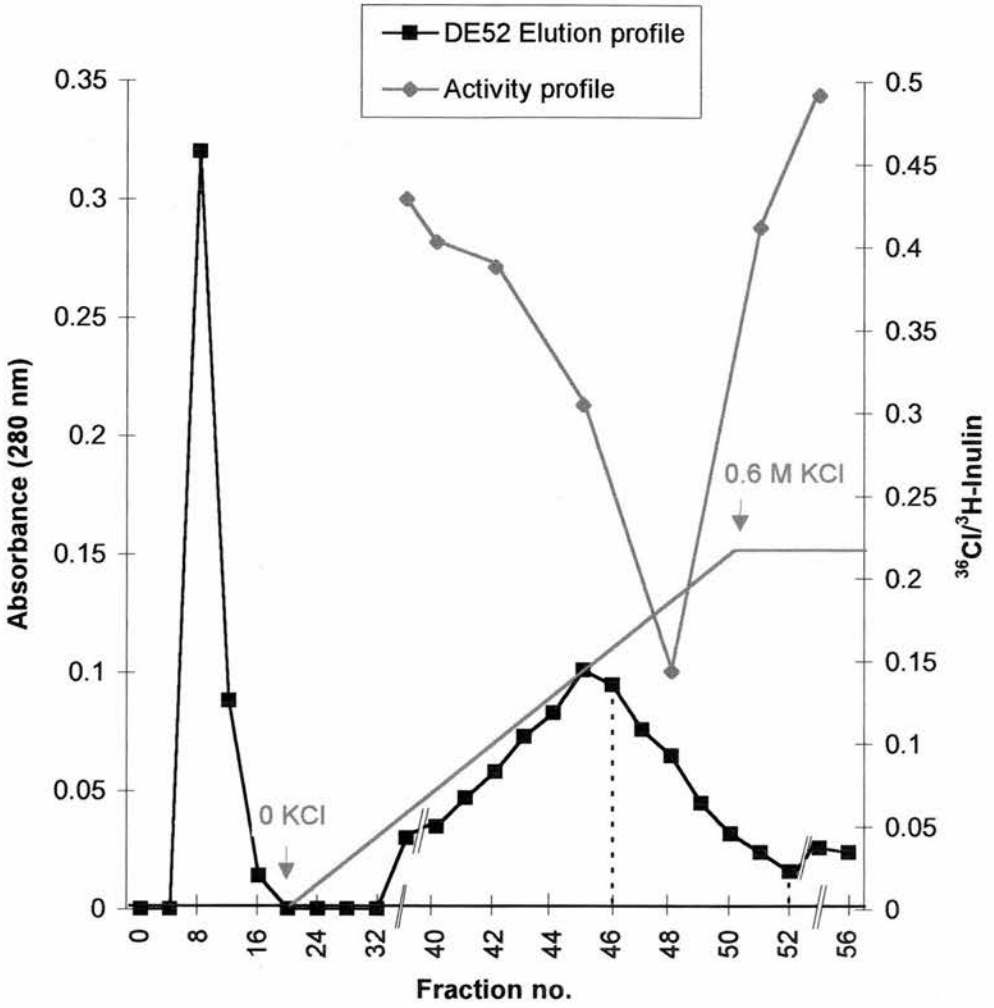

Figure 4.5.1 Elution and activity profile after DE52 anion-exchange column. Chromotography of CHAPS solubilised sheep brain microsomes is shown after DE52 column. Relative absorbances were read at 280 nm after elution with 0-600 mM KCl gradient. Maximal Cl^- transport activity was shown at fraction 48 and fractions 46 to 52 were pooled.

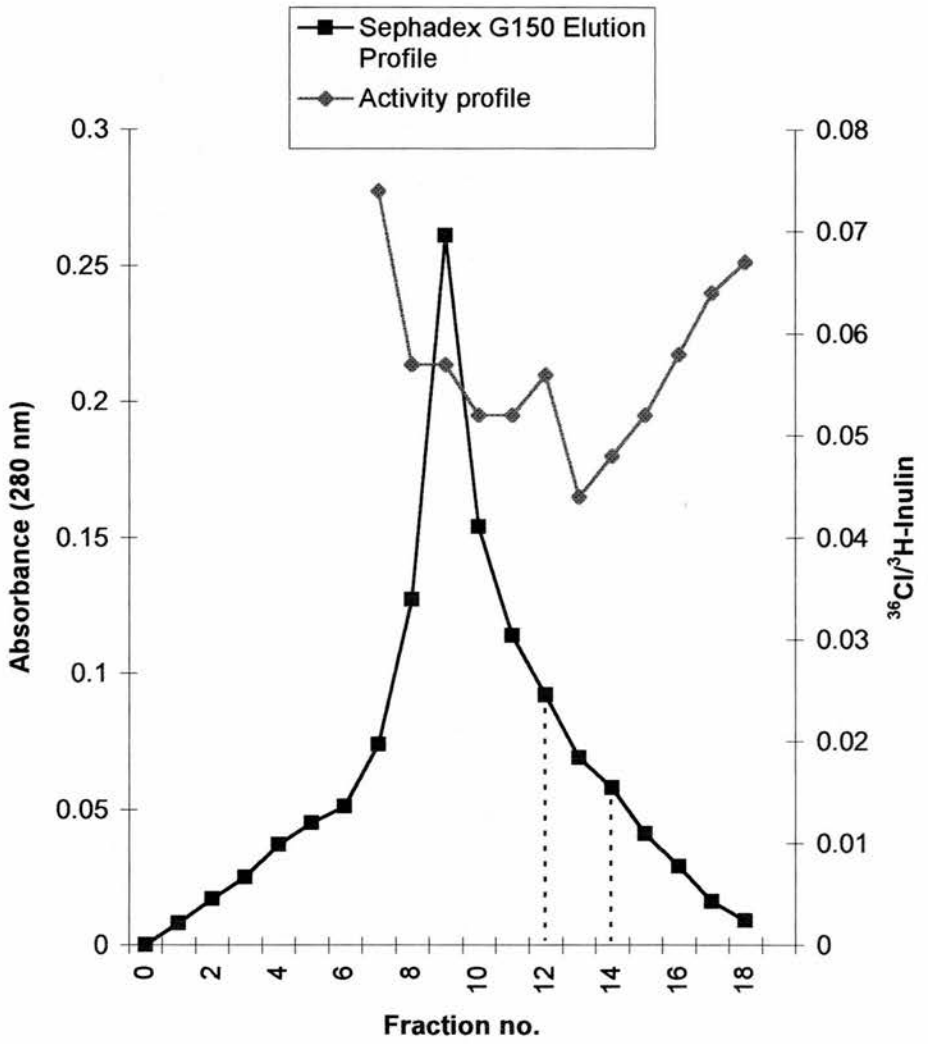

Figure 4.5.2 Elution and activity profile after Sephadex G150 gel exclusion column. Elution profile is shown with relative absorbances at 280 nm. Two peaks of activity were shown with maximal Cl^- transport activity at fraction 13. Fractions 12, 13 & 14 were pooled.

Sample	^{36}Cl (cpm)	[^{3}H]-inulin (cpm)	^{36}Cl/[^{3}H]-inulin	Efflux (%)
Direct Ct	176 214	16 345	-	-
Direct P	176 214	16 345	-	-
Ct	4 783	1 945	2.46	0
P	680	1 450	0.47	81
$P_{NPPB\ (100\ \mu M)}$	555	1 371	0.40	84
$P_{IAA\text{-}94\ (100\ \mu M)}$	858	1 869	0.46	81
$P_{DIDS\ (100\ \mu M)}$	944	2 178	0.43	83

Table 4.5.1 Example of an efflux assays with inhibitors after Sephadex G150. The ^{36}Cl and [^{3}H]-inulin values are an average of two points. Ct and P represent the controls and proteoliposomes which were normalised and cpm are the counts per minute.

Protein	Mr	log Mr	Ve (ml)	Ve/Vo
Cytochrome C	12.4	4.09	265.5	2.11
Carbonic anhydrase	29	4.46	247.5	1.96
Albumin	66	4.82	189	1.50
Alcohol dehydragenase	150	5.18	171	1.36
β-amylase	200	5.30	153	1.21
Dextran blue	Void volume	-	126	-
Fraction 13	170 (graph)	5.23	156	1.24

Table 4.5.2 Molecular weight sizing of active Cl^- transporting fraction
From these data a plot of Log Mr v. Ve/Vo gave the approximate molecular weight of the active fraction (molecular weights from S.Howell, unpublished observations). Where Ve is the elution volume and Vo is the void volume.

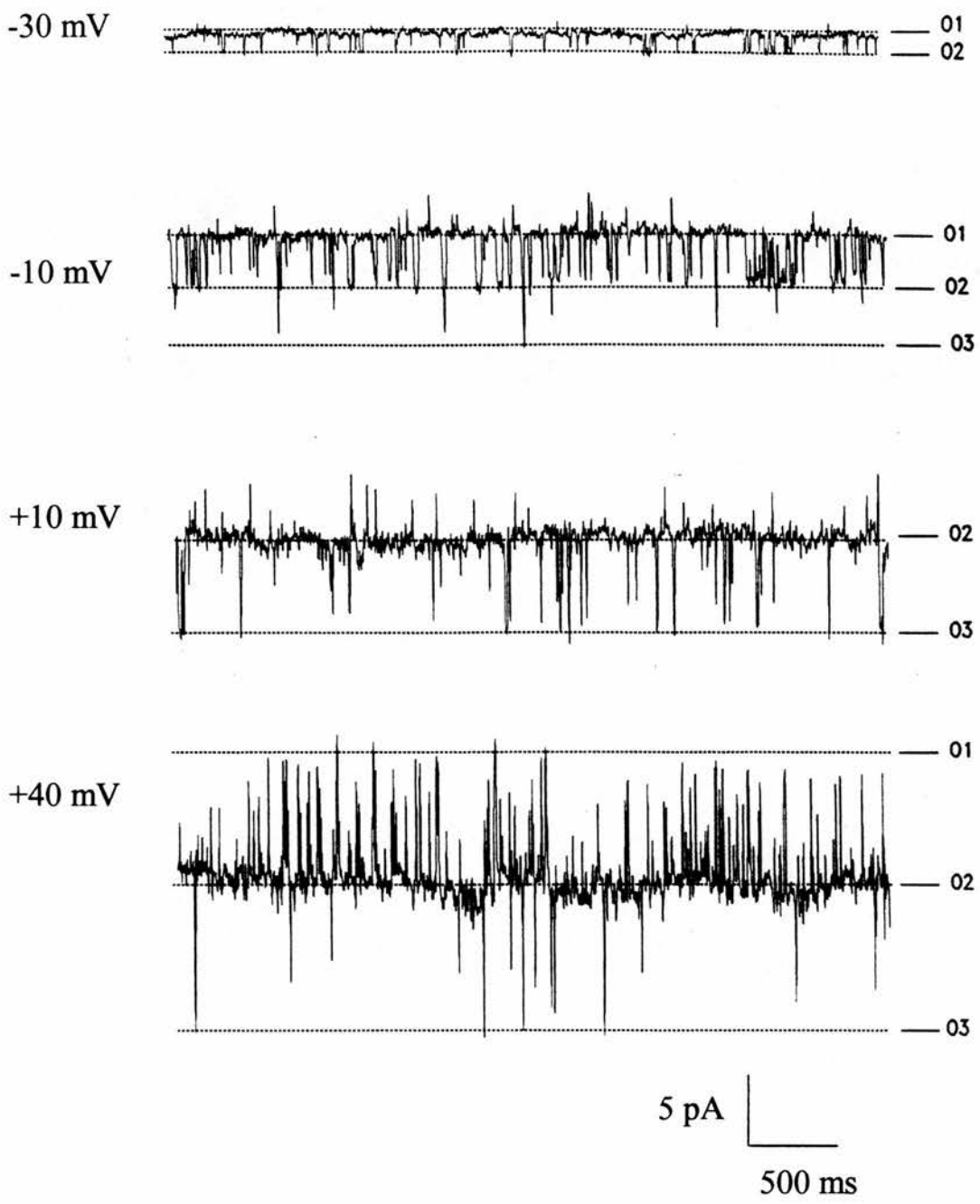

Figure 4.5.3 Reconstitution of proteoliposomes into planar lipid bilayers.
A multichannel recording of K^+ channels from Sephadex G-150 fraction I is shown at a range of holding potentials in asymmetric 450 mM/50 mM KCl, 5 mM Tris-HCl, pH 7.4. The open levels are indicated (...). Low-pass filtered at 0.15 kHz.

Figure 4.5.4 SDS-PAGE after partial purification.
A coomassie-stained 7.5 % gel is shown under reducing conditions. A, Mr markers, B, native membranes, C, solubilised membranes, D, active fraction after DE52 column, E, active fraction after sephadex G-150 column, F, active fraction after Concanavalin A column, G, Concanavalin A control.

simple 3-stage purification. The efflux assay gave compelling evidence of Cl^- transporting activity but it remains difficult to identify the proteins responsible for Cl^- efflux . The next stage of purification was Concanavalin A although the efflux diminished to 8 % in the most active 1M α-methylmannoside fraction (data not shown). The absence of a high-affinity ligand therefore made it very difficult to continue to select for the sheep brain ER anion channel.

4.6 Discussion

The basic properties of a sheep brain microsomal anion channel were investigated using planar lipid bilayers. The channel was of intermediate conductance, permeable to both anions and cations and possessed several subconductance states at approximately 25, 50 and 75% of the main open state. The channel was completely blocked by DIDS at 100 μM in the *cis* chamber (Figure 4.3.1, Panel A) and also by Zn^{2+} when added to the *cis* chamber at 1 mM (Figure 4.3.1, Panel B). These results were very similar to the rat brain anion channel and therefore the explanations of block were consistent with DIDS binding to lysine residues and Zn^{2+} with histidine or cysteine residues. When added to both chambers at 100 μM (Figure 4.3.2) NPPB gave a characteristic time-dependent block which was also observed in the rat brain ER channel over a 4 minute timescale. This could be explained in a similar fashion to the rat brain channel where it is believed NPPB partitions into the membrane due to its lipophilic nature. When 100 μM and 150 μM IAA-94 were added to both chambers an "intermediate" or flickery block was observed (Figure 4.3.3) which was very similar to that described in rat brain. Due to a lack of single-channel data resulting from co-incorporation of contaminating channels, including a higher-conductance Cl^- channel, relative anion & cation permeabilities and data for analysis of IAA-94 block were not obtained.

The results showing the presence of a similar anion channel from sheep brain microsomes facilitated the development of a partial purification protocol. Cl^- transporting activity was measured using an efflux assay and active fractions were pooled at n+1 to n+7 after DE52 anion-exchange chromotography and n +3,4,5 after

sephadex G150 gel-exclusion chromotography. There were two peaks of Cl^- channel activity after sephadex G150 and these were designated fraction I and fraction II. Inhibition of fraction II efflux using NPPB, IAA-94 and DIDS was unsuccessful probably due to leak pathways such as K^+ channels in the proteoliposomes. No Cl^- channels were reconstituted from fraction I or II in Choline Cl but K^+ channels were observed in fraction I in KCl. This may be explained by the fact KCl was a consistently better solution for fusion when compared with Choline Cl and proteoliposomes were also more difficult to fuse than native membranes probably due to the absence of attachment factors. The Cl^- transporting activity after sephadex G150 was shown to be present at ~170 kDa. using molecular weight sizing of the column. The coomassie gel does not support this evidence although it is possible that total efflux may result from a single Cl^- channel protein. The final stage of the purification consisted of Concanavalin A-sepharose B chromatography and the 1M α-methyl-mannoside eluted fraction contained some activity although this was greatly reduced. The Cl^- channel may not possess a glycoprotein moeity, and it was therefore difficult to obtain data beyond this point using standard biochemical techniques. A detailed study on the inhibition of these channels is needed to find a high-affinity ligand in the submicromolar range to further the purification (by affinity-chromatography) with the ultimate aim of molecular characterisation.

Overall, the sheep brain anion channel results when compared with the rat brain microsomal anion channel displayed remarkable similarities. The rat brain channel has been shown to be co-localised with ryanodine-sensitive Ca^{2+}-release channels in the ER. Although co-localisation experiments were not carried out with

the sheep brain microsomes it is so similar in its ionic conductance and substate behaviour would be reasonable to assume that the channel also originated from the ER.

Chapter 5

Final Discussion

5. Final Discussion

A novel rat brain anion channel has been characterised using voltage-clamping of planar lipid bilayers. They are present in brain ER and are co-localised with ryanodine-sensitive Ca^{2+}-release channels (Ashley, 1989). A novel sheep brain ER anion channel was also discovered and this was similar to the rat brain channel. The channels from rat and sheep brain microsomes incorporated into the bilayer usually after 15-30 mins of the addition of vesicles in the presence of Ca^{2+} and osmotic gradient. Channels were more difficult to obtain from sheep brain microsomes and generally had higher background "noise". The vesicles consistently fused in the outside-out configuration as co-localised Ca^{2+}-release channels from rat brain became incorporated with their binding sites for cytoplasmic ligands facing the *cis* chamber.

The brain ER channel was poorly-selective between anions and also discriminated poorly between anions and cations ($P_{Cl}/P_{Choline}$=3.2 +/-1.2). From exclusion sizing of the pore using permeant ions the minimum pore diameter was approximately 7 Å. The single channel conductance saturated at ~170 pS which was relatively lower than expected given the pore size. A considerably higher conductance would be expected and suggests the channel may have have an unusual permeation mechanism. The relatively poor fit of the conductance-concentration data (Figure 3.3.6) and the surprisingly low Km for Choline Cl argued against a one-ion pore. The concentration-dependence of relative anion-cation permeabilities suggests that the channel are possibly multi-ion pores with a transport mechanism in which anions and cations complex through the channel (Franciolini & Nonner, 1994). Data for the

sheep brain channel was limited but the conductance was very similar to the rat brain channel.

The rat brain channel behaves functionally as a "multimeric" complex with more than one conduction pathway (Matsuda *et al*, 1989). In this model the protomers would be identical and describes the substates at regular of nearly regular intervals. This is also the case in the sheep brain channel. It is possible that the substates may be due to changes that occur within a single pore (Dani & Fox, 1991) although in the rat brain channel binomial analysis strongly supports the "multimeric" model and together with the information that HEPES and other blockers interact with individual protomers reinforces the case.

The rat brain channel was blocked completely by 100μM DIDS and 1 mM Zn^{2+} and on a "slow" timescale by HEPES and frusemide. It was blocked on an intermediate timescale by 200 μM EA, 25-200 μM IAA-94, and 15-100 μM NPPB and on a "fast" timescale by 0.5 mM Zn^{2+}. These data led to an investigation into block of the sheep brain anion channel. DIDS, Zn^{2+}, IAA-94, & NPPB added at the same concentrations led to very similar modes of block. This information that a similar anion channel exists in sheep and was blocked with the same drugs led to a partial purification protocol being developed. Using a $^{36}Cl^-$ efflux assay transport activity was found after DE52, sephadex G150 but diminished after Concanavalin A. This suggested that the Cl^- channel protein did not possess a glycoprotein moeity. The fraction containing activity was sized after sephadex G150 and was found to be ~170 kDa. The identification of more potent inhibitors for use in an affinity column is needed before the purification can be advanced any further.

The physiological role of the brain ER Cl^- channel is currently unknown although it may be involved with a 'charge-compensating' mechanism primarily concerned with Ca^{2+}-uptake and release (Bayerdorffer *et al.*, 1984). It has been demonstrated in SR with work on the Ca-ATPase that potentials develop in liposomes without the presence of counter-ion channels although the ER has not been shown to be polarised. It is also unknown about membrane potential variations within the ER during Ca^{2+} release. Different pathways may allow counter-ion flow during Ca^{2+} release and reuptake and channels have been implicated including an intracellular double-barrelled Cl^- channel from rat liver ER (Morier & Sauvé, 1994). However, the voltage-dependence of the brain ER channel means that it is not maximally active to function as a charge compensator during Ca^{2+}-release. This is consistent with results found in some SR Cl^- channels (Kourie *et al.*, 1996a,b, Sukhareva *et al.*, 1994). Clues to the physiological function of the channel may be obtained from the relative lack of selectivity. Cations may also pass through the channel from lumen to cytoplasm and although physiologically it is not maximally active to do this it may be a back-up mechanism for charge-compensation. It is therefore possible that the brain ER anion channel plays an important role in charge-compensating the positive luminal potential produced through the calcium pump during calcium loading.

These novel anion channels from rat and sheep brain microsomes are very likely to be present in the ER membrane. The rat brain channel can be characterised as poorly-selective between anions and cations and also discriminates poorly between different anions. It has characteristic subconductance behaviour and functions as a "multimer" composed of four protochannels. Individual protomers could be blocked

on a "slow" timescale and the channel gating was well described by the binomial equation. The basic characteristics of the sheep brain channel showed striking similarities to the rat brain channel and it is possible that these intracellular Cl^- channels exist in mammalian brain with conserved physiological roles.

References

Ackerman, M.J., Wickmamn, K.D., & Clapham, D.E. 1994. Hypotonicity activates a native chloride current in *Xenopus* oocytes. *J. Gen. Physiol.* **103**, 153-179.

Alvarez, O. 1986. How to set up a bilayer system. In *Ion Channel Reconstitution,* ed. Miller, C. pp. 115-130. Plenum, New York.

Anderson, M.P., Gregory, R.J., Thompson, S., Souza, D.W., Paul, S., Mulligan, R.C., Smith, A.E., & Welsh, M.J. 1991. Demonstration that CFTR is a chloride channel by alteration of its ion selectivity. *Science* **253**, 202-205.

Aprison, M.H. 1978. Glycine as a neurotransmitter. In *Psychopharmacology: A generation of progress,* ed. Lipton, M.A., Di Massio, A., & Killam, K.F. pp. 333-346. Raven, New York.

Ashley, R.H. 1995. Intracellular calcium channels. In *Essays in Biochemistry* **30**, pp. 98-117.

Ashley, R. H. 1989. Activation and conductance properties of ryanodine-sensitive calcium channels from brain microsomal membranes incorporated into planar lipid bilayers. *J.Membr.Biol.* **111**, 179-189.

Attali, B., Guillemare, E., Lesage, F., Honoré, E., Romey, G., Lazdunski, M., & Barhanin, J. 1993 The protein IsK is a dual activator of K^+ and Cl^- channels. *Nature* **365**, 850-852.

Bader, C.R., Bertrand, D. & Schwartz, E.A. 1982. Voltage-activated and calcium-activated currents studied in solitary rod inner segments from the

salamander retina. *J. Physiol.* **331**, 253-284.

Bae, H.-R. & Verkman, A.S. 1990. Protein kinase A regulates chloride conductance in endocytic vesicles from proximal tubule. *Nature* **348**, 637-639.

Barhanin, J., Lesage, F., Guillemare, E., Fink, M., Lazdunski, M. & Romey, G. 1996. K_vLQT1 and IsK (minK) proteins associate to form the I_{Ks} cardiac potassium current. *Nature* **384**, 78-80.

Bauer, C. K., Steinmeyer, K., Schwarz, J. R. & Jentsch, T. J. 1991. Completely functional double-barrelled chloride channel expressed from a single *Torpedo* cDNA. *Proceedings of the National Academy of Sciences of the United States of America* **88**, 11052-11056.

Bayerdörffer, E., Streb, H., Eckhardt, L., Haase, W. & Schulz, I. 1984. Characterisation of calcium uptake into rough endolasmic reticulum of rat pancreas. *J. Membr. Biol.* **81**, 69-82.

Bégault, B., Anagnostopoulos, T. & Edelman, A. 1993. ATP-regulated chloride conductance in endoplasmic reticulum (ER)-enriched pig pancreas microsomes. *Biochim. Biophys. Acta* **1152**, 319-327.

Benz, R. 1994. Permeation of hydrophilic solutes through mitochondrial outer membranes. Review on mitochondrial porins. *Biochim. Biophys. Acta* **1197**, 167-196.

Berridge, M. J. 1993. Inositol trisphosphate and calcium signalling. *Nature* **361**, 315-325.

Betz, H., 1992. Structure and function of the inhibitory glycine receptor. *Q. Rev.*

Biophys. **25**, 381-394.

Blachly-Dyson, E., Peng, S., Colombini, M. & Forte, M. 1990. Selectivity changes in site-directed mutants of the VDAC ion channel: Structural implications. Science **247**, 1233-1236.

Blatz, A. L. 1991. Properties of single functional chloride channels from rat cerebral cortex neurones. *J.Physiol.* **441**, 1-21.

Blatz, A. L. & Magleby, K. L. 1983. Single voltage-dependent chloride-selective channels of large conductance in cultured rat muscle. *Biophys. J.* **243**, 237-241.

Blatz, A. L. & Magleby, K. L. 1985. Single chloride-selective channels active at resting membrane potentials in cultured rat skeletal muscle. *J.Physiol.* **47**, 119-123.

Brandt, S. & Jentsch, T.J. 1995. ClC-6 and ClC-7 are two novel broadly expressed members of the CLC chloride channel family. *FEBS Letters* **377**, 15-20.

Bureau, M.H., Khrestchatisky, M., Heeren, M.A., Zambrowicz, E.B., Kim, H., Grisar, T.M., Colombini, M., Tobin, A.J. & Olsen, R.W. 1992. Isolation & cloning of a voltage-dependent anion channel-like Mr 36,000 polypeptide from mammalian brain. *J. Biol.Chem.* **267**, 8679-8684.

Buyse, G., Voets, T., Tytgat, J., De Greef, C., Droogmans, G., Nilius, B., & Eggermont, J. 1997. Expression of human pI_{Cln} and ClC-6 in *Xenopus* oocytes induces an identical endogenous chloride conductance. *J. Biol. Chem.* **272**, 3615-3621.

Cabantchik, Z.I. & Greger, R. 1992. Chemical probes for anion transporters of mammalian cell membranes. *Am. J. Physiol.* **262** *(Cell Physiol. 31-4)*, C803-C827.

Cahalan, M.D. & Lewis, R.S. 1988. Role of potassium and chloride channels in volume regulation by T-lymphocytes. In *Cell Physiology of Blood,* ed. Gunn, R.B., & Parker, J.C., pp. 281-301. Rockefeller University Press, New York.

Cahalan, M.D. & Lewis, R.S. 1994. Regulation of chloride channels in lymphocytes. In *Current Topics in Membranes and Transport*, ed. Guggino, W., pp. 281-301. Academic Press, New York.

Chua, M. & Betz, W.J. 1991. Characterisation of ion channels on the surface membrane of adult rat skeletal muscle. *Biophys. J.* **59**, 1251-1260.

Cohen, F. S. 1986. Fusion of liposomes to planar bilayers. In *Ion Channel Reconstitution,* ed. Miller, C. pp. 131-139. Plenum, New York.

Colombini, M. 1979. A candidate for the permeability pathway of the outer mitochondrial membrane. *Nature* **279**, 643-645.

Colombini, M. 1994. Anion channels in the mitochondrial outer membrane. *Chloride Channels: Curr.Top.Membr.* **42**, 73-101.

Colquhoun, D. & Sigworth, F.J. 1983. Fitting and statistical analysis of single-channel records. In *Single-Channel Recording*, 1st edn., ed. Sakmann, B. & Neher, E., Plenum, NY, pp. 191-263.

Cotman, C. W. 1974. Isolation of synaptosomal and synaptic plasma membrane fractions. *Meth.Enzymol.* **31**, 445-452.

Cutting, G.R., Lu, L., O'Hara, B.F., Kasch, L.M., Montrose-Rafizadeh, C., Donovan, P.M., Shimada, S., Antonarakis, S.E., Guggino, W.B., Uhl, G.R. & Kazazian, H.H. Cloning of the gamma-aminobutyric acid (GABA) rho1 cDNA: A GABA receptor subunit highly expressed in the retina. 1991. *Proc. Natl.Acad.Sci.* USA **88**, 2673-2677.

Dani, J. A. & Fox, J. A. 1991. Examination of subconductance levels from a single ion channel. *J.Theor.Biol.* **153**, 401-423.

DeBin, J.A., Wood, M.R., Pfenninger, K.H. & Strichartz, G.R. 1994. A chloride channel reconstituted from fetal rat brain growth cones. *J. Membr. Biol.* **141**, 7-19.

De Pinto, V. & Palmieri, F. 1992. Transmembrane arrangement of mitochondrial porin or voltage-dependent anion channel (VDAC). *J. Bioenenerg. Biomembr.* **24**, 21-26.

Diaz, M., Valverde, M.A., Higgins, C.F., Rucareanu, C. & Sepulveda, F.V. 1992. *Pflugers Arch.* **422**, 347-353.

Doring, C. & Colombini, M. 1985. Voltage dependence and ion selectivity of the mitochondrial channel, VDAC, are modified by succinic anhydride. *J. Membr. Biol.* **83**, 81-86.

Duszyk, M., Liu, D., French, A.S. & Man, S.F.P. 1995. Evidence that pH-titratable groups control the activity of a large epithelial chloride channel. *Biochem. Biophys. Res. Commun.* **215**, 355-360.

Ehring, G.R., Osipchuk, Y.V. & Cahalan, M.D. 1994. Swelling-activated chloride

channels in multidrug-sensitive and -resistant cells. *J. Gen. Physiol.* **104**, 1129-1161.

Evans, M.G. & Marty, A. 1986. Calcium-dependent chloride currents in isolated cells from rat lacrimal glands. *J. Physiol.(London)* **378**, 437-460.

Feigenspan, A., Wassle, H. & Bormann, J. 1993. Pharmacology of GABA-receptor Cl^- channels in rat retinal bipolar cells. *Nature* **361**, 159-164.

Fischer, H., Illek, B. & Machen, T.E. 1995. The actin filament disrupter cytochalasin D activates the recombinant cysic fibriosis transmembrane conductance regulator Cl^- channel in mouse 3T3 fibroblasts. *J. Physiol.* **489.3**, 745-754.

Fisher, S.E., Van Bakel, I., Lloyd, S.E., Pearce, S.H.S., Thakker, R.V. & Craig, I.W. 1995. Cloning and characterisation of CLCN5, the human kidney chloride channel gene implicated implicated in Dent disease (an X-linked hereditary nephrolithiasis). *Genomics* **29**, 598-606.

Franciolini, F. & Nonner, W. 1987. Anion and cation permeability of a chloride channel in rat hippocampal neurones. *J.Gen.Physiol.* **90**, 453-478.

Franciolini, F. & Nonner, W. 1994. A multi-ion permeation mechanism in neuronal background chloride channels. *J.Gen.Physiol.* **104**, 725-746.

Frizzell, R.A. & Halm, D.R. 1990. Chloride channels in epithelial cells (chapter 8, vol 37) in *Channels and Noise in Epithelial Tissues*, ed. Bronner, F., Helman, S.I. & van Driessche, W. Academic Press, New York.

Glickman, J., Croen, K., Kelly, S., & Al-Awqati, G. 1983. Golgi membranes contain an electrogenic H^+ pump in parallel to a chloride conductance. *J. Cell. Biol.*

97, 1303-1308.

Goldberg, A.F.& Miller, C. 1991. Solubilisation and functional reconstitution of a chloride channel from *Torpedo californica* electroplax. *J. Membr. Biol.* **124**, 199-206.

Gray, P.T.A., Bevan, S. & Ritchie, J.M. 1984. High conductance anion-selective channels in rat cultured Schwann cells. *Proc.R.Soc.Lond.(Biol.)* **221**, 395-409.

Gray, M.A., Plant, S. & Argent, B.E. 1993. cAMP-regulated whole cell chloride currents in pancreatic duct cells. *Am. J. Physiol.* **264** *(Cell Physiol. 33)*, C591-C602.

Greger, R., Schlatter, E. & Gögelein, H. 1987. Chloride channels in the luminal membrane of the rectal gland of the dogfish (*Squalas acanthias*). Properties of the 'larger' conductance channel. *Pflugers Arch.* **409**, 114-121.

Grenningloh, G., Schmeiden, V., Schofield, P.R., Seeburg, P.H., Siddiqque, T., Mohandas, T.K., Becker, C.-M. & Betz, H. 1990a. Alpha subunit variants of the human glycine receptor: primary structures, functional expression and chromosomal localization of the corresponding genes. *EMBO J.* **9**, 771-776.

Grenningloh, G., Pribilla, I., Prior, P., Multhaup, G., Beyreuther, K., Taleb, O. & Betz, H. 1990b. Cloning and expression of the 58 kd beta subunit of the inhibitory glycine receptor. *Neuron* **4**, 963-970.

Grinstein, S., Clarke, C.A., Dupre, A. & Rothstein, A. 1982. Volume-induced

increase of anion permeability in human lymphocytes. *J.Gen. Physiol.* **80**, 801-823.

Gründer, S., Thiemann, A., Pusch, M. & Jentsch, T.J. 1992. Regions involved in the opening of ClC-2 chloride channel by voltage & cell volume. *Nature Lond.* **360**, 759-763.

Guinamard, R., Paulais, M. & Teulon, J. 1995. Inhibition of a small-conductance cAMP-dependent Cl^- channel in the mouse thick ascending limb at low internal pH. *J. Physiol.* **490.3**, 759-765.

Hall, S.K., Zhang, J. & Lieberman, M. 1995. Cyclic AMP prevents activation of a swelling-induced chloride-sensitive conductance in chick heart cells. *J.Physiol.* **488.2**, 359-369.

Hall, Z.W. 1992. In *An Introduction to Molecular Neurobiology*, ed. Hall Z.W., p10. Sinauer, Sunderland, MA..

Hanrahan, J. W. & Tabcharini, J. A. 1990. Inhibition of an outwardly rectifying anion channel by HEPES and related buffers. *J.Membr.Biol.* **116**, 65-77.

Hayman, K. A. & Ashley, R. H. 1993. Structural features of a multisubstate cardiac mitoplast anion channel: inferences from single-channel recording. *J.Membr.Biol.* **136**, 191-197.

Hill, D.R. & Bowery, N.G. 1981. ^{3}H-baclofen and^{3}H-GABA bind to bicuculline-insensitive $GABA_B$ sites in rat brain. *Nature* **290**, 149-152.

Hille, B. 1984. Elementary properties of pores. In *Ionic Channels of Excitable Membranes,* pp. 181-204. Sinauer, Sunderland, MA.

Howell, S., Duncan, R.R. & Ashley, R.H. 1996. Identification and characterisation of a homologue of p64 in rat tissues. *FEBS Lett.* **390**, 207-210.

Ide, T., Sakamoto, H., Morita, T., Taguchi, T., & Kasai, M. 1991. Purification of a Cl^--channel protein of sarcoplasmic reticulum by assaying the channel activity in the planar bilayer system. *Biochem. Biophys. Res. Commun.* **176**, 38-44.

Jentsch, T.J., Günther, W., Pusch, M. & Schwappach, B. 1995. Properties of voltage-gated chloride channels of the ClC gene family. *J. Physiol.* **482.P**, 19-25S.

Jentsch, T.J., Steinmayer, K. & Schwarz. G. 1990. Primary structure of *Torpedo marmorata* chloride channel isolated by expression cloning in *Xenopus* oocytes. *Nature Lond.* **348**, 510-514.

Johnston, G.A.R. 1994. GABA receptors : As complex as ABC?. *Clin. Exp. Pharmacol. Physiol* **21**, 521-526.

Kasai, M. & Kometani, T. 1979. Inhibition of anion permeability of sarcoplasmic reticulum vesicles by 4-acetamido-4-isothiocyanatostilbene-2,2-disulfonate. *Biochim. Biophys. Acta.* **557**, 243-247.

Kawano, S., Nakamura, F., Tanaka, T. & Hiraoka, M. 1992. Cardiac sarcoplasmic reticulum chloride channels regulated by protein kinase A. *Circ.Res.* **71**, 585-589.

Kawasaki, M., Uchida, S., Monkawa, T., Miyawaki, A., Mikoshiba, K., Marumo, F. & Sasaki, S. 1994. Cloning and expression of a protein kinase C-regulated chloride channel abundantly expressed in rat brain neuronal cells. *Neuron* **12**,

597-604.

Kemmer, T.P., Bayerdörffer, E., Will, H. & Schulz, I. 1987. Anion dependence of Ca^{2+} transport amd (Ca^{2+}+K^{+})- stimulated Mg^{2+}-dependent transport ATPase in rat pancreatic endoplasmic reticulum. *J. Biol. Chem.* **202**, 13758-13764.

Kleene, R., Pfanner, N., Pfaller, R., Link, T.A., Sebald, W., Neupart, W. & Tropschug, M. 1987. Mitochondrial porin of *Neurospora crassa*. cDNA cloning, *in vitro* expression and import into mitochondria. *EMBO J.* **6**, 2627-2633.

Koumi, S.-I., Sato, R. & Aramaki, T. 1995. Activation of the plasma membrane chloride channel by protein kinase C in isolated guinea-pig hepatocytes. *J. Physiol.* **487.2**, 379-394.

Kourie, J.I., Laver, D.R., Junankar, P.R., Gage, P.W. & Dulhunty, A.F. 1996a. Characteristics of two types of chloride channel in sarcoplasmic reticulum vesicles from rabbit skeketal muscle. *Biophys. J.* **70**, 202-221.

Kourie, J.I., Laver, D.R., Ahern, G.P. & Dulhunty, A.F. 1996b. A calcium-activated chloride channel in sarcoplasmic reticulum vesicles from rabbit skeletal muscle. *Am. J. Physiol.* **270** (Cell Physiol. 39), C1675-C1686.

Kowdley, G.C., Ackerman, S.J., John, J.E., Jones, L.R. & Moorman, J.R. 1994. Hyperpolarization-activated chloride currents in *Xenopus* oocytes. *J. Gen. Physiol.* **103**, 217-230.

Krapivinsky, G.B., Ackerman, M.J., Gordon, E.A., Krapivinsky, L.D. & Clapham, D.E. 1994. Molecular characterisation of a sweeling-induced chloride

conductance regulatory protein, pI_{Cln}. *Cell* **76**, 439-448.

Kubo, M. & Okada, Y. 1992. Volume-regulatory Cl channel currents in cultured human epithelial cells. *J. Physiol.* **456**, 351-371.

Kuhse, J., Schmieden, V. & Betz, H. 1990. A single amino acid exchange alters the pharmacology of neonatal rat glycine receptor subunit. *Neuron* **5**, 867-873.

Kunzelmann, K., Pavenstadht, H. & Greger, R. 1989. Properties and regulation of chloride channels in cystic fibrosis and normal airway cells. *Pflügers Arch.* **415**, 172-182.

Kürz, L.L., Wagner, S., George Jr., A.L., & Rüdel, R. 1997. Probing the major skeletal muscle chloride channel with Zn^{2+} and other sulfhydryl-reactive compounds. *Pflügers Arch.* **433**, 357-363.

Labarca, P. & Lattorre, R. 1992. Insertion of ion channels into planar lipid bilayers by vesicle fusion. *Meth.Enzymol.* **207**, 447-463.

Landry, D. W., Akabas, M. A., Redhead, C. & Al-Awqati, Q. 1990. Purification and reconstitution of epithelial chloride channels. *Meth.Enzymol.* **191**, 572-582.

Landry, D.W., Akabas, M.H., Redhead, C., Edelman, A., Cragoe, E.J., Jr., & Al-Awqati, Q. 1989. Purification and reconstitution of chloride channels from kidney and trachea. *Science* **244**, 1469-1472.

Landry, D. W., Reitman, M., Cragoe, E. R. & Al-Awqati, Q. 1987. Epithelial chloride channels: development of inhibitory ligands. *J.Gen.Physiol.* **90**, 779-798.

Landry, D., Sullivan, S., Nicolaides, M., Redhead, C., Edelman, A., Field, M., Al-

Awqati, Q. & Edwards, J. 1993. Molecular cloning and characterisation of p64, a chloride channel protein from kidney microsomes. *J. Biol. Chem.* **268**, 14948- 14955.

Lewis, T.M., Roberts, M.L. & Bretag, A.H. 1994. Immunolabelling for VDAC, the mitochondrial voltage-dependent anion channel on sarcoplasmic reticulum from amphibian skeletal muscle. *Neurosci. Lett.* **181**, 83-86.

Lloyd, S.E., Pearce, S.H.S., Fisher, S.E., Steinmeyer, K., Schwappach, B., Scheinman, S.J., Harding, B., Bolino, A., Devoto, M., Goodyer, P., Rigden, S.P.A., Wrong, O., Jentsch, T.J., Craig, I.W., & Thakker, R.V. 1996. A common molecular basis for three inherited kidney stone diseases. *Nature* **379**, 445-449.

Loo, D.D.F., Zeuthen, T., Chandy, G. & Wright E.M. 1996. Cotransport of water by the Na^+/glucose cotransporter. *Proc. Natl.Acad. Sci.* USA **93**, 13367-13370.

Ludwig, O., De Pinto, V., Palmieri, F. & Benz, R. 1986. Pore formation by the mitochondrial porin of rat brain in lipid bilayer membranes. *Biochim. Biophys. Acta.* **860**, No. 2, 268-276.

Ludewig, U., Pusch, M. & Jentsch, T.J. 1996. Two physically distinct pores in the dimeric ClC-0 chloride channel. *Nature* **383**, 340-343.

MacDonald, R.L. & Olsen, R.W. 1994. $GABA_A$ receptor channels. *Annu. Rev. Neurosci.* **17**, 569-602.

Malenka, R.C., Madison, D.V. & Nicoll, R.A. 1986. Potentiation of synaptic transmission in the hippocampus by phorbol esters. *Nature* **321**, 175-177.

Malinowska, D.H., Kupert, E.Y., Bahinski, A., Sherry, A.M. & Cuppoletti, F. 1995. Cloning, functional expression, and characterization of a PKA-activated gastric Cl^- channel. *Am. J. Physiol.* **268** (*Cell Physiol. 37*), C191-C200.

Mannella, C.A. 1990. Structural analysis of mitochondrial pores. *Experientia*, **46**, 137-145.

Marten, I., Busch, H., Rashke, K., & Hedrich, R. 1993. Modulation and block of the plasma membrane anion channel of guard cells by stilbene derivatives. *Biophys. J.* **21**, 403-408.

Martin, C. & Ashley, R. H. 1993. Reconstitution of a voltage-activated calcium conducting cation channel from brain microsomes. *Cell Calcium* **14**, 427-438.

Martinac, B., Buechner, M., Delcour, A.H., Adler, J. & Kung, C. 1987. Pressure-sensitive ion channel in *Escherichia coli. Proc. Natl. Acad. Sci.* USA **84**, 2297-2301.

Mason, S.J., Paradiso, A.M. & Boucher, R.C. 1991. Regulation of transepithelial ion transport and intracellular calcium by extracellular ATP in human normal and cystic fibrosis airway epithelium. *Br. J. Pharmacol.* **103**, 1649-1656.

Matsuda, H., Matsuura, H. & Noma, A. 1989. Triple-barrelled structure of inwardly-rectifying K^+ channels revealed by Cs^+ and Rb^+ block in guinea-pig heart cells. *J.Physiol.(Lond)* **413**, 139-157.

Matsuoka, T., Nishizaki, T. & Ikeuchi, Y. 1996. Regulation of the serum-activated Ca^{2+}-dependent chloride channel on *Xenopus* oocytes. *Biochem. Biophys. Res. Commun.* **218**, 633-637.

Meldolesi, L., Madeddu, L. & Pozzan, T. 1990. Intracellular Ca^{2+} storage organelles in non-muscle cells: heterogeneity and functional assignment. *Biochim. Biophys.Acta* **1055**, 130-140.

Middleton, R.E., Pheasant, D.J. & Miller, C. 1996. Homodimeric architecture of a ClC-type chloride on channel. *Nature* **383**, 337-340.

Mihara, K. & Sato, R. 1985. Molecular cloning and sequencing of cDNA for yeast porin, an outer mitochondrial membrane protein: a search for targeting signal in the primary structure. *EMBO J.* **4**, 769-774.

Miller, C. & Richard, E.A. 1990. The voltage-dependent chloride channel of *Torpedo* electroplax. Intimations of molecular structure from quirks of single-channel function. In *Chloride channels and Carriers in Nerve, Muscle, and Glial Cells*, ed. Alvarez-Leefmans, F.J. & Russell, J.M. pp. 383-405. Plenum, New York.

Miller, C. & White, M. M. 1980. Dimeric structure of Cl^- channels from *Torpedo* electroplax. *Proc. Natl. Acad. Sci.USA* **81**, 2772-2775.

Moorman, J.R., Palmer, C.T., John, J.E., Durieux, M.E. & Jones, L.R. 1992. Phospholemman expression induces a hyperpolarisation-actived chloride current in *Xenopus* oocytes. *J. Biol. Chem.* **267**, 14551-14554.

Morier, N. & Sauvé, R. 1994. Analysis of a novel double-barrelled anion channel from rat liver rough endoplasmic reticulum. *Biophys. J.* **67**, 590-602.

Nelson, D.J., Tang, J.M. & Palmer, L.G. 1984. Single-channel recordings of apical membrane chloride conductance in A6 epithelial cells. *J. Membr. Biol.* **80**,

81-89.

Owen, D.G., Segal, M. & Barker, J.L. 1984. A Ca-dependent Cl^- conductance in cultured mouse spinal neurons. *Nature* **311**, 567-576.

Pahapill, P.A. & Schlichter, L.C. 1992. Cl^- channels in intact human T-lymphocytes. *J. Physiol.* **445**, 407-430.

Palade, P. T. & Barchi, R. L. 1977. On the inhibition of membrane chloride channels by aromatic carboxylic acids. *J.Gen.Physiol.* **69**, 879-896.

Palade, P., Dettbarn, C., Volpe, P., Alderson, B. & Otero, A.S. 1989. Direct inhibition of inositol-1,4,5-trisphosphate-induced Ca^{2+} release from brain microsomes by K^+ channel blockers. *Mol. Pharmacol.* **36**, 664-672.

Paulmichl, M., Li, Y., Wickman, K., Ackerman, M., Peralta, E. & Clapham, D. 1992. New mammalian chloride channel identified by expression cloning. *Nature* **356**, 238-241.

Pozzan, T., Rizzuto, R., Volpe, P. & Meldolesi, J. 1994. Molecular and cellular physiology of intracellular calcium stores. *Physiol.Rev.* **74**, 595-636.

Pusch, M. & Jentsch, T. J. 1994. Molecular physiology of voltage-gated chloride channels. *Physiol.Rev.* **74**, 813-827.

Pusch, M., Steinmeyer, K. & Jentsch, T.J. 1994. Low single channel conductance of the major skeletal muscle chloride channel, CLC-1. *Biophys. J.* **66**, 149-152.

Reeves, W.B. & Gurich, R.W. 1994. Calcium-dependent chloride channels in endosomes from rabbit kidney cortex. *Am. J. Physiol.* **266** (Cell Physiol 35), C741-C750.

Robinson, R.A., & Stokes, R.H. 1955. In *Electrolyte solutions: The measurement and interpretation of conductance, chemical potential and diffusion in solution of simple electrolytes.* p 479, Butterworths, London, England.

Roos, N., Benz, R. & Brdiczka, D. 1982. Identification and characterisation of the pore-forming protein in the outer membrane of rat liver mitochondria. *Biochim. Biophys. Acta.* **686**, 204-214.

Rousseau, E., Roberson, M. & Meissner, G. 1988. Properties of single chloride selective channel from sarcoplasmic reticulum. *Eur.Biophys.J.* **16**, 143-151.

Sanguinetti, M.C., Curran, M.E., Zou, A., Shen, J., Spector, P.S., Atkinson, D.L. & Keating, M.T. 1996. Coassembly of K_vLQT1 and minK (IsK) proteins to form cardiac I_{Ks} potassium channel. *Nature* **384**, 80-83.

Sardini, A., Mintenig, G.M. & Valverde, M.A. 1995. Drug efflux mediated by the human multidrug resistance P-glycoprotein is inhibited by cell swelling. *J. Cell. Sci.* **107**, 3281-3290.

Schein, S.J., Colombini, M. & Finkelstein, A. 1976. Reconstitution in planar lipid bilayers of a voltage-dependent anion-selective channel obtained from *Paramecium* mitochondria. *J. Membr. Biol.* **30**, 99-120.

Schmid, A., Dehlinger-Kremer, M., Schulz, I. & Gogelein, H. 1990. Voltage-dependent $InsP_3$-insensitive calcium channels in membranes of pancreatic endoplasmic reticulum vesicles. *Nature* **346**, 374-376.

Schmid, A., Gogelein, H., Kemmer, T. P. & Schulz, I. 1988. Anion channels in giant liposomes made of endoplasmic reticulum vesicles from rat exocrine

pancreas. *J.Membr.Biol.* **104**, 275-282.

Schmieden, V., Kuhse, J. & Betz, H. 1992. Agonist pharmacology of neonatal and adult glycine receptor a subunits: identification of amino acid residues involved in taurine activation. *EMBO J.* **11**, 2025-2032.

Schwiebert, E.M., Light, D.B., Fejes-Toth, G., Fejes-Toth, N. & Stanton, B.A. 1990. A GTP-binding protein activates chloride channels in a renal epithelium. *J. Biol. Chem.* **265**, 7725-7728.

Sheppard, D.N., Rich, D.P., Ostedgaard, L.S., Gregory, R.L., Smith, A.E. & Welsh, M.J. 1993. Mutations in CFTR associated with mild disease from Cl^- channels with altered pore properties. *Nature* **362**, 160-164.

Shintani, Y. & Marunaka, Y., 1996. Regulation of single Cl^- channel conductance by insulin and tyrosine phosphatase. *Biochem. Biophys. Res. Commun.* **218**, 142-147.

Shivers, B.D., Killisch, I., Sprengel, R., Sontheimer, H., Köhler, M., Schofield, P.R. & Seeburg, P.H. 1989. Two novel $GABA_A$ receptor subunits exist in distinct neuronal subpopulations. *Neuron* **3**, 327-337.

Sigel, E., Stephenson, F.A., Mamalaki, C. & Bernard, E.A. 1983. A gamma-aminobutyric acid/ benzodiazepine receptor complex of bovine cerebral cortex. Purification & partial characterization. *J. Biol. Chem.* **258**, 6965-6971.

Simon, S. M. & Blobel, G. 1991. A protein-conducting channel in the endoplasmic reticulum. *Cell* **65**, 371-380.

Smith, J. S., Coronado, R. & Meissner, G. 1985a. Sarcoplasmic reticulum contains

adenine nucleotide-activated calcium channels. *Nature* **316**, 446-449.

Smith, J.S., Coronado, R. & Meissner, G. 1985b. Single-channel measurements of the calcium-release channel from skeletal muscle sarcoplasmic reticulum. *J.Gen.Physiol.* **88,** 573-588.

Sorgato, M. C. & Moran, O. 1993. Channels in mitochondrial membranes: knowns, unknowns and prospects for the future. *Crit.Rev.Biochem.Molec.Biol.* **18**, 127-171.

Steinmeyer, K.,Lorenz, C., Pusch, M., Koch, M.C. & Jentsch T.J. 1994. Multimeric structure of ClC-1 chloride channel revealed by mutations in dominant myotonia (Thomsen). *EMBO J.* **13**,737-743.

Steinmeyer, K., Ortland, C. & Jentsch, T.J. 1991. Primary structure and functional expression of a developmentally regulated skeletal muscle chloride channel. *Nature Lond.* **354**, 301-304.

Strange, K., Emma, F. & Jackson, P.S. 1996. Cellular and molecular physiology of volume-sensitive anion channels. *Am. J. Physiol.* **270**, C711-C730.

Suarez-Isla, B.A., Orozco, C., Heller, P.F. & Froehlich, J.P. 1986. Single calcium channel in native sarcoplasmic reticulum membranes from skeletal muscle. *Proc. Natl. Acad. Sci. USA* **79**, 7749-7753.

Tabares, L., Mazzanti, M. & Clapham, D. E. 1991. Chloride channels in the nuclear envelope. *J.Membr.Biol.* **123**, 49-54.

Taleb, O., Feltz, P., Bossu, J.L. & Feltz, A. 1988. Small-conductance chloride channels activated by calcium on cultured endocrine cells from mammalian

pars intermedia. *Pflugers Arch.* **412**, 641-646.

Tanifuji, M., Sokabe, M. & Kasai, M. 1987. An anion channel of sarcoplasmic reticulum incorporated into planar bilayers: Single-channel behavior and conductance properties. *J.Membr.Biol.* **99**, 103-111.

Thévenod, F., Gasser, K.W. & Hopfer, U. 1990. Dual modulation of chloride conductance by nucleotides in pancreatic and parotid zymogen granules. *Biochem. J.* **272**, 119-126.

Thiemann, A., Gründer, S., Pusch, M. & Jentsch, T.J. 1992. A chloride channel widely expressed in epithelial and non-epithelial cells. *Nature Lond.* **356**, 57-60.

Tilly, B.C., Kansen, M., Van Gageldonk, P.G.M., Van Den Berghe, N., Galgaard, H., Bijmann, J. & De Jonge, H.R. 1991. G-proteins mediate intestinal chloride channel activation. *J. Biol. Chem.* **266**, 2036-2040.

Tilly, B.C., Mancini, G.M.S., Bijmann, J., Van Gageldonk, P.G.M., Beerens, C.E.M.T., Bridges, R.J., De Jonge, H.R. & Verheijen, F.W. 1992. Nucleotide-activated chloride channels in lysosomal membranes. *Biochem. Biophys. Res. Commun.* **187**, 254-260.

Tominaga, M., Tominaga, T., Miwa, A. & Okada, Y. 1995 Volume-sensitive chloride channel activity does not depend on endogenous p-glycoprotein. *J. Biol. Chem.* **270**, 27887-27893.

Townsend, C., & Rosenberg, R.L. 1995 Characterisation of a chloride channel reconstituted from cardiac sarcoplasmic reticuulum. *J. Membr. Biol.* **147**,

121-136.

Troll, H., Malchow, D., Muller-Taubenberger, A., Humbel, B., Lottspeich, F., Ecke, M., Gerisch, G., Schmid, A. & Benz, R. 1992. Purification, functional characterisation, and cDNA sequencing of mitochondrial porin from *Dictyostelium dicoideum*. *J. Biol. Chem.* **267**, 21072-21079.

Uchida, S., Sasaki, S., Furukawa, T., Hiraoka, M., Imai, T., Hirata, Y. & Marumo, F. 1993. Molecular cloning of a chloride channel that is regulated by dehydration and expressed predominantly in kidney medulla. *J. Biol. Chem.* **268**, 3821-3824.

Vaca, L. & Kunze, D. L. 1993. cAMP-dependent phosphorylation modulates voltage-gating in an endothelial Cl^- channel. *Am.J.Physiol.* **264**, C370-C375.

Valkanov, M., Martin, R.J., & Dixon, D.M. 1994. The Ca-activated chloride channel of *Ascaris suum* conducts volatile fatty acids produced by anaerobic respiration: A patch-clamp study. *J. Membr. Biol.* **138**, 133-141.

Valverde, M.A., Diaz, M., Sepulveda, F.V., Gill, D.H., Hyde, S.C. & Higgins, C.F. 1992. Volume-regulated chloride channels associated with the multidrug resistance P-glycoprotein. *Nature* **355**, 830-833.

Vandenberg, R.J., Handford, C.A. & Schofield, P.R. 1992. Distinct agonist and antagonist-binding sites on the glycine receptor. *Neuron* **9**, 491-496.

Van Slegtenhorst, M.A., Bassi, M.T., Borsani, G., Walpenar, M.C., Ferrero, G.B., De Concilis, L., Rugarti, E.I., Grillo, A., Franco, B., Zoghbi, H.Y. & Ballabio, A. 1994. A gene from Xp22.3 region shares homology with

voltage-gated chloride channels. *Human molecular genetics* **3, 547-552.**

Vogel, H. & Jähnig, F. 1986. Models for the structure of outer-membrane proteins of *Escherichia coli* derived from Raman spectroscopy and prediction methods. *J. Mol. Biol.* **190**, 191-199.

Walaas, S.I., Czernik, A.J., Olstad, O.K., Sletten, K. & Walaas, O. 1991. Protein kinase C and cyclic AMP-dependent protein kinase phosphorylate phospholemman, an insulin and adrenaline-regulated membrane phosphoprotein, at specific sites in the carboxy terminal domain. *Biochem. J.* **304**, 635-640.

Wangemann, P., Wittner, M., Di Stefano, A., Englert, H.C., Lang, H.J., Schlatter, E. & Greger, R. 1986. Cl^- channel blockers in the thick ascending limb of the loop of Henle. Structure activity relationship. *Pflugers Arch. (Suppl. 2)*, S128-S141.

Welsh, M.J., Anderson, M.P., Rich, D.P., Berger, H.A., Denning, G.M., Ostedgaard, L.S., Sheppard, D.N., Cheng, S.H., Gregory, R.J., & Smith, A.E. 1992. Cystic fibrosis transmembrane regulator: A chloride channel with novel regulation. *Neuron* **8**, 821-829.

Werman, R., Davidoff, R.A. & Aprison, M.H. 1968. Inhibitory action of glycine on spinal neurons in the cat. *J Neurophysiol* **31**, 81-95.

Williams, A. J. 1995. The measurement of the function of single ion channels reconstituted into artificial lipid membranes. In *Ion Channels, a Practical Approach*, ed. Ashley, R. H. pp. 43-67. IRL/OUP, Oxford, UK.

Woodhull, A.M. 1973. Ionic blockage of sodium channels in nerve. *J. Gen. Physiol.* **61**, 687-708.

Woll, K.H., Leibowitz, M.D., Neumcke, B. & Hille, B. 1987. A high-conductance anion channel in adult amphibian skeletal muscle. *Pflugers Arch.* **410**, 632-640.

Wright, E.M. & Diamond, J.M. 1977. Anion selectivity in biological systems. *Physiol. Rev.* **57**, 109-153.

Yamamoto, D. & Suzuki, N. 1987. Blockage of chloride channels by HEPES buffer. *Proc. Roy. Soc. Lond. B.* **230**, 93-100.

Young, A.B. & Snyder, S.H. 1973. Strychnine binding associated with glycine receptors of the central nervous system. *Proc. Natl. Acad. Sci.* **70**, 2832-2836.

Yuto, J., Ide, T. and Kasai, M. 1997. ATP-sensitive anion channel from rat brain synaptosomal membranes incorporated into planar lipid bilayers. *Biophys. J.* **72,** 720-727.

Zizi, M., Fisher, R., & Guillo, F.G. 1991. Formation of cation channels in planar lipid bilayers by brefeldin A. *J. Biol. Chem.* **266**, 18443-18445.

Zygmunt, A.C. & Gibbons, W.R. 1991. Calcium-activated chloride current in rabbit ventricular myocytes. *Circulation Research* **68**, 424-437.